

150
1/30/80
M.M.

10. 1567

DOE/ET/04712-1
BAW-1532-1
NOVEMBER 1979

MASTER

DEVELOPMENT OF AN EXTENDED-BURNUP MARK B DESIGN

FIRST SEMI-ANNUAL PROGRESS REPORT: JULY-DECEMBER 1978

PREPARED FOR
THE UNITED STATES
DEPARTMENT OF ENERGY

Burnable
Poison
Assembly

Fuel Assembly

Fuel Rod



Babcock & Wilcox

DISCLAIMER

This report was prepared as an account of work sponsored by an agency of the United States Government. Neither the United States Government nor any agency Thereof, nor any of their employees, makes any warranty, express or implied, or assumes any legal liability or responsibility for the accuracy, completeness, or usefulness of any information, apparatus, product, or process disclosed, or represents that its use would not infringe privately owned rights. Reference herein to any specific commercial product, process, or service by trade name, trademark, manufacturer, or otherwise does not necessarily constitute or imply its endorsement, recommendation, or favoring by the United States Government or any agency thereof. The views and opinions of authors expressed herein do not necessarily state or reflect those of the United States Government or any agency thereof.

DISCLAIMER

Portions of this document may be illegible in electronic image products. Images are produced from the best available original document.

DISCLAIMER

This report was prepared as an account of work sponsored by the United States Government. Neither the United States nor the United States Department of Energy, nor any of their employees, makes any warranty, express or implied, or assumes any legal liability or responsibility for the accuracy, completeness, or usefulness of any information, apparatus, product, or process disclosed, or represents that its use would not infringe privately owned rights. Reference herein to any specific commercial product, process, or service by trade name, mark, manufacturer, or otherwise, does not necessarily constitute or imply its endorsement, recommendation, or favoring by the United States Government or any agency thereof. The views and opinions of authors expressed herein do not necessarily state or reflect those of the United States Government or any agency thereof.

DEVELOPMENT OF AN EXTENDED-BURNUP

MARK B DESIGN

First Semi-Annual Progress Report
for the Period July-December 1978

DISCLAIMER

This book was prepared as an account of work sponsored by an agency of the United States Government. Neither the United States Government nor any agency thereof, nor any of their employees, makes any warranty, express or implied, or assumes any legal liability or responsibility for the accuracy, completeness, or usefulness of any information, apparatus, product, or process disclosed, or represents that its use would not infringe privately owned rights. Reference herein to any specific commercial product, process, or service by trade name, trademark, manufacturer, or otherwise, does not necessarily constitute or imply its endorsement, recommendation, or favoring by the United States Government or any agency thereof. The views and opinions of authors expressed herein do not necessarily state or reflect those of the United States Government or any agency thereof.

Prepared for

United States Department of Energy

Under Contract ET-78-C-02-4712

by

BABCOCK & WILCOX
Power Generation Group
Nuclear Power Generation Division
P.O. Box 1260
Lynchburg, Virginia 24505

BABCOCK & WILCOX
- Research and Development Division
Lynchburg Research Center
P. O. Box 1260
Lynchburg, Virginia 24505

Submitted by

BABCOCK & WILCOX
Contract Research Division
P.O. Box 835
Alliance, Ohio

Arkansas Power & Light Company
P.O. Box 551
Little Rock, Arkansas 72203

~~DISTRIBUTION OF THIS DOCUMENT IS UNLIMITED~~

Babcock & Wilcox

CONTRIBUTING AUTHORS

The following B&W personnel are contributing authors: J. B. Andrews, T. A. Coleman, P. J. Henningson, C. M. Hove, S. S. Kere, R. E. Lide, R. S. Piascik, S. W. Spetz, K. O. Stein, V. O. Uotinen, T. N. Wampler, B. L. Wilks, H. W. Wilson, and J. R. Worsham of the Nuclear Power Generation Division; and R. E. Womack of the Research and Development Division.

ACKNOWLEDGMENT

As with any project or program of this magnitude, the work reported herein is the product of many individuals at Babcock & Wilcox Company, Arkansas Power & Light Company and the U. S. Department of Energy. The authors gratefully recognize their help and efforts in the extended burnup program.

SUMMARY

The primary objective of this program is to develop and demonstrate an improved PWR fuel assembly design capable of batch average burnups of 45,000-50,000 MWd/mtU. To accomplish this, a number of technical areas must be investigated to verify acceptable extended-burnup fuel performance. These areas range from fuel cycle and core physics considerations at high burnup to various mechanical performance considerations related to ensuring fuel integrity.

This report is the first semi-annual progress report for the program, and it describes work performed during the July-December 1978 time period. Efforts during this period included the definition of a preliminary design for a high-burnup fuel rod, physics analyses of extended-burnup fuel cycles, studies of the physics characteristics of changes in fuel assembly metal-to-water ratios, and development of a design concept for post-irradiation examination equipment to be utilized in examining high-burnup lead-test assemblies.

An initial design for a high-burnup fuel rod capable of 60,000 MWd/mtU rod average burnup was derived from parametric studies of key fuel rod design variables. In these studies, the effects of a change in a fuel rod design parameter, such as plenum volume, were investigated to determine whether the change would result in a fuel performance improvement. The results of these parametric studies indicated that end-of-life fuel rod internal pressure was the burnup limiting restraint for fuel rods of current design. Thus, changes in the fuel rod design that reduce end-of-life fuel rod internal pressure were pursued. A preliminary fuel rod design meeting the design goal of 60,000 MWd/mtU was developed by increasing the fuel rod plenum volume by about 50% and increasing cladding thickness by 3 mils. The increased cladding thickness improves fuel rod resistance to creep and provides added margin for corrosion.

Detailed fuel management evaluations were performed which verified both the technical feasibility and the uranium utilization improvement of extended burnup fuel cycles. These cycles covered discharge batch average burnup in excess of 45,000 MWd/mtU. They were successfully designed to satisfy standard

nuclear design criteria for uranium reloads. A uranium utilization improvement of 17% resulted from one of the fuel management schemes.

Two approaches to changing fuel assembly metal-to-water ratios were investigated. One approach, decreasing fuel rod outside diameter and proportionately reducing the uranium loading, showed large potential savings in both uranium and enrichment requirements — on the order of 8% of annual reactor requirements. The other approach, maintaining present fuel rod dimensions and reducing the uranium content of the rod by dilution with a metallic oxide did not yield favorable results.

A conceptual design was completed for post-irradiation examination equipment for examining the high-burnup lead-test assemblies planned for irradiation in the Arkansas Nuclear One, Unit 1 (ANO-1) reactor. The conceptual design employs a removable system installed in the cask loading pit in the auxiliary building at the ANO-1 site. Several simultaneous operations are allowed with this design in order to obtain a large number of measurements in a short time span.

Babcock & Wilcox
Power Generation Group
Nuclear Power Generation Division
Lynchburg, Virginia

Report BAW-1532-1

October 1979

Development of an Extended-Burnup Mark B Design -
First Semi-Annual Progress Report: July-December 1979

Key Words: UO₂ Fuel, Fuel Cycle, Fuel Assembly, Fuel
Burnup, Pressurized Water Reactor

ABSTRACT

The United States Department of Energy (DOE), Arkansas Power & Light Company (AP&L), and The Babcock & Wilcox Company (B&W) are participating in an extended burnup program which is a part of the national effort to improve the utilization of uranium in light water reactors by increasing the amount of energy extracted from each ton of uranium ore. This joint effort program includes development of fuel management schemes and fuel assembly designs for extended burnup. In addition, tests of extended burnup fuel assembly designs will be conducted to support the implementation of extended burnup fuel cycles in light water reactors.

The goal of the DOE/AP&L/B&W program is to extend the burnup of light water reactor fuel assemblies beyond presently allowable limits to the 45,000-50,000 Mwd/mtU batch average burnup range. Extending fuel burnup from the current level of ~30,000 Mwd/mtU to the 50,000 Mwd/mtU level would result in a 15-20% improvement in uranium utilization.

During the last half of 1978, detailed fuel management evaluations of extended burnup fuel cycles, parametric studies of fuel rod design variables, physics analyses of assembly hydrogen to uranium atom ratios, and design of post-irradiation examination equipment were conducted. This report is the first semi-annual progress report for the program.

CONTENTS

	Page
1. INTRODUCTION	1-1
2. DISCUSSION OF TECHNICAL CONSIDERATIONS	2-1
3. PROGRAM SCOPE	3-1
4. PHASE I PROGRAM DESCRIPTION	4-1
4.1. Task 1 - Fuel Utilization Studies	4-1
4.1.1. Objectives	4-1
4.1.2. Technical Workscope	4-1
4.2. Task 2 - Parametric Studies	4-3
4.2.1. Objectives	4-3
4.2.2. Technical Workscope	4-4
4.3. Task 3 - Engineering and Design of Improved Poolside Examination Equipment	4-4
4.3.1. Objective	4-4
4.3.2. Technical Workscope	4-4
5. PROGRESS TO DATE - TASK 1, "FUEL UTILIZATION STUDIES"	5-1
5.1. Subtask 1A - Optimum Burnup Determination	5-1
5.1.1. Introduction	5-1
5.1.2. Design Methods and Criteria	5-2
5.1.3. Summary	5-3
5.2. Subtask 1D - Reduction of Uranium in Fuel Rods	5-5
5.2.1. Introduction	5-5
5.2.2. Reduced-Diameter Fuel Rods	5-6
5.2.3. Fuel Density Reductions	5-9
6. PROGRESS TO DATE - TASK 2, "PARAMETRIC STUDIES"	6-1
6.1. Introduction	6-1
6.2. Subtask 2A - Fuel Rod Analyses	6-2
6.2.1. Introduction	6-2
6.2.2. Power History Sensitivity Study	6-2
6.2.3. Fuel Temperature and Rod Internal Pressure Study	6-3
6.2.4. Fuel Rod Cladding Ovality Study	6-4
6.2.5. Preliminary Extended Burnup Fuel Rod Design	6-5
6.3. Subtask 2B - Basic Structural Component Design	6-6
6.3.1. Introduction	6-6
6.3.2. Material Property Changes	6-6
6.3.3. Geometry Changes	6-7

CONTENTS (Cont'd)

	Page
6.3.4. Fatigue	6-8
6.3.5. Preliminary Conclusions	6-8
7. PROGRESS TO DATE — TASK 3, "ENGINEERING AND DESIGN OF IMPROVED POOLSIDE EXAMINATION EQUIPMENT"	7-1
7.1. Introduction	7-1
7.2. Examination Scope	7-1
7.3. Design Guidelines	7-2
7.4. Results and Discussion	7-2
7.4.1. Operating Location Selection	7-2
7.4.2. System Description	7-3

APPENDIXES

A. Description of Fuel Cycle Study	A-1
B. Description of Fuel Cycle Study	B-1
C. Description of Fuel Cycle Study	C-1
D. Description of Fuel Cycle Study	D-1
E. Description of Fuel Cycle Study	E-1

List of Tables

Table

5-1. Uranium Utilization — 177 FA Plant	5-12
5-2. Margin to Maximum Allowed Pin Power Peak (%)	5-12
5-3. Discharge Burnups	5-13
5-4. Shutdown Margin	5-13
5-5. Standard Mark B Fuel Parameters	5-14
6-1. Standard Mark B Fuel Parameters	6-9
6-2. Fuel Temperature/Rod Internal Pressure Study	6-10
6-3. Parametric Temperature/Pressure Analysis	6-11
6-4. Fuel Rod Design Parameters	6-11
6-5. Preliminary Fuel Rod Design	6-12
7-1. PIE System Test Capabilities	7-5
A-1. Fuel Inventory Plan	A-4
A-2. Fuel Burnup Distribution	A-5
A-3. Control Rod Worths	A-6
B-1. Fuel Inventory Plan	B-3
B-2. Fuel Burnup Distribution	B-4
B-3. Control Rod Worths	B-5
C-1. Fuel Inventory Plan	C-4
C-2. Fuel Burnup Distribution	C-5
C-3. Control Rod Worths	C-6

List of Tables (Cont'd)

Table		Page
D-1.	Fuel Inventory Plan	D-3
D-2.	Fuel Burnup Distribution	D-4
D-3.	Control Rod Worths	D-5
E-1.	Fuel Inventory Plan	E-4
E-2.	Fuel Burnup Distribution	E-5
E-3.	Control Rod Worths	E-6

List of Figures

Figure		
5-1.	Reduced Diameter Fuel Rod Enrichment Vs Hydrogen to Uranium Atom Ratio	5-15
5-2.	Reduced Diameter Fuel Rod Separative Work Unit Savings Vs Hydrogen to Uranium Atom Ratio	5-16
5-3.	Reduced Diameter Fuel Rod Yellowcake Savings Vs Hydrogen to Uranium Atom Ratio	5-17
5-4.	Reduced Diameter Fuel Rod Potential Dollar Savings Vs Hydrogen to Uranium Atom Ratio	5-18
5-5.	UO ₂ -ZrO ₂ Fuel Rod Enrichment Vs Hydrogen to Uranium Atom Ratio	5-19
5-6.	UO ₂ -ZrO ₂ Fuel Rod Separative Work Unit Penalty Vs Hydrogen to Uranium Atom Ratio	5-20
5-7.	UO ₂ -ZrO ₂ Fuel Rod Yellowcake Savings Vs Hydrogen to Uranium Atom Ratio	5-21
5-8.	UO ₂ -ZrO ₂ Fuel Rod Economics Vs Hydrogen to Uranium Atom Ratio	5-22
5-9.	Cycle Average K _∞ for Constant Fuel Enrichment Vs Hydrogen to Uranium Atom Ratio	5-23
6-1.	Fuel Rod Radial Peaking Factor Power History	6-13
6-2.	Fuel Rod Radial Peaking Factor Power History	6-14
6-3.	Fuel Rod Radial Peaking Factor Power History	6-15
6-4.	EOL Internal Rod Pressure Vs Fuel Densification	6-16
6-5.	EOL Internal Rod Pressure Vs Initial Rod Pressure	6-16
6-6.	EOL Internal Rod Pressure Vs Fuel Pellet Outside Diameter	6-17
6-7.	EOL Internal Rod Pressure Vs Rod Plenum Volume	6-18
6-8.	Maximum Fuel Temperature Vs Burnup	6-19
6-9.	Maximum Fuel Temperature Vs Burnup	6-20
6-10.	Maximum Fuel Temperature Vs Burnup	6-21
6-11.	Creep Ovality Vs Cladding Wall Thickness	6-22
6-12.	Creep Ovality Vs Fuel Rod Plenum Volume	6-22

List of Figures (Cont'd)

Figure	Page
6-13. Creep Ovality Vs Fuel Rod Initial Pressure	6-23
6-14. Creep Ovality Vs Fuel Densification	6-24
6-15. Creep Ovality Vs Burnup	6-25
6-16. EOL Creep Ovality as a Function of Wall Thickness and Prepressure	6-26
6-17. EOL Internal Rod Pressure Vs Burnup	6-27
6-18. Mark B Fuel Assembly	6-28
6-19. Holddown Spring Net Operating Force	6-29
6-20. Fuel Assembly Growth as Function of Assembly Average Fluence	6-30
6-21. Fuel Rod Growth as Function of Assembly Average Fluence	6-31
7-1. Cask Loading Pit Area in Auxiliary Building	7-6
7-2. PIE System Arrangement in Cask Loading Pit	7-7
7-3. PIE Operations Flow Plan	7-8
A-1. Cycle 4 Core Loading Plan	A-7
A-2. Cycle 5 Core Loading Plan	A-8
A-3. Cycle 6 Core Loading Plan	A-9
A-4. Cycle 7 Core Loading Plan	A-10
A-5. Cycle 8 Core Loading Plan	A-11
A-6. Cycle 9 Core Loading Plan	A-12
A-7. Cycle 4, Core Power Distribution — 36-FA Feed	A-13
A-8. Cycle 5, Core Power Distribution — 36-FA Feed	A-14
A-9. Cycle 6, Core Power Distribution — 36-FA Feed	A-15
A-10. Cycle 7, Core Power Distribution — 36-FA Feed	A-16
A-11. Cycle 8, Core Power Distribution — 36-FA Feed	A-17
A-12. Cycle 9, Core Power Distribution — 36-FA Feed	A-18
B-1. Cycle 5 Core Loading Plan	B-6
B-2. Cycle 6 Core Loading Plan	B-7
B-3. Core Loading Plan for Cycles 7 and 8	B-8
B-4. Cycle 5 Core Power Distribution — 60-FA Feed, Rodded	B-9
B-5. Cycle 6 Core Power Distribution — 60-FA Feed, Rodded	B-10
B-6. Cycle 7 Core Power Distribution — 60-FA Feed, Rodded	B-11
B-7. Cycle 8 Core Power Distribution — 60-FA Feed, Rodded	B-12
C-1. Cycle 5 Core Loading Plan	C-7
C-2. Cycle 6 Core Loading Plan	C-8
C-3. Core Loading Plan For Cycles 7 and 8	C-9
C-4. Cycle 5 Core Power Distribution — 60 Feed, Feed and Bleed	C-10
C-5. Cycle 6 Core Power Distribution — 60 Feed, Feed and Bleed	C-11
C-6. Cycle 7 Core Power Distribution — 60 Feed, Feed and Bleed	C-12
C-7. Cycle 8 Core Power Distribution — 60 Feed, Feed and Bleed	C-13
D-1. Cycle 5 Core Loading Plan	D-6
D-2. Cycle 6 Core Loading Plan	D-7
D-3. Core Loading Plan For Cycles 7 and 8	D-8
D-4. Cycle 5 Core Power Distribution — 68-FA Feed	D-9
D-5. Cycle 6 Core Power Distribution — 68-FA Feed	D-10
D-6. Cycle 7 Core Power Distribution — 68-FA Feed	D-11
D-7. Cycle 8 Core Power Distribution — 68-FA Feed	D-12

List of Figures (Cont'd)

Figures	Page
E-1. Cycle 4 Core Loading Plan	E-7
E-2. Cycle 5 Core Loading Plan	E-8
E-3. Cycle 6 Core Loading Plan	E-9
E-4. Cycle 7 Core Loading Plan	E-10
E-5. Cycle 4 Core Power Distribution - 80-FA Feed	E-11
E-6. Cycle 5 Core Power Distribution - 80-FA Feed	E-12
E-7. Cycle 6 Core Power Distribution - 80-FA Feed	E-13
E-8. Cycle 7 Core Power Distribution - 80-FA Feed	E-14

1. INTRODUCTION

A major new constraint was introduced into nuclear fuel cycle considerations as a result of the decision of the United States government to defer indefinitely the reprocessing of spent fuel and the recycling of plutonium and uranium. For a number of years the traditional practice in the LWR industry has been to discharge fuel after it has been irradiated for three or four cycles and has achieved a batch average burnup in the 25,000-33,000 MWd/mtU range. The discharge batch average burnup limit of about 33,000 MWd/mtU had been established through economic optimization studies based on the assumption that spent fuel reprocessing would make it possible to reclaim and reuse the residual fissile materials that exist in spent fuel. In addition to representing an economic optimum, this burnup limit of about 33,000 MWd/mtU has been demonstrated over the last decade to be conservative from a mechanical performance standpoint and to give ample assurance of cladding integrity and safe operating performance.

In the absence of reprocessing and recycling, however, conventional LWR fuel management strategies no longer represent optimum approaches. The industry must now assume that residual fissile materials in spent fuel cannot be reclaimed and reused. This currently imposed "once-through" fuel cycle has created an economic incentive to look for ways to minimize uranium requirements in this new mode of operation.

One of the more straightforward and most readily employable means of achieving substantial improvements in uranium utilization in LWRs in the near term is to increase the discharge batch average burnup limit. Engineering projections have indicated that uranium utilization improvements of 15-20% can be achieved when the discharge batch average burnup is increased from the current 30,000 MWd/mtU to the 45,000-50,000 MWd/mtU range. This improved uranium utilization results in lower fuel cycle costs and also reduces requirements for spent fuel storage.

The United States Department of Energy (DOE) has initiated a research, development, and demonstration effort involving the Arkansas Power & Light Company, Duke Power Company, and The Babcock & Wilcox Company. The goal is to demonstrate improved fuel utilization, mainly through the successful operation of PWR fuel assemblies to extended burnups.

The overall fuel utilization improvement effort between B&W/Duke/AP&L/DOE is divided into two separate but interrelated programs. In one of the programs, B&W and Duke are seeking to demonstrate that the batch average burnup limit of current PWR assemblies can be safely increased from ~33,000 to ~38,000 MWd/mtU. This program, which does not involve design changes in current fuel assemblies, but instead will extend the current fuel performance data base, will pave the way for the wide-scale implementation of higher batch average burnups beginning as early as 1981. This burnup extension will allow substantial improvement (~5%) in uranium utilization beginning within 2-3 years.

In the program reported herein, B&W and AP&L are undertaking the development and demonstration of an improved fuel assembly design that will be capable of achieving batch average burnups in the 45,000-50,000 MWd/mtU range. The B&W/AP&L program is a longer term effort, which is expected to lead to full-scale implementation of such higher burnup fuel assemblies by the late 1980's with an additional 10 to 15% improvement in uranium utilization.

This report is the first semi-annual progress report for the B&W/AP&L program (contract No. ET-78-C-02-4712). It covers the progress made between July 1 and December 31, 1978.

THIS PAGE
WAS INTENTIONALLY
LEFT BLANK

cladding, and data are needed to verify that corrosion and hydriding are not accelerated at high burnups. Dimensional and structural changes include such effects as irradiation growth, fretting, wear, and component relaxation, which must be addressed in the design process. Pellet-cladding interaction encompasses a broad category of events involving contact between the fuel pellets and the cladding that lead to the loss of cladding integrity through chemical or mechanical means. Since the availability of aggressive fission products and the number of rods experiencing pellet-cladding contact will both increase with burnup, attention must be focused on ways to prevent PCI failures, thereby maintaining cladding integrity.

The practical concerns discussed above are being addressed through a series of analytical studies and demonstration irradiations. The aim of these studies is to perform the necessary research, development, and demonstration as expeditiously as possible so that the resource savings potential of extended burnup can be implemented in a timely fashion.

The following section is a brief discussion of the overall scope of the AP&L/B&W program.

3. PROGRAM SCOPE

As mentioned earlier, the objectives of this program are to develop and demonstrate an improved PWR fuel assembly that will be capable of achieving batch average burnups from 45,000 to 50,000 MWd/mtU. The successful completion of this program will allow substantial uranium utilization improvements to be realized in pressurized water reactors. The program is divided into two phases:

Phase I: Development and Design of Extended Burnup Fuel Assemblies

Phase II: Fabrication, Licensing, Irradiation and Evaluation of
Extended Burnup Lead Test Assemblies

Phase I comprises the nuclear, mechanical, and thermal-hydraulic analyses required to develop and design a PWR fuel assembly capable of burnups in the desired range. The major output of Phase I will be a design for the improved fuel assembly. In addition, Phase I includes assessments of selected uranium utilization improvement options and the design of improved equipment for conducting nondestructive measurements on extended burnup fuel assemblies.

Phase II of the program includes manufacturing of lead test assemblies using the design developed in Phase I. Phase II also includes irradiation and examination of the lead test assemblies, which will support the eventual implementation of a full batch of extended burnup assemblies.

Work is underway on Phase I of this program, which is divided into three major tasks:

Task 1: Fuel Utilization Studies

Task 2: Parametric Studies

Task 3: Engineering and Design of Improved Poolside
Examination Equipment

These Phase I tasks are described in detail in section 4.

4. PHASE I PROGRAM DESCRIPTION

4.1. Task 1 - Fuel Utilization Studies

4.1.1. Objectives

The objectives of Task 1 are as follows:

1. To verify the feasibility of extended-burnup cycles.
2. To determine the "optimum" fuel burnup based on current fuel cycle economics.
3. To examine control techniques for the removal of partial-length control rods.
4. To estimate potential uranium yellowcake savings from a program of moderator temperature control.
5. To evaluate potential uranium yellowcake savings from optimization of fuel assembly water: fuel ratio.
6. To assess the uranium yellowcake benefits accruing from improved utilization of discharged fuel from the initial reactor core.

4.1.2. Technical Workslope

4.1.2.1. Subtask 1A - Optimum Burnup Determination

Both the feasibility and the economics of extended burnup fuel cycles will be analyzed through a series of fuel management evaluations. Fuel cycle calculations using the PDQ-07 diffusion theory code¹ and B&W's standard two-dimensional reactor model will be performed to develop acceptable fuel management plans for achieving high discharge batch average burnups. The fuel cycle designs will define enrichment requirements, fuel loadings, power distributions, fuel burnup data, selected control rod worths, and isotopics. Using the fuel cycle analyses, fuel cycle costs will be evaluated and the optimum burnup determined.

4.1.2.2. Subtask 1B - APSR Removal

The use of anticipatory movements of the full-length control rods (a priori control techniques) to dampen xenon, reactivity, and power oscillations caused by withdrawing the partial-length control rods or axial power shaping rods

(APSRs) will be investigated using the three-dimensional nodal code FLAME.² FLAME is a Babcock & Wilcox computer code used for licensing analyses of core operating limits. Removal of the APSRs is expected to have a reactivity worth of 0.3 to 0.5% $\Delta\rho$. Therefore, the removal of APSRs near end of a cycle will provide a 1-3% uranium utilization improvement.

A fuel cycle for an operating B&W 177-fuel assembly plant will be selected for the analysis. As a first approach, removal of the partial-length control rods will be studied near the end of the cycle because the core power distribution generally flattens with burnup, thus reducing power peaking and increasing margins to design limits. Reactor power, imbalance, xenon distribution, and power peaking will be tracked during the maneuver.

4.1.2.2. Subtask 1C -- Moderator Temperature Control

It may be possible to extend cycle lifetime by employing moderator temperature increases to reduce reactor power rather than inserting neutron poisons such as control rods or soluble boron, which are normally used to accomplish the power reduction. An increased moderator temperature can reduce power by hardening the neutron spectrum, which results in increased neutron absorption in ²³⁸U and increased production of ²³⁹Pu. The net effect is to shift from parasitic neutron absorption to increased plutonium production.

The advantages of a program of moderator temperature increases during a fuel cycle will be investigated in this subtask. Analyses will be performed on a fuel assembly basis using the B&W computer code NULIF to assess the most beneficial time in life for increased moderator temperature.³ The fuel cycle lifetimes from these studies will be used to ascertain the potential uranium utilization improvement available from the increased moderator temperature concept.

4.1.2.3. Subtask 1D -- Reduction of Uranium in Fuel Rods

Existing PWR fuel designs were developed assuming recovery of their discharge fissile content by reprocessing and recycling. Improvements in uranium utilization can be achieved in the once-through fuel cycle by optimizing the moderator-to-fuel ratio of the fuel assembly to obtain the maximum benefit from the fuel assembly's fissile content during incore residence.

Two approaches to improving the moderator-to-fuel ratio for the once-through fuel cycle will be investigated and the potential uranium utilization improvement quantified.

The first approach involves assessing the benefits of reducing fuel rod diameter with a proportional decrease in uranium content. This assessment will identify the enrichment levels, yellowcake requirements, uranium utilization improvement, and economics associated with reducing the fuel rod diameter.

The second approach involves diluting the uranium content of the fuel rod with a metallic oxide while maintaining standard Mark B fuel rod dimensions. Outputs from the study will be enrichment levels, yellowcake requirements, uranium utilization improvement, and economic analyses.

This subtask quantifies the potential uranium utilization improvement from these two approaches to reducing the uranium content of the fuel rods.

4.1.2.4. Subtask 1E - Improved Utilization of Discharged Fuel

Fuel management plans that call for reinserting discharged fuel assemblies from the first and second batches of fuel for additional irradiation will be developed and compared to typical three-batch refueling, which does not include reinsertion. The fuel management program to be investigated is shown in Table 4-1. The PDQ07 diffusion theory computer code and B&W's standard two-dimensional reactor model will be used to develop the fuel management schemes for a B&W 205-fuel assembly (FA) core. The fuel management analyses will yield enrichment requirements, fuel loading patterns, core power distributions, fuel burnup data, and isotopics. The information from the fuel management analyses will be evaluated to determine the uranium utilization and fuel cycle costs for both typical three-batch refueling and reinsertion cases. A direct comparison of the uranium utilization will be performed to identify the potential utilization improvement from reinserting discharged fuel.

4.2. Task 2 - Parametric Studies

4.2.1. Objectives

The objectives of Task 2 are as follows:

1. To evaluate the effects of changes in fuel rod design parameters on fuel performance.
2. To develop lead test assembly designs capable of 50,000 MWd/mtU burnup.

4.2.2. Technical Workscope

Under this task, the mechanical design for high burnup lead test assemblies will be developed. These assemblies will be interchangeable with the current Mark B 15 x 15 fuel assemblies. The lead test assemblies will be prototypes for subsequent full batch implementation and will provide valuable performance data to assist in licensing activities.

The first four lead test assemblies are planned for insertion in cycle 5 of the ANO-1 reactor (currently scheduled for mid-November 1980). The design of these assemblies will be based on B&W's existing analytical models, which have been verified and updated based on post-irradiation examinations of fuel assemblies at burnups of approximately 31,000 MWd/mtU. Fuel performance data at burnups in excess of 40,000 MWd/mtU are expected in 1980 from the companion Duke Power Company/DOE program, "Qualification of the B&W Mark B Fuel Assembly for High Burnup." These experimental data will be used to optimize the high-burnup lead test assembly design. Thus, a second set of four lead test assemblies is planned for ANO-1, cycle 6.

4.3. Task 3. Engineering and Design of Improved Poolside Examination Equipment

4.3.1. Objective

The objective of Task 3 is to design a nondestructive measurement system for characterizing and collecting fuel performance data on extended burnup fuel assemblies.

4.3.2. Technical Workscope

The system to be designed will consist of the following components:

1. Visual station for periscope observation and photography as well as television, TV-video taping, and length measurement capabilities to determine rod and assembly growths.
2. Gamma scanner capable of full-length isotopic gamma scans of the corner rods of fuel assemblies.
3. Line scan testing and auxiliaries for dimensional measurements taken on individual peripheral fuel rods and full water channel measurements at selected axial elevations of a fuel assembly. Measurements on individual rods will consist of diametral profilometry and lateral bow (along face of

assembly). The auxiliaries consist of the measurement heads and associated electronics and recorders for the line scan tester.

4. Computerized data acquisition system to facilitate the handling, reduction, and subsequent analysis of the data generated at poolside (optional).
5. Crud collection system for sampling crud from selected fuel rods at various locations of interest.
6. Grid spring tester to determine the spacer grid spring loads on fuel rods.
7. Holddown spring tester to determine irradiation effects on assembly hold-down spring load and deflection characteristics.

Table 4-1. Improved Utilization of Discharged Fuel —
Fuel Management Program, 205-FA Core

Three-Batch Refueling

Batch No.	No. FAs	Cycle No. and planned EFPD					
		460 1	307 2	307 3	307 4	307 5	307 6
1	69	69	--	--	--	--	--
2	68	68	68	--	--	--	--
3	68	68	68	68	--	--	--
4	69	--	69	69	69	--	--
5	68	--	--	68	68	68	--
6	68	--	--	--	68	68	68
7	69	--	--	--	--	69	69
8	68	--	--	--	--	--	68

Reinsertion of Discharged Fuel

Batch No.	No. FAs	Cycle No. and planned EFPD					
		307 1	307 2	307 3	307 4	307 5	307 6
1	69	69	5	--	--	--	16
2	68	68	68	13	21	25	9
3	68	68	68	68	--	--	--
4	64	--	64	64	64	--	--
5	60	--	--	60	60	60	--
6	60	--	--	--	60	60	60
7	60	--	--	--	--	60	60
8	60	--	--	--	--	--	60

5. PROGRESS TO DATE - TASK 1, "FUEL UTILIZATION STUDIES"

The work effort during this reporting period has addressed Subtask 1A, "Optimum Burnup Determination," and Subtask 1D, "Reduction of Uranium in Fuel Rods." The progress to date on these subtasks is discussed below. Work on the remaining subtasks is scheduled for the following report period.

5.1. Subtask 1A - Optimum Burnup Determination

5.1.1. Introduction

The major emphasis during this report period has been the verification of uranium utilization improvement and technical feasibility of extended burnup fuel cycles through detailed fuel management evaluations. Fuel management plans resulting in discharge batch average burnups from ~34,000 to ~48,500 MWd/mtU were analyzed. The results from the fuel management evaluations confirmed previous predictions of the improvement in uranium utilization as a function of discharge burnup. Furthermore, extended burnup fuel cycles were successfully designed to satisfy standard design criteria for uranium reloads. Five fuel management plans for 177-FA (fuel assembly) plants were selected for study to determine the technical feasibility of designing fuel cycles with relatively high discharge burnups. The five selected combinations of reload batch size and fuel cycle length were as follows:

1. 80 fuel assembly feed, 460 EFPD cycle @ 2772 MWt, feed and bleed
2. 68 fuel assembly feed, 460 EFPD cycle @ 2772 MWt, feed and bleed
3. 60 fuel assembly feed, 460 EFPD cycle @ 2772 MWt, feed and bleed
4. 60 fuel assembly feed, 497 EFPD cycle @ 2568 MWt, rodded
5. 36 fuel assembly feed, 292 EFPD cycle @ 2772 MWt, feed and bleed

These selections, which were made in conjunction with AP&L, Duke, and the DOE, represent a spectrum of fuel cycles that are of interest to utilities with operating PWRs. Utilities have been showing a preference for 18-month fuel cycles because of their higher annual availability and capacity factor. Thus, it was decided to pursue three fuel management approaches to 18-month

fuel cycles that would result in discharge burnups in the range of interest, i.e., 33,000 to 50,000 MWd/mtU. Because annual or semi-annual fuel cycles are inherently more efficient from a fuel management standpoint than the 18-month cycle, a reduced feed batch for an annual fuel cycle was also chosen for analysis. The annual cycle allows replacement of a smaller fraction of the core during each refueling, which increases fuel management efficiency.

To obtain data of generic applicability to B&W 177-FA plants, four of the fuel management evaluations were conducted at the maximum licensed power level of 2772 MWt. For comparison, a fuel management plan for operation at 2568 MWt in the "rodded" mode was also developed.

The 2772-MWt plants operate in a feed-and-bleed mode, which primarily utilizes soluble boron to control reactivity changes. In this mode, control rods are almost fully withdrawn from the core during full power operation. In the rodded mode, a bank of control rods is deeply inserted during full power operation.

The "low leakage" or lumped burnable poison (LBP) shuffle scheme was selected for the extended burnup fuel management evaluations because previous studies performed by B&W indicated that a substantial improvement in uranium utilization (~4%) can be achieved with this scheme. In the LBP shuffle scheme illustrated in Figure C-1, fresh fuel assemblies containing LBP clusters are interspersed in the core interior with the highest burnup fuel. The lowest burnup fuel from the previous cycle is placed on the core periphery. Radial core neutron leakage is thereby reduced relative to the out-in fuel management scheme in which fresh fuel is loaded on the core periphery.

5.1.2. Design Methods and Criteria

The diffusion theory program PDQ-7 with thermal-hydraulic feedback was used for the detailed fuel management evaluations.¹ Two-dimensional, quarter-core geometry was used with one mesh interval per cell pitch. Two-group neutron cross sections used in PDQ-7 are fit as functions of several variables, including ²³⁵U enrichment and fuel burnup in MWd/mtU. Because relatively high ²³⁵U enrichments and fuel burnups were projected for the extended burnup cycles, the cross section library was expanded to 5.25% ²³⁵U enrichment and 80,000 MWd/mtU.

Beginning-of-cycle (BOC) isotopics for four of the five fuel management evaluations were obtained from previously licensed out-in, rodded fuel cycles.

Annual cycles employing the out-in shuffle scheme and the feed-and-bleed mode of operation were used to obtain BOC isotopics for the fifth fuel management evaluation, the 36-FA feed case.

For all cases except the 80-FA feed case, the projected equilibrium cycle feed enrichment was loaded for each cycle, the cycle was depleted, and cycle lifetime was determined. The first two cycles (N+1, N+2) are transition cycles from the conventional out-in scheme to the low-leakage shuffle scheme, which incorporates high burnup and higher feed enrichments. In the design of an actual plant, the feed enrichment of the transition cycles would probably be different than that of the equilibrium cycle in order to make the transition more gradual and to reduce power peaking. It was decided for this study to load the equilibrium enrichment immediately, to reach the equilibrium cycle sooner, and to test the ability to control power peaking by shuffling fuel assemblies and by choice of burnable poison concentrations. The 80-FA feed case used enrichments that were varied by cycle to demonstrate the possible reductions in power peaking that could be achieved during transition cycles.

The design criteria used during the fuel management evaluations were (1) a maximum radial relative pin power of less than 1.651, (2) a 1.0% $\Delta\rho$ shutdown margin with the most reactive control rod assumed stuck out of the core, (3) moderator temperature coefficient less than or equal to zero at rated power, and (4) a negative power coefficient in the operating range of 15-100% rated power.

The details of the fuel management evaluations and conclusions are discussed in the following sections.

5.1.3. Summary

The results of the fuel cycle analyses that are of primary interest are the uranium utilization, power distributions, fuel burnups, and control rod worths. The uranium utilization of a fuel cycle scheme is a measure of how efficiently uranium ore is used. Power distributions are required to establish the reactor operating limits that could be imposed for a given cycle. Fuel burnups and control rod worths are needed to verify that the fuel cycle scheme is within the design limits of the fuel and that adequate shutdown margin is maintained.

The base case against which various options were compared utilized three-batch refueling (hypothetical 59-FA feed), the LBP shuffle scheme, and annual

(292 EFPD) fuel cycles at a power level of 2568 MWt. The discharge batch average burnup for the base case is 27,413 MWd/mtU, and its uranium utilization is 11.73 MWt/2000 lb U₃O₈ (assuming 1% fabrication overage and a 0.5% gas conversion loss).

Table 5-1 shows the uranium utilization for each of the five fuel management schemes. As expected, the 36-FA feed case (approximately five-batch refueling) with annual cycles gave the highest uranium utilization, 13.76 MWt/2000 lb U₃O₈, which represents a 17.3% increase over the base case. Of the 18-month fuel cycles, the best fuel utilization was achieved by the 60-FA feed case (approximately three-batch refueling). The utilization in this case was 12.54 MWt/2000 lb U₃O₈, which represents a 6.9% increase over the base case. Thus, a substantial improvement in uranium utilization can be realized from extended burnup in either annual or 18-month fuel cycles relative to annual, three-batch refueling.

The power distributions for the extended burnup cycles resulted in no significantly increased peaking for the equilibrium cycle compared to typical three-batch fuel management. Therefore, no major restrictions to nuclear operating limits for extended burnup equilibrium cycles are expected. This statement is confirmed by the margins to the maximum pin power peaks displayed in Table 5-2. The 80-FA feed case gave the lowest peaking, even in the transition cycles, because the enrichment of the fresh fuel introduced during the transition was adjusted to reduce peaking, and there are simply more fresh fuel assemblies to share power with the 80-FA feed case. The results from the detailed fuel management evaluations indicate that power peaking in extended burnup fuel cycles can be controlled to within the nuclear design criteria currently accepted for light water reactors. Transition cycle power peaking will be more difficult to control, but adequate design margin can be maintained by careful selection of fuel enrichment and feed batch size.

Discharge batch average burnups and maximum FA discharge burnups are given in Table 5-3 for each of the five fuel management schemes. The ratio of maximum assembly burnup to batch average discharge burnup is higher for extended burnup cycles than it is for the base case. Some reduction in the ratio of maximum assembly burnup to batch average discharge burnup can be achieved in extended burnup fuel cycle designs by placing more emphasis on equalizing discharge burnups during the fuel cycle design process.

The control rod worths and shutdown margins for the extended burnup fuel cycles were not significantly different from the base case. The equilibrium extended burnup cycles met the shutdown reactivity margin requirement of 1.0% $\Delta\rho$ shutdown margin. Table 5-4 gives the shutdown margin for the equilibrium fuel cycles.

The detailed fuel management evaluations of various extended burnup fuel cycle schemes confirmed that the uranium utilization improvements projected by simplified reactor models are achievable. Furthermore, the extended burnup cycles can be designed within existing design criteria without unduly restricting reactor operating limits.

Appendixes A through E describe the five fuel management evaluations in detail.

5.2. Subtask 1D - Reduction of Uranium in Fuel Rods

5.2.1. Introduction

Current PWR fuel designs employ cylindrical, high-density UO_2 pellets. The fuel rod design employs as much UO_2 as possible in the fuel rod to minimize enrichment requirements and to maximize plutonium production. This represented an optimal approach under the assumption that reprocessing would be implemented. However, under the assumption of no reprocessing, the uranium fuel assembly requires reoptimization to more effectively utilize the plutonium in situ as it is generated rather than striving for maximum discharged plutonium content.

Previous analyses have demonstrated that optimum plutonium fuel utilization in LWRs requires a greater hydrogen-to-fuel atom ratio (wetter lattice) than is required for uranium fuel. Therefore, an increase in the hydrogen-to-fuel atom ratio is a means to utilize the bred-in plutonium fuel more efficiently.

Hydrogen-to-fuel atom ratio changes can be accomplished in several ways. For example, it can be accomplished by increasing the lattice pitch without changing the rod dimensions. Second, it can be accomplished by reducing the diameter of the fuel rods, without changing the lattice pitch. Third, it can be accomplished by reducing the quantity of uranium in the fuel pellet without changing either the rod or assembly dimensions. Of these alternatives, the last two could be implemented with the least perturbations on the overall core design. Thus, it is the uranium savings that could be achieved by these two approaches that is being investigated in this subtask.

5.2.2. Reduced-Diameter Fuel Rods

The studies described herein show that potentially significant savings in uranium resources and fuel cycle costs can be achieved by reducing the fuel rod diameter while maintaining a constant fuel rod pitch. The increased neutron moderation from the larger water volume surrounding the reduced-diameter fuel rod provides improved neutron thermalization, a softer thermal energy spectrum, and a significant reactivity benefit. The net result is that both the amount of uranium and the total separative work units are reduced relative to the standard Mark B fuel assembly design while maintaining equivalent energy production capability. The maximum potential uranium savings occurs at a fuel volume reduction of about 25% and is equivalent to a savings of approximately 8% of the annual yellowcake requirements for three-batch refueling of a B&W 177-FA plant operating at 2568 MWt. The maximum potential front end uranium cost savings occurs at a fuel volume reduction of about 15% and is estimated to be equivalent to a savings of approximately 6% of the annual uranium material and separative work costs.

5.2.2.1. Methods of Analysis

The indicated savings was calculated using the B&W neutron spectrum and fuel depletion computer program NULIF.³ The fuel assembly was represented as a fuel pin cell, with the effects of the remaining components of the fuel assembly (control rod guide tubes, instrument tube, and water) being accounted for by appropriate flux and volume weighting.

The NULIF model assumed a fuel rod enrichment of 2.80 wt % ²³⁵U for the standard Mark B fuel rods. Dimensions for the standard Mark B fuel rod are given in Table 5-5. The fuel burnup for the standard Mark B fuel rod in these calculations is 28,915 Mwd/mtU at the end of three 308-EFPD cycles. The soluble boron concentration was decreased stepwise from 1000 ppmB at the beginning of each cycle to 10 ppmB at the end of each cycle.

The NULIF calculations for fuel rods of reduced diameters used the same assumptions of power output, cycle length, and soluble boron concentration as the standard Mark B fuel rod. For the reduced-diameter fuel rods, the cladding outside diameter and the fuel pellet diameter were reduced proportionally to produce a given fuel rod volume reduction. The fuel pellet-to-cladding gap cross-sectional area was maintained at the nominal standard Mark B value. The

average EOC infinite multiplication factor (k_{∞}) from NULIF was used as the basis for cycle lifetime determination.

5.2.2.2. Results

As fuel volume is reduced, an increase in fuel enrichment is required to maintain the same energy production capability. This fuel enrichment is shown as a function of hydrogen-to-uranium atom ratio (H/U ratio) in Figure 5-1. Also shown in this figure is the fuel enrichment that would result if the separative work units were held constant as the fuel volume was reduced. The difference between the two curves in Figure 5-1 represents the enrichment benefit resulting from increased neutron moderation due to the additional water volume around the fuel rod. Figure 5-2 illustrates the potential separative work unit savings as a function of H/U ratio.

The net savings in yellowcake is a function of both the enrichment required for equal energy production and the fuel rod volume reduction. For a constant fuel enrichment, the savings in yellowcake for a given fuel rod volume reduction is directly proportional to the volume reduction as shown by the solid line in Figure 5-3. However, since higher enrichments are required for the reduced-diameter fuel rods to maintain equal energy production, the yellowcake savings from the fuel rod volume reduction are decreased by the amount of yellowcake required for the increased enrichment. The net savings in yellowcake for reduced-diameter fuel rods is shown as a dashed line in Figure 5-3 over a range of H/U ratios from 4.0 to 6.5. The maximum savings occurs at an H/U ratio of approximately 6.5, which corresponds to a volume reduction of about 25%. The maximum potential net savings would be 7.8% of the annual three-batch refueling requirements of the reactor.

The uranium material costs for the standard Mark B fuel rod and for the reduced-diameter fuel rods were also compared to determine the reduction in fuel volume for which the total dollar savings is potentially the greatest. The dollar savings in yellowcake, gas conversion, and separative work units were summed to obtain the total potential dollar savings. The total potential dollar savings are given as a function of H/U ratio in Figure 5-4. The separative work unit dollar savings was based on a cost of \$88.65 per SWU. The yellowcake dollar savings was based on a cost of \$43.00 per pound of U_3O_8 , and the cost of converting U_3O_8 to UF_6 gas was priced at \$4.50 per kilogram of uranium.

The maximum total potential dollar savings i.e., the sum of the yellowcake, conversion, and separative work unit dollar savings, occurred at an H/U ratio of about 5.3, corresponding to a fuel volume reduction of around 15%. The maximum total potential dollar savings was approximately 6% relative to the standard Mark B assembly uranium material cost.

The fuel rod volume reduction at which optimum uranium and fuel cost savings occur is expected to decrease as burnup and enrichment increase because of the lower conversion efficiency for smaller rods and because of the additional yellowcake requirements for higher enrichments. However, on the basis of the study described above, the use of a reduced-diameter rod appears promising.

5.2.2.3. Recommendations

In addition to the evaluation of the effects of fuel volume reductions at higher burnups and enrichments, the following areas need to be addressed for reduced-diameter fuel rods.

Initial studies have shown that the moderator temperature coefficient is more positive for reduced-diameter fuel rods than for standard Mark B fuel rods. Although the moderator temperature coefficient can probably be controlled with lumped burnable poison, quantification of the moderator temperature coefficient limitation associated with fuel rod volume reduction is needed for evaluation of reduced-diameter fuel rods in fuel cycle designs that do not use lumped burnable poison and to assess the increase in poison requirements for LBP schemes. A more positive moderator temperature coefficient at EOC, especially in 18-month cycles, could be a beneficial effect because of constraints on the allowable negative moderator coefficient. Reduced-diameter fuel rods must be irradiated to higher burnups than standard Mark B fuel rods to yield the same total energy production. Since fission gas release increases as a function of burnup and EOL fuel rod internal pressure is a major concern at high burnup, evaluations of the mechanical and thermal characteristics of the reduced-diameter fuel rods are needed to compare their benefits at the same total energy production to standard Mark B rods. In addition, many of the hydraulic parameters for the fuel rod and fuel assembly would differ from standard Mark B values.

In summary, the use of reduced-diameter rods appears to offer substantial uranium and cost savings, and further work might be merited.

5.2.3. Fuel Density Reductions

An evaluation has also been made of the uranium resource and dollar savings available from a reduction in fuel density by dilution with a zirconium oxide (ZrO_2) filler. Although a savings of approximately 2% of the annual yellowcake requirements was found, the increase in enrichment needed to maintain equal energy production capability would result in an economic penalty.

5.2.3.1. Method of Analysis

The B&W neutron spectrum and fuel depletion computer program NULIF was used to study the effects of a reduced fuel density.³ The methods used were the same as those described in the reduced-diameter fuel rod study in section 5.2.2.1.

The fuel rod dimensions were those of the standard design, but the fuel volume was diluted with zirconium oxide to obtain the desired reduction in fuel density.

5.2.3.2. Results

As the amount of fuel in the rod was reduced, an increase in fuel enrichment was required to maintain the same energy production capability. However, for the UO_2-ZrO_2 fuel rods, the increase in enrichment required for equivalent energy production capability was much larger than for reduced-diameter fuel rods. For equivalent energy production, the enrichment and separative work units for the UO_2-ZrO_2 fuel rods were always greater than for the standard Mark B fuel rod. Figure 5-5 shows the relationship between the UO_2-ZrO_2 fuel rod enrichment and the standard Mark B enrichment as a function of H/U ratio for both equal energy production capability and equal separative work units. Figure 5-6 displays the increased separative work unit requirements for the UO_2-ZrO_2 fuel rod for equivalent energy production capability as a function of H/U ratio.

Figure 5.2-7 illustrates the savings in yellowcake for a given fuel density reduction as a function of H/U ratio. The dashed line on Figure 5-7 shows the net yellowcake savings for a given H/U ratio of the UO_2-ZrO_2 fuel rods. The net yellowcake savings for the UO_2-ZrO_2 fuel rods is the yellowcake savings from the fuel density reduction minus the amount of yellowcake required for the increased enrichment to obtain equivalent energy production capability. The net yellowcake savings for the UO_2-ZrO_2 fuel rod was much lower than that for the reduced-diameter fuel rod at the same H/U ratio.

Next, the uranium material cost in dollars per assembly for the standard Mark B fuel rod and for the UO_2 - ZrO_2 fuel rod were compared to determine the total dollar savings or penalty as a function of fuel density reduction. The dollar savings penalties for yellowcake, gas conversion, and separative work units were summed to obtain the total potential dollar savings or penalty. The total potential dollar penalty is shown as a function of H/U ratio in Figure 5-8. The separative work unit dollar costs were based on a price of \$88.65 per SWU. The yellowcake dollar savings was based on a cost of \$43.00 per pound of U_3O_8 , and the cost of converting U_3O_8 to UF_6 gas was priced at \$4.50 per kilogram of uranium.

There was a net total dollar penalty for the UO_2 - ZrO_2 fuel rod relative to the standard Mark B fuel rod for all the fuel density reductions investigated. Thus, a small savings in yellowcake — potentially about 2% of the annual yellowcake requirement — could be obtained from fuel density reductions, but fuel costs would be increased.

The difference in benefits between the reduced-diameter fuel rod concept and the reduced uranium density concept was somewhat unexpected. Conceptually each design relied on an increased H/U ratio to effect an improvement in uranium utilization. However, the results from the analysis showed a large utilization improvement by increasing the H/U ratio for the reduced-diameter fuel rod design but only a minimal utilization improvement by increasing the H/U ratio for the design with reduced uranium density.

In evaluating the causes of the differences, the reasons became apparent. The economic advantage of the reduced-diameter design was much greater than that for the reduced-density design because at the same value of H/U the reduced-density design had twice the change in fuel loading of the reduced diameter design. Thus, the enrichment requirement change for the reduced-density design was at least twice that of the reduced-diameter design. While the increased enrichment requirement may be linear, the increased enrichment costs are exponential. Clearly then, the reduced-diameter design should offer a much greater economic benefit than the reduced-density design.

The greater uranium utilization benefit of the reduced-diameter design must be a direct consequence of the physics results. The physics implications are that the reduced-diameter design must be more efficient neutronically. Consequently, if we analyzed both new designs at the same enrichment, the reduced-diameter

design should have a higher multiplication rate as a function of H/U than the reduced-density design. Figure 5-9 demonstrates that, indeed, the core average value of κ_{∞} for the reduced-diameter design does show a much greater reactivity benefit than the reduced-density design. Thus, the greater uranium utilization benefit of the reduced-diameter design is readily understandable.

Therefore, while it was expected conceptually that both designs would show significant uranium utilization improvements with an increased H/U, the larger water region in the reduced-diameter fuel rod case significantly increased the number of neutrons slowing down to thermal energies, resulting in a substantial benefit relative to the reduced uranium density design.

Table 5-1. Uranium Utilization - 177-FA Plant,
15 x 15 Rod Assemblies

Feed batch size	Core power, MWt	Equil. cycle length, EFPD	Equil. discharge burnup, MWd/mtu	Actual ^(a) U utilization, MWY/STU ₃₀₈	Change in uranium utilization, %
59 ^(b)	2568 R	292	27,413	11.73	0.0
80	2772 FB	460	34,382	11.24	-4.2
68	2772 FB	460	40,448	12.13	+3.4
60	2772 FB	460	45,838	12.54	+6.9
60	2568 R	497	45,838	12.52	+6.7
36	2772 FB	292	48,500	13.76	+17.3

(a) Verified by completed PDQ analysis of four fuel cycles.

(b) Base case.

Table 5-2. Margin to Maximum Allowed Pin Power Peak (%)

Feed batch size	Core power, MWt	Cycle margin, %					
		1	2	3	4	5	6
59 ^(a)	2568 R	--	--	--	5.0		--
80	2772 FB	15.5	15.5	11.7	8.4	--	--
68	2772 FB	7.0	6.3	3.3	4.9	--	--
60	2772 FB	5.2	6.2	8.5	4.5	--	--
60	2568 R	0.8	0.4	4.4	4.5	--	--
36	2772 FB	5.6	8.7	8.1	9.5	9.3	9.7

(a) Base case.

Table 5-3. Discharge Burnups

<u>Feed batch size</u>	<u>Core power, MWt</u>	<u>Burnup, MWd/mtU</u>		<u>Ratio maximum to avg.</u>
		<u>Batch</u>	<u>Maximum assembly</u>	
59 ^(a)	2568 R	27,413	30,700	1.12
80	2772 FB	34,770	39,552	1.14
68	2772 FB	40,806	49,967	1.22
60	2772 FB	45,891	54,506	1.19
60	2568 R	45,673	55,713	1.22
36	2772 FB	49,376	51,553	1.04

(a) Base case.

Table 5-4. Shutdown Margin

<u>Feed batch size</u>	<u>Core power, MWt</u>	<u>Transition cycle</u>		<u>Equilibrium cycle</u>	
		<u>BOC</u>	<u>EOC</u>	<u>BOC</u>	<u>EOC</u>
59 ^(a)	2568 R	--	--	2.87	1.45
80	2772 FB	3.02	2.10	3.27	1.91
68	2772 FB	3.43	1.94	3.13	1.70
60	2772 FB	3.48	1.59	3.55	2.20
60	2568 R	2.67	1.80	2.49	1.51
36	2772 FB	1.90	1.26	1.83	1.28

(a) Base case.

Table 5-5. Standard Mark B Fuel Parameters

Total number of FAs in core	177
Number of fuel rods per FA	208
Number of control rod guide tubes per assembly	16
Number of instrumentation tubes per assembly	1
Fuel rod outside diameter, in.	0.430
Cladding thickness, in.	0.0265
Pellet diameter, in.	0.3695
Fuel rod pitch, in.	0.568
Fuel assembly pitch, in.	8.587
Cladding material	Zircaloy-4

Figure 5-1. Reduced Diameter Fuel Rod Enrichment Vs Hydrogen to Uranium Atom Ratio

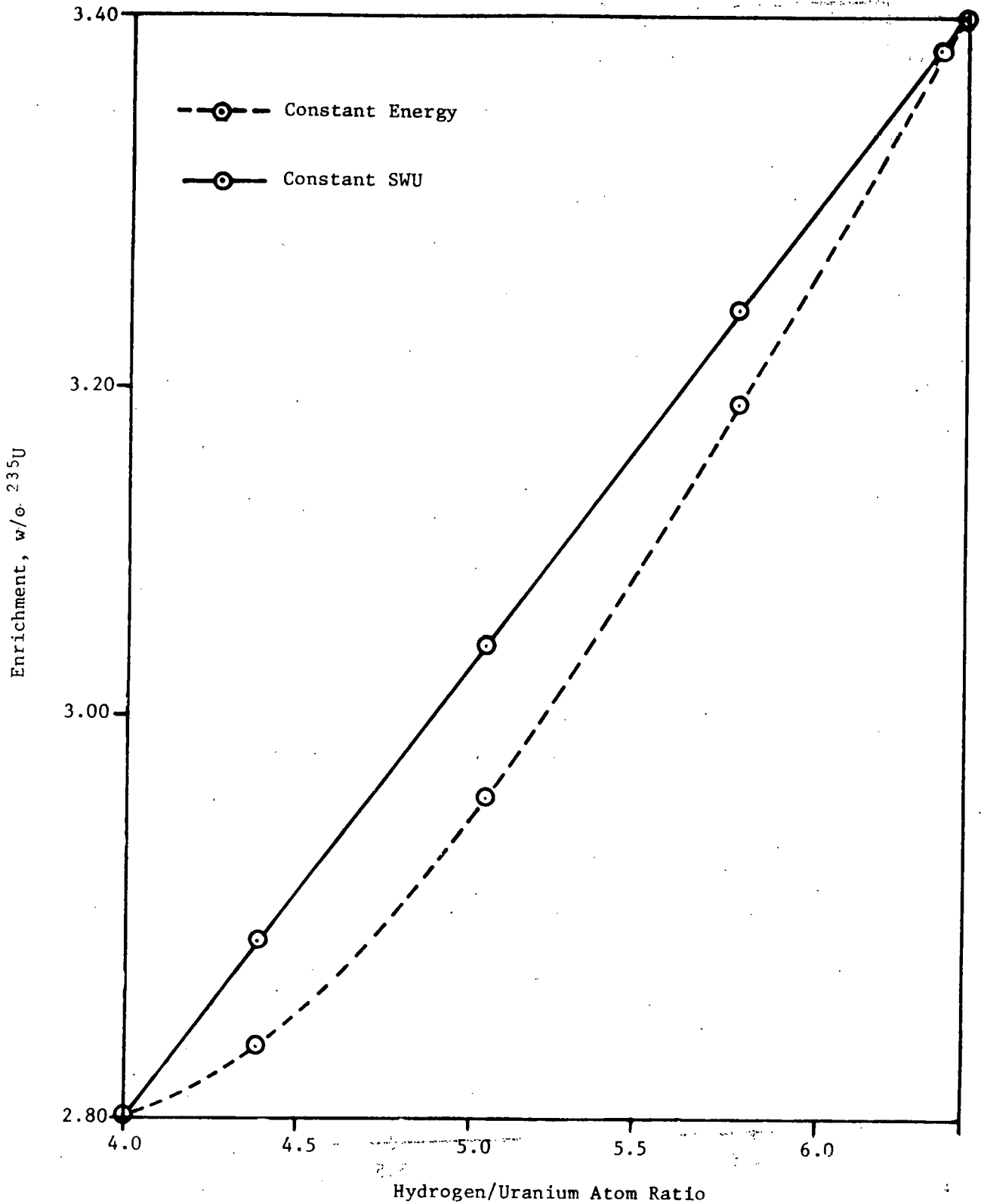


Figure 5-2. Reduced Diameter Fuel Rod Separative Work Unit Savings Vs Hydrogen to Uranium Atom Ratio

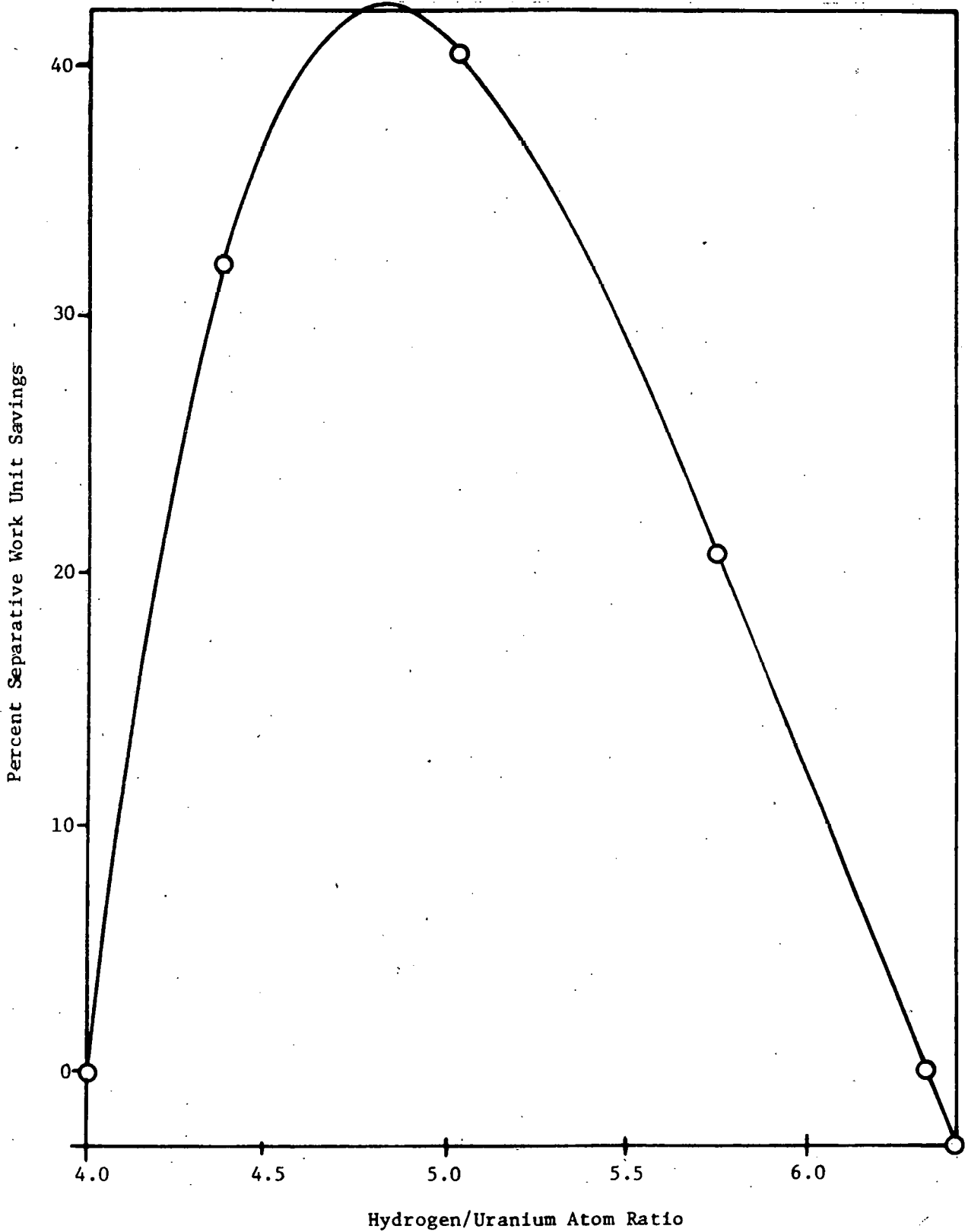


Figure 5-3. Reduced-Diameter Fuel Rod Yellowcake Savings Vs Hydrogen to Uranium Atom Ratio

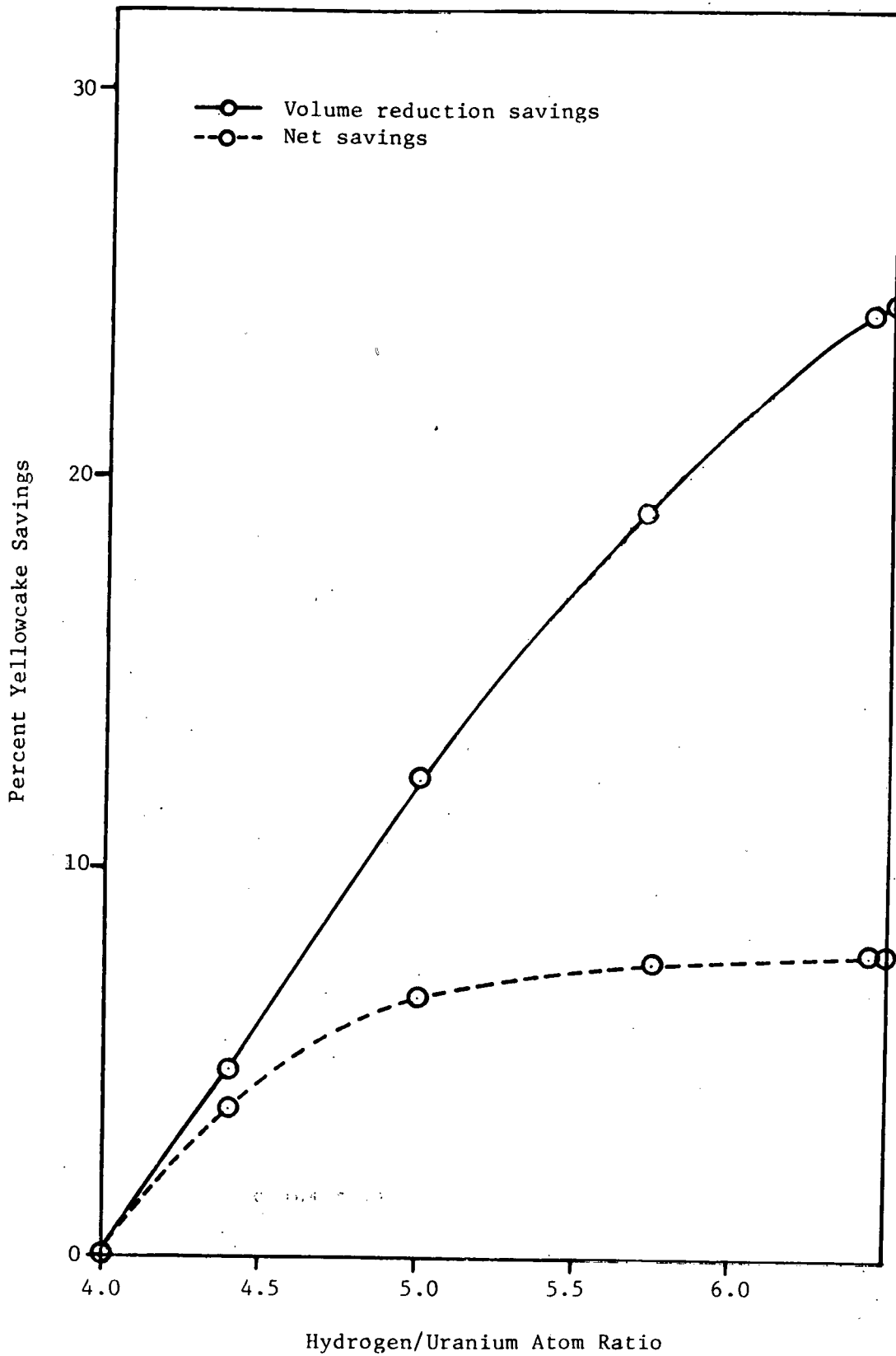


Figure 5-4. Reduced-Diameter Fuel Rod Potential Dollar Savings Vs Hydrogen to Uranium Atom Ratio

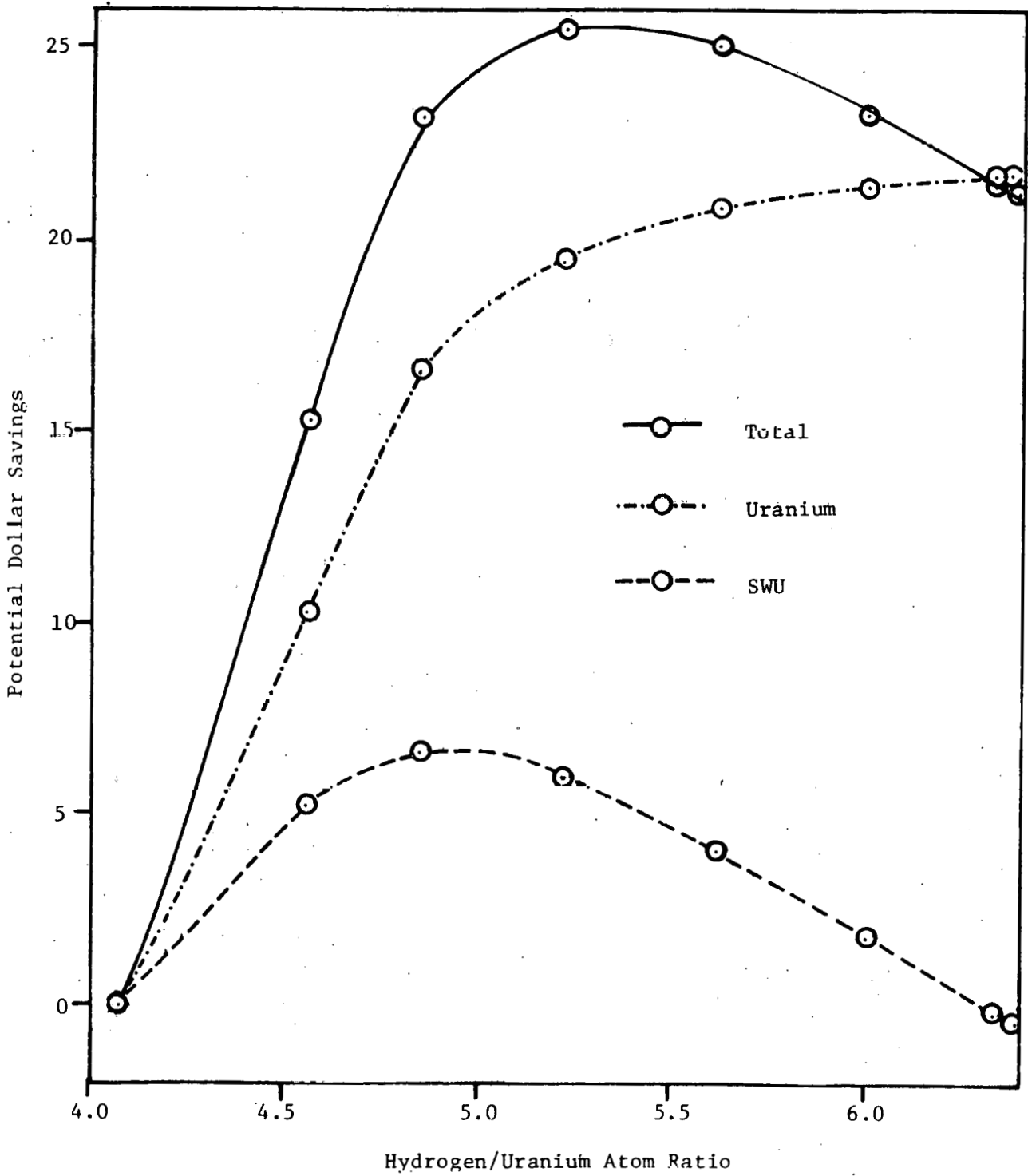


Figure 5-5. UO_2-ZrO_2 Fuel Rod Enrichment Vs Hydrogen to Uranium Atom Ratio

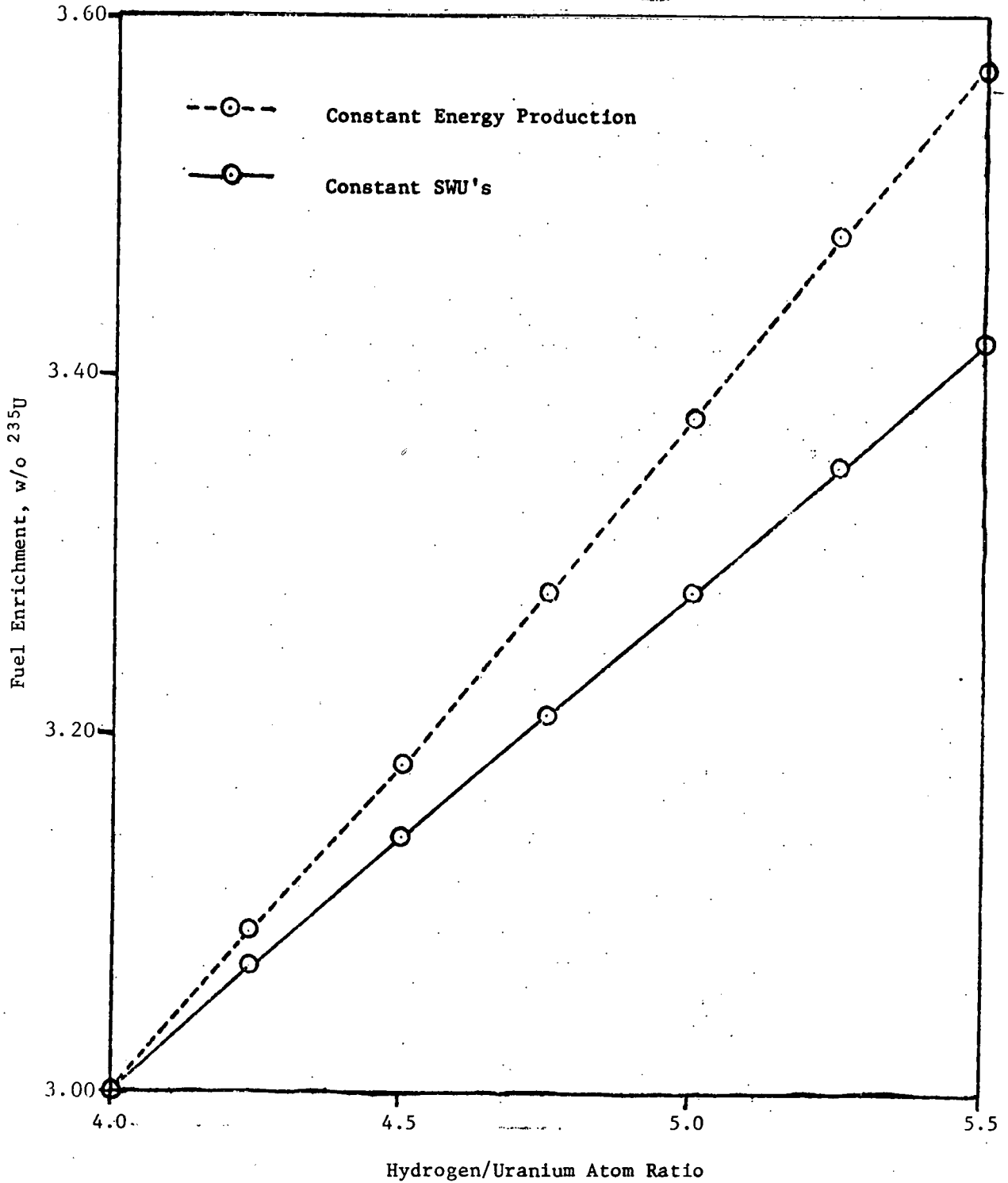


Figure 5-6. $\text{UO}_2\text{-ZrO}_2$ Fuel Rod Separative Work Unit Penalty Vs Hydrogen to Uranium Atom Ratio

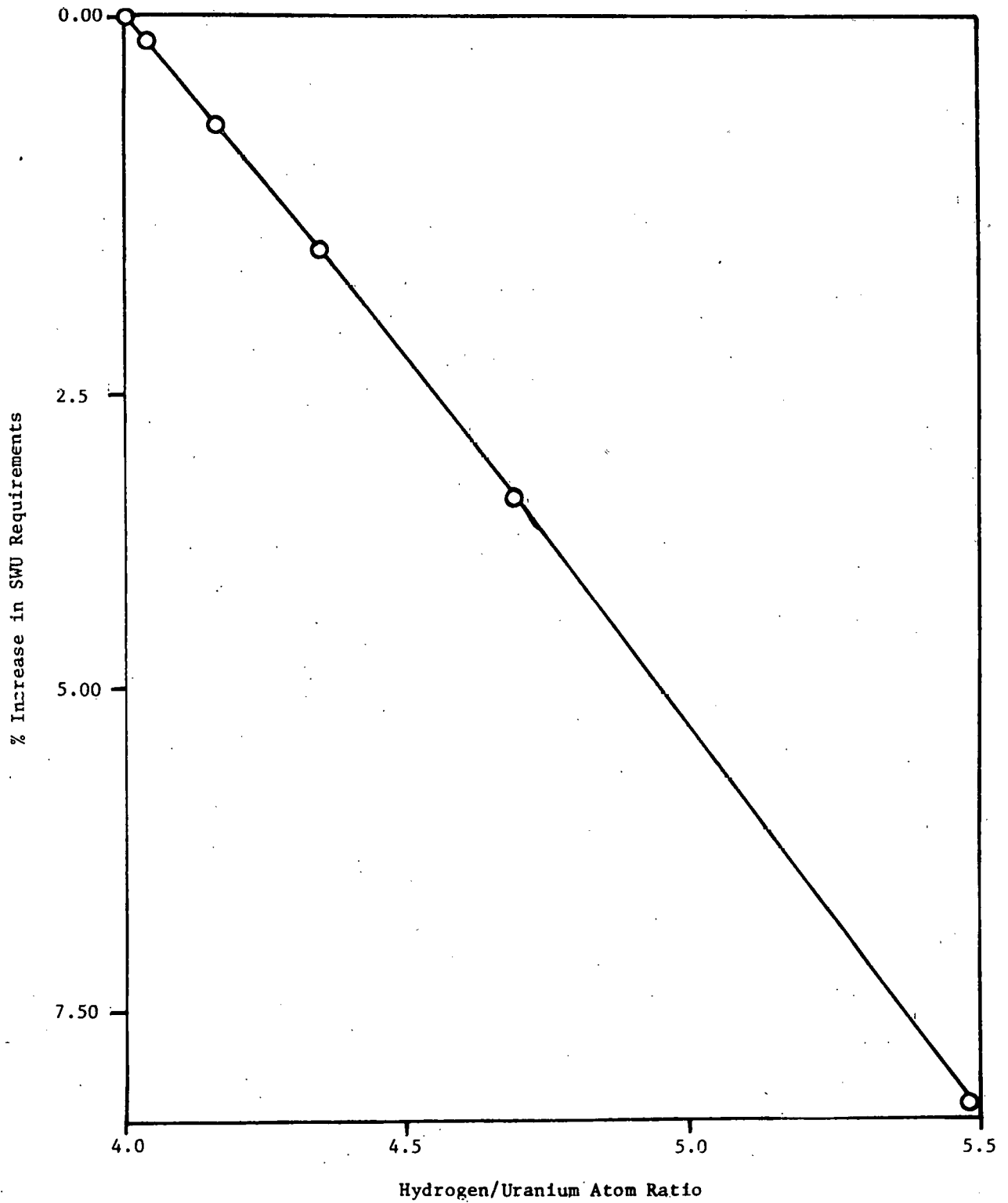


Figure 5-7. UO_2 - ZrO_2 Fuel Rod Yellowcake Savings Vs Hydrogen to Uranium Atom Ratio

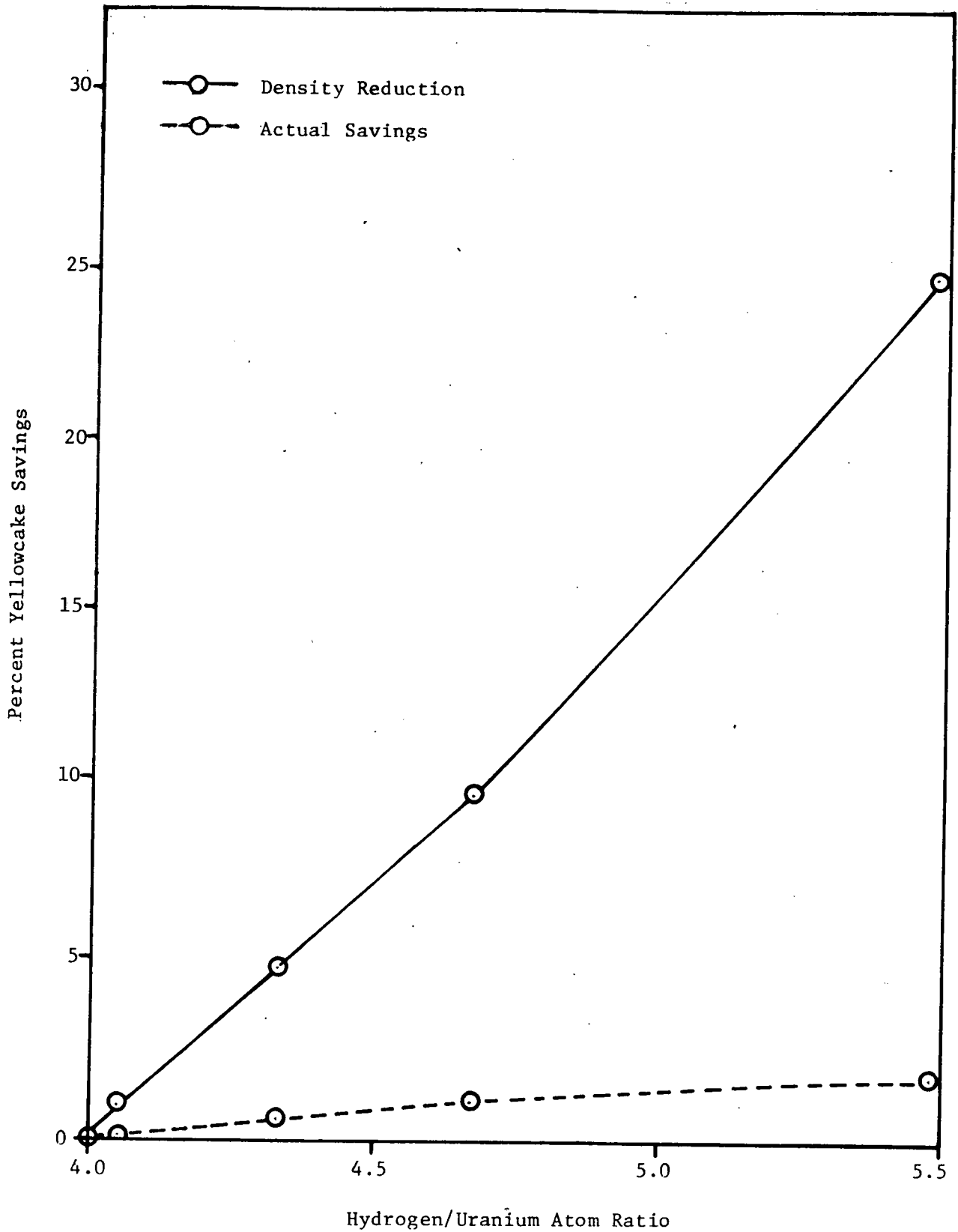


Figure 5-8. $\text{UO}_2\text{-ZrO}_2$ Fuel Rod Economics Vs Hydrogen to Uranium Atom Ratio

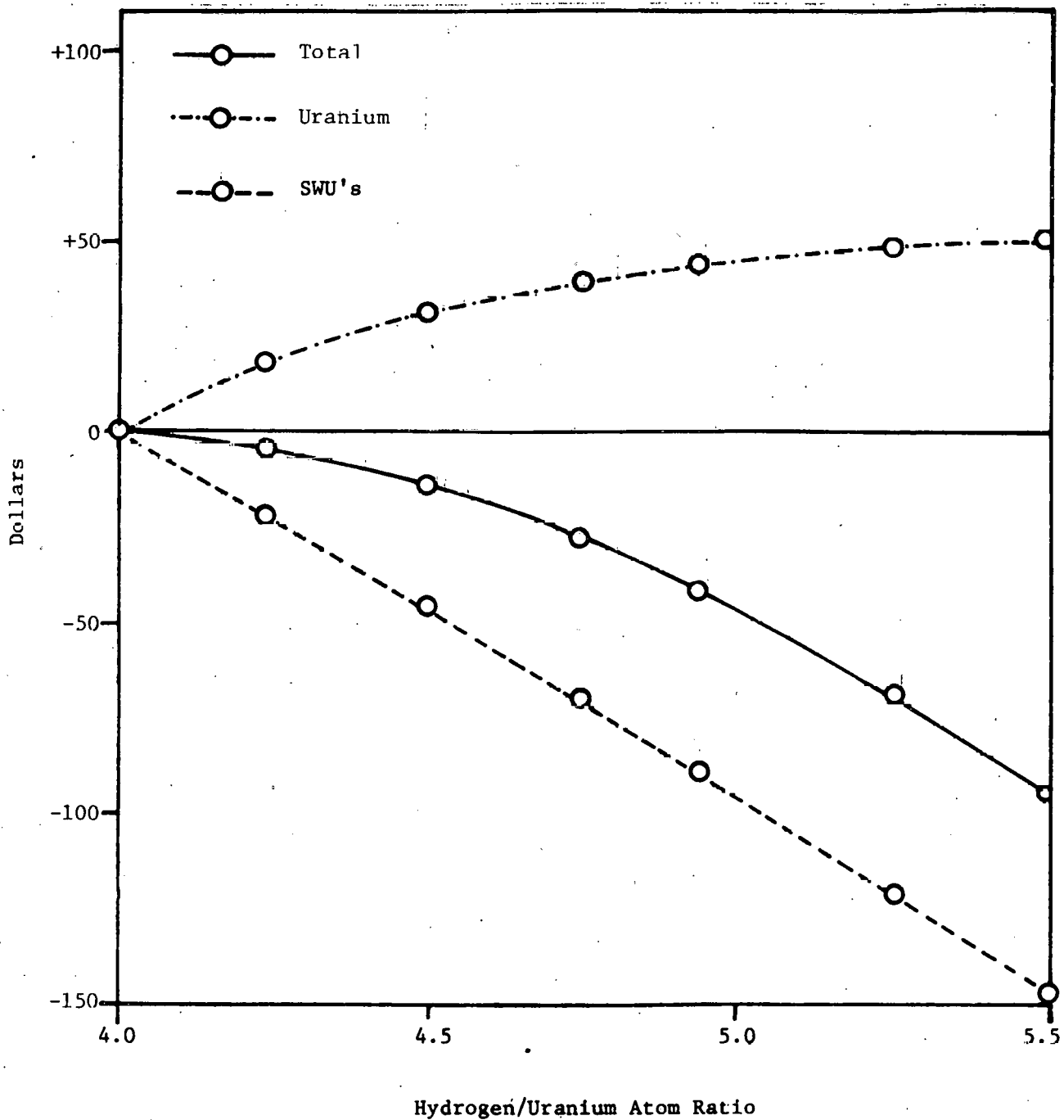
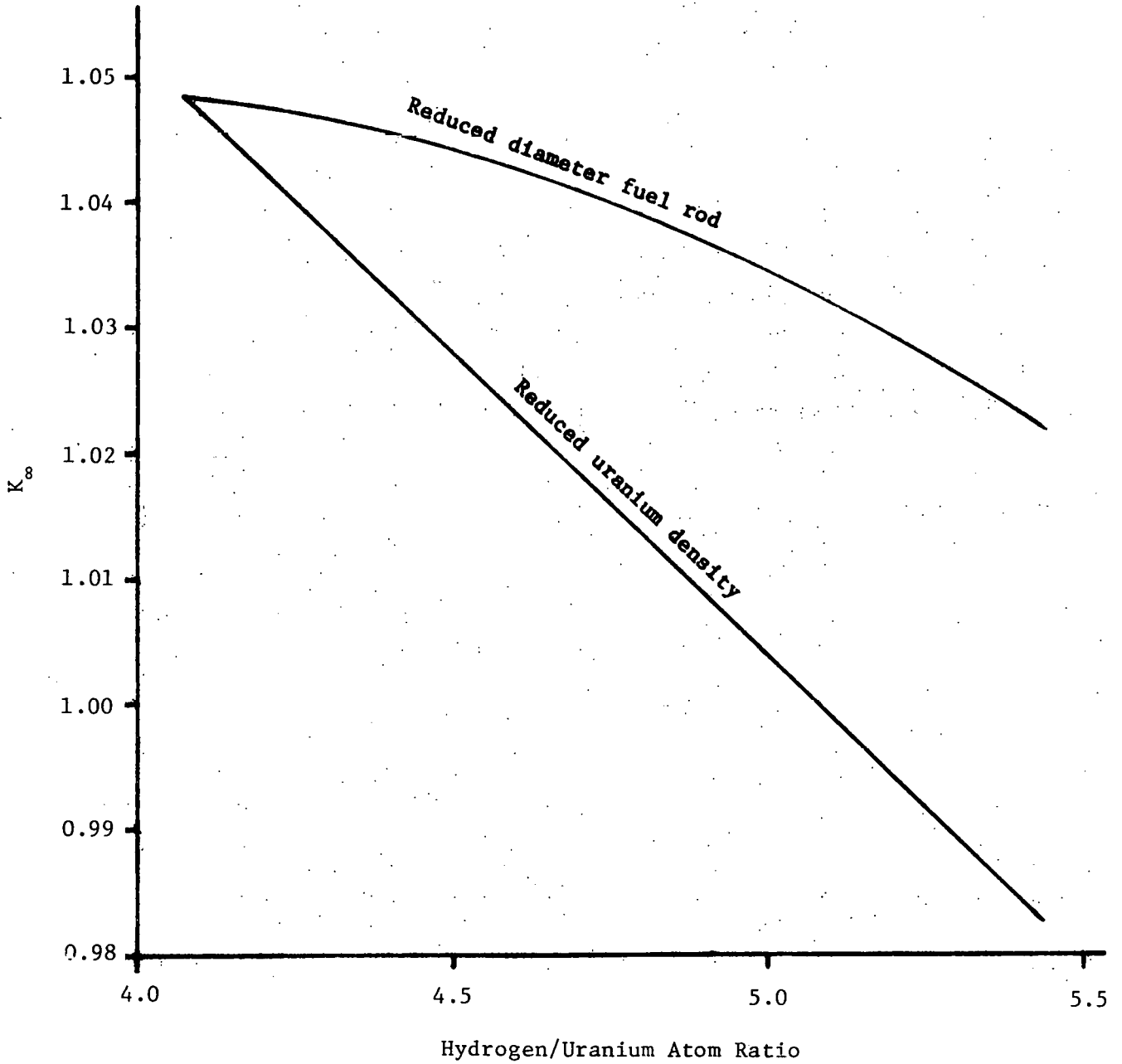


Figure 5-9. Cycle Average K_{∞} for Constant Fuel Enrichment Vs Hydrogen to Uranium Atom Ratio



6. PROGRESS TO DATE — TASK 2, "PARAMETRIC STUDIES"

6.1. Introduction

To realize the economic and fuel utilization benefits of extended burnup, fuel rods must be capable of operating to extended burnups in a safe and reliable manner. Fuel rods have typically been designed for operation up to 40,000 to 45,000 MWd/mtU. Extended burnup will require fuel rods capable of burnups of up to 60,000 MWd/mtU. Therefore, fuel rod designs with extended burnup capability must be developed and evaluated.

Parametric studies were conducted to investigate how changes in key fuel rod parameters affect fuel rod performance at extended burnup. These studies, plus benchmark irradiation data from post-irradiation examination of current design Mark B fuel assemblies, will be used to develop specifications for a fuel assembly with extended-burnup capability.

The extended-burnup fuel assembly design will be compatible with existing cores. Such core interfaces as reactor internals, adjacent assemblies, incore instrumentation, and control components dictate the fuel assembly outside envelope and the lattice spacing. Therefore, the design effort is focused on fuel rod parameters, and on strengthening the basic structure of the assembly when needed. The characteristics of the current Mark B (15×15) assembly, which serve as the reference design for the parametric studies, are given in Table 6-1.

The first extended-burnup design is to be used for four lead-test fuel assemblies planned for insertion in cycle 5 of the Arkansas Nuclear One, Unit 1 (ANO-1) reactor. It is expected that cycle 5 will commence in late 1980. Post-irradiation data at 40,000 MWd/mtU will not be available until 1980 under a companion project entitled, "Qualification of the B&W Mark B Fuel Assembly for High Burnup," which B&W is conducting with Duke Power Company and the Department of Energy.⁴ Thus, a conservative approach will be used in the design evaluations for the initial lead-test assemblies.

The manufacture and irradiation of the lead-test assemblies will be addressed in Phase II of this program.

6.2. Subtask 2A - Fuel Rod Analyses

6.2.1. Introduction

The objective of the fuel rod analyses was to provide guidance in selecting changes in fuel rod design that will have a beneficial effect on fuel performance and to quantify the relationship between a design change and its effect on performance. During this report period, studies were performed in three areas: a power history sensitivity study, a fuel temperature and rod internal pressure study, and a fuel rod cladding ovality study. The details of these studies are discussed below.

6.2.2. Power History Sensitivity Study

A primary concern in PWR fuel rod design is the buildup of pressure in the rod due to the release of the noble gases xenon and krypton from the fuel pellet. Fuel rod power histories have a large effect on fuel rod internal pressure because both the amount and rate of gas release from the fuel are dependent on power level and burnup. Using the standard Mark B fuel rod as a base, the effects of various power histories on end-of-life fuel rod internal pressure were evaluated.

The analyses were performed using TACO2⁵, a fuel rod thermal analysis code that includes the effects of cladding creep, fuel densification, fuel relocation, and fission gas release. The conservatism of TACO2 for design application has been demonstrated with both thermal and fission gas release benchmark data. The USNRC is reviewing TACO2 for approval of its use in licensing submittals.

Three fuel rod power histories were analyzed. The histories are shown in Figures 6-1, 6-2, and 6-3. Figure 6-1 is based on fuel cycle data from Mark B cores involving fuel rod burnups of up to ~38,000 MWd/mtU. The power and burnup of individual rods are tracked and plotted through several cycles. A design envelope that encompasses all the histories is then drawn; the trend of this envelope was extended from 38,000 to 60,500 MWd/mtU to assess fuel rod internal pressure at extended burnup. An end-of-life (EOL) fuel rod internal pressure of 2300 psia resulted.

For the second power history, Figure 6-2, the shape of the envelope was adjusted proportionally to 60,500 MWd/mtU. An EOL fuel rod internal pressure of 2500 psia resulted.

In the third power history, individual rod power histories from 18-month fuel cycles were enveloped and extended to 60,500 MWd/mtU. An EOL fuel rod internal pressure of 2400 psia was calculated. Relative to the design criterion that EOL fuel rod internal pressure must be less than system pressure (2200 psia), the results from these studies were encouraging. The calculated EOL fuel rod internal pressures were only modestly greater than the system pressure and can be accommodated by design changes, such as an increase in plenum volume. The study also showed the sensitivity of EOL fuel rod internal pressure to fuel rod power history.

6.2.3. Fuel Temperature and Rod Internal Pressure Study

Using the current Mark B fuel rod described in Table 6-1 as a base case, the fuel rod parameters given in Table 6-2 were individually varied from their nominal values to determine the effect on EOL fuel rod internal pressure and temperature. The TACO2 fuel rod model in conjunction with the fuel rod power history shown in Figure 6-2 was used for these analyses. As indicated in Table 6-2, many fuel rod parameters were studied; however, only the parameters given in Table 6-3 significantly affected fuel rod internal pressure and temperature.

The calculated dependence of EOL (60,500 MWd/mtU) fuel rod internal pressure on degree of fuel densification, initial fuel rod fill pressure, initial fuel pellet outside diameter, and fuel rod plenum volume (the parameters that had significant effects) are illustrated in Figures 6-4 through 6-7, respectively. The results from these calculations can be summarized as follows:

1. EOL fuel rod internal pressures increased as initial fill gas pressure was increased. Over the 400 to 500 psia range for initial fill gas pressure, the EOL fuel rod internal pressure increased by approximately 4 psia for each psia increase in initial fill gas pressure.
2. As the initial fuel pellet outside diameter was increased, thereby decreasing the pellet-to-cladding gap, EOL fuel rod internal pressure decreased due to lower fuel temperatures.
3. Significant decreases in EOL fuel rod internal pressure can be achieved by increasing the fuel rod plenum volume. The minimum pressure experienced

by the fuel rod was not as sensitive to plenum volume changes as was EOL internal pressure, indicating that plenum volume could be increased without prohibitively affecting the creep collapse resistance of the fuel rod.

4. Increased incore densification of the fuel caused a decrease in end of life fuel rod pressure.

The calculated variations in maximum fuel temperature versus burnup are shown in Figures 6-8, 6-9, and 6-10, respectively, as a function of initial fuel pellet outside diameter, fuel initial density, and degree of incore fuel densification. The following conclusions can be drawn from these curves:

1. Fuel temperature decreased as initial fuel pellet outside diameter was increased due to the reduced pellet-to-cladding gap.
2. Higher-initial density fuel resulted in lower fuel temperatures because of increased thermal conductivity.
3. An increase in incore fuel densification caused higher fuel temperatures because of the larger pellet-to-cladding gap. The changes yielding lower fuel temperatures (higher initial fuel density and reduced pellet-to-cladding gap) would provide greater margin to centerline fuel melt limits and improve fuel performance through reduced fission product release. Reduced fission product release will result in lower EOL fuel rod internal pressures and possibly less susceptibility to stress corrosion cracking (SCC). All these effects will have a positive impact on operating limits and overall fuel performance.

6.2.4. Fuel Rod Cladding Ovality Study

As in the fuel temperature and rod internal pressure analyses, individual fuel rod parameters were varied from their nominal values to evaluate the effects of such changes on fuel rod cladding ovality. The CROV computer code was used to perform the ovality studies.⁶ CROV calculates ovality changes in fuel rod cladding due to thermally induced and irradiation-induced creep.

The parameters that significantly affected ovality were cladding wall thickness, fuel rod plenum volume, fuel rod initial fill gas pressure, and degree of incore fuel densification. The predicted behavior of cladding ovality as a function of these parameters is shown in Figures 6-11 through 6-14, respectively. An examination of these curves supports the following conclusions:

1. Thicker cladding can be used to counteract ovality.
2. An increase in fuel rod plenum volume or a decrease in initial fill gas pressure increased cladding ovality.
3. Ovality increased as the degree of incore fuel densification increased.

6.2.5. Preliminary Extended Burnup Fuel Rod Design

Based on the results from the parametric studies, it was judged that an increase in plenum volume was a necessary change and that an increase in cladding thickness would allow a decrease in fuel rod initial fill gas pressure while maintaining satisfactory creep collapse resistance. Thus, the preliminary designs described in Table 6-4 were developed as test cases for determining the effects of combining several changes.

The increase in plenum volume was obtained by reducing the fuel column length and extending the fuel rod length. Thermal and creep collapse analyses were then performed for the range of cladding outside diameters, inside diameters, and wall thicknesses given in Table 6-4.

The fuel temperatures from the analyses were acceptable. The fuel rod internal pressures indicated that EOL fuel rod internal pressure can be maintained within acceptable limits by proper selection of initial fill gas pressure and judicious fuel management.

Using these temperatures and pressures, a creep collapse analysis was performed for each case. A typical EOL creep ovality curve is shown in Figure 6-15. The strong interrelationship between fuel rod parameters (cladding wall thickness/fuel rod prepressure and EOL creep ovality) is shown by the curves on Figure 6-16. By proper selection of cladding wall thickness and fuel rod initial fill gas pressure, acceptable creep collapse resistance can be obtained.

The preliminary fuel rod design given in Table 6-5 was selected for the lead-test assemblies based on the results above. The features of this design relative to the standard Mark B design are (1) thicker cladding accommodated by a change in cladding inside diameter and fuel pellet outside diameter, (2) increased fuel theoretical density, and (3) decreased fuel stack height and increased rod length to give a larger plenum volume. Figures 6-15 and 6-17 illustrate the enhanced EOL creep resistance and lower EOL internal rod pressure, respectively, for this design relative to the standard Mark B. The design goal of a 60,500 MWd/mtU capability fuel rod is met by this preliminary

design. This design is also compatible with manufacturing and scheduling constraints for ANO-1 cycle 5, which dictate no major modifications to the fuel assembly structural cage.

6.3. Subtask 2B - Basic Structural Component Design

6.3.1. Introduction

The objective of this subtask is to design a fuel assembly incorporating the high-burnup fuel rod design described in subtask 2A to obtain a fuel assembly capable of 50,000 MWd/m²U burnup. The design effort was divided into two parts: (1) reduction and evaluation of fuel assembly operating performance data to identify areas in which changes are required to extend the burnup capability of the fuel assembly and (2) accommodation of the fuel rod design changes from subtask 2A. As discussed in section 6.2 of this report, the extended-burnup fuel rod design development is currently in progress. Thus, efforts to date have been focused on identifying fuel assembly burnup limits.

The B&W Mark B fuel assembly is shown in Figure 6-18. The assembly can be considered in two parts - the fuel rods and the structural cage. The structural cage comprises two end fittings connected by guide tubes. Along the guide tubes are the spacer grids, which hold the fuel rods in a coolable array. The two end grids are attached to the end fittings by skirts. The upper end fitting contains a helical holddown spring to prevent fuel assembly lift due to coolant flow.

When consideration is given to exposing the fuel assembly to higher burnups, the critical factors are neutron fluence and residence time. These factors cause three different effects on the assembly: material property changes, geometry changes, and fatigue.

6.3.2. Material Property Changes

The generalized effects of irradiation on the structural metals are to increase strength and decrease ductility. For conservatism, stress analyses for the structural cage design use the BOL (beginning of life) strengths. For components that may experience plastic strain after significant irradiation, the strain is limited by the design to low values to ensure a conservative margin allowing for ductility loss.

Stress relaxation due to irradiation and to the temperature in the material under constant stress is a concern for the helical holddown spring. Stress relaxation will cause a loss of free height of the spring after irradiation. Thus, this effect can result in loss of the holddown force required to prevent fuel assembly lift. As a counter-effect, fuel assembly growth causes greater spring compression, which increases holddown force. The net effect is almost no change in holddown force ($\sim 1\%$) at the operating condition. This conclusion is based on analysis of the PIE (post-irradiation examination) data obtained on the high-burnup lead assemblies at the 30,000 MWd/mtU point and PIE data from other B&W programs and is demonstrated by the holddown force data presented in Figure 6-19.

6.3.3. Geometry Changes

Growth of Zircaloy under irradiation causes dimensional changes in the fuel assemblies, including increases in the length of the fuel rods and guide tubes. The allowable length changes impose limits on the fluence (burnups) to which the fuel assembly can be exposed. The design interface between the reactor vessel internals and the fuel assemblies includes a gap between the upper end of the fuel assembly and the upper grid plate of the internals. The gap is necessary to accommodate differential thermal expansion and fuel assembly growth. Because the fuel assemblies expand less than the internals as the temperature increases, the gap is smallest at the cold shutdown condition.

Figure 6-20 shows the mean growth curve for fuel assembly (guide tube) growth based on a linear least-squares fit of post-irradiation growth data from Mark B fuel assemblies with burnups ranging from 0 to 31,000 MWd/mtU. A statistical analysis considering the variability in as-built fuel assembly dimensions and the variance of the growth data showed that the allowable probability of gap closure occurred at a fast fluence of 7.3×10^{21} neutron/cm² ($E > 1$ MeV), which corresponds to a fuel assembly average burnup of 43,000 MWd/mtU. This burnup limitation is conservative but does establish a bounding limit on fast fluence and consequently on fuel assembly average burnup. Since the target burnup for the lead-test assemblies is 50,000 MWd/mtU, design changes to accommodate fuel assembly growth will be pursued.

Collection of growth data at the 40,000 MWd/mtU level is planned in late 1979. These data will allow better definition of the burnup limit arising from growth considerations.

The fuel rods also grow due to irradiation as shown in Figure 6-21. This curve is based on PIE data for burnups up to 31,000 MWd/mtU. The distance between the upper and lower end fittings is greater than the fuel rod length, which provides a gap to accommodate fuel rod growth. The rate at which this gap is closed is reduced because the guide tube growth increases the gap. The result is that the fuel assembly burnup at which there would be a 0.5% probability of gap closure is beyond 50,000 MWd/mtU fuel assembly average burnup.

6.3.4. Fatigue

The increased assembly residence time will result in more fatigue cycles. For the purpose of determining the number of fatigue cycles resulting from flow-induced vibration, residence time is defined as the time in core with two or more primary coolant pumps running. Analyses also include low cycle events, such as heatup and cooldown and head removal. However, fatigue is not expected to be a limiting factor on burnup due to large initial design margins for fatigue.

6.3.5. Preliminary Conclusions

Based on the PIE data available up to the 30,000 MWd/mtU burnup level, it appears that fuel assembly (guide tube) growth will be the primary constraint that will limit the standard Mark B fuel assembly burnup. The collection of additional high-burnup PIE data planned under this program is expected to better define growth limits.

Table 6-1. Standard Mark B Fuel Parameters

Total number of FAs in core	177
Number of fuel rods per FA	208
Number of control rod guide tubes per assembly	16
Number of instrumentation tubes per assembly	1
Fuel rod outside diameter, in.	0.430
Cladding thickness, in.	0.0265
Pellet diameter, in.	0.3695
Fuel rod pitch, in.	0.568
Fuel assembly pitch, in.	8.587
Cladding material	Zircaloy-4

Table 6-2. Fuel Temperature/Rod Internal
Pressure Study

Fuel

Outer diameter
Density
Surface roughness
Volume fraction-dished ends
Radius of pellet dish
Fuel enrichment
Power factor
Densification

Cladding

Inner diameter
Outer diameter
ID surface roughness
Length
Plenum volume

Rod

Fuel column length
System pressure
Pin backfill pressure
Sorbed gas
Swelling rate
Gas release model

Table 6-3. Parametric Temperature/Pressure Analysis

Fuel pellet density, % TD	93-96
Fuel pellet OD, in.	0.3685-0.3700
Fuel pellet densification, % TD	1-4
Fuel rod plenum volume, in. ³	0.959-1.801
Fuel rod prepressure, psia	400-520

Table 6-4. Fuel Rod Design Parameters

<u>Parameter</u>	<u>Mark-B nominal</u>	<u>Case 1</u>	<u>Case 2</u>	<u>Case 3</u>
Clad OD, in.	0.4300	0.4300-0.4320	0.4280-0.4320	0.4300
Clad ID, in.	0.3770	0.3710-0.3730	0.3710-0.3730	0.3730-0.3750
Clad thickness, in.	0.0265	0.0285-0.0305	0.0275-0.0305	0.0275-0.0295
Clad length, in.	153.13	153.63	153.63	153.63
Pellet OD, in.	0.3695	0.3635	0.3635	0.3635
Pellet density, % TD	94	95	95	95
Pellet column Length, in.	142.25	138.60	138.60	138.60
Rod plenum vol, in. ³	0.959	1.445	1.445	1.445

Table 6-5. Preliminary Fuel Rod Design

<u>Parameter</u>	<u>Initial design</u>	<u>Change from standard Mark-B design</u>
Clad OD, in.	0.4300	None
Clad ID, in.	0.3710	Decrease 0.006 in.
Clad wall thickness, in.	0.0295	Increase 0.003 in.
Diametral gap 0.0075, in.	0.0075	None
Pellet density, % TD	95	Increase 1% TD
Pellet OD, in.	0.3635	Decrease 0.006 in.
UO ₂ loading, g UO ₂	2410.4	Decrease ~120 g UO ₂
UO ₂ loading, g U	2124.8	Decrease ~104 g U
Stack height, in.	138.60	Decrease ~4 in.
Plenum volume, in. ³	~1.445	Increase ~0.486 in. ³
Prepressure, psia	450-480	
Fuel rod length, in.	154-3/16	Increase 0.5 in.
Tube length, in.	153-5/8	Increase 0.5 in.

Figure 6-1. Fuel Rod Radial Peaking Factor Power History

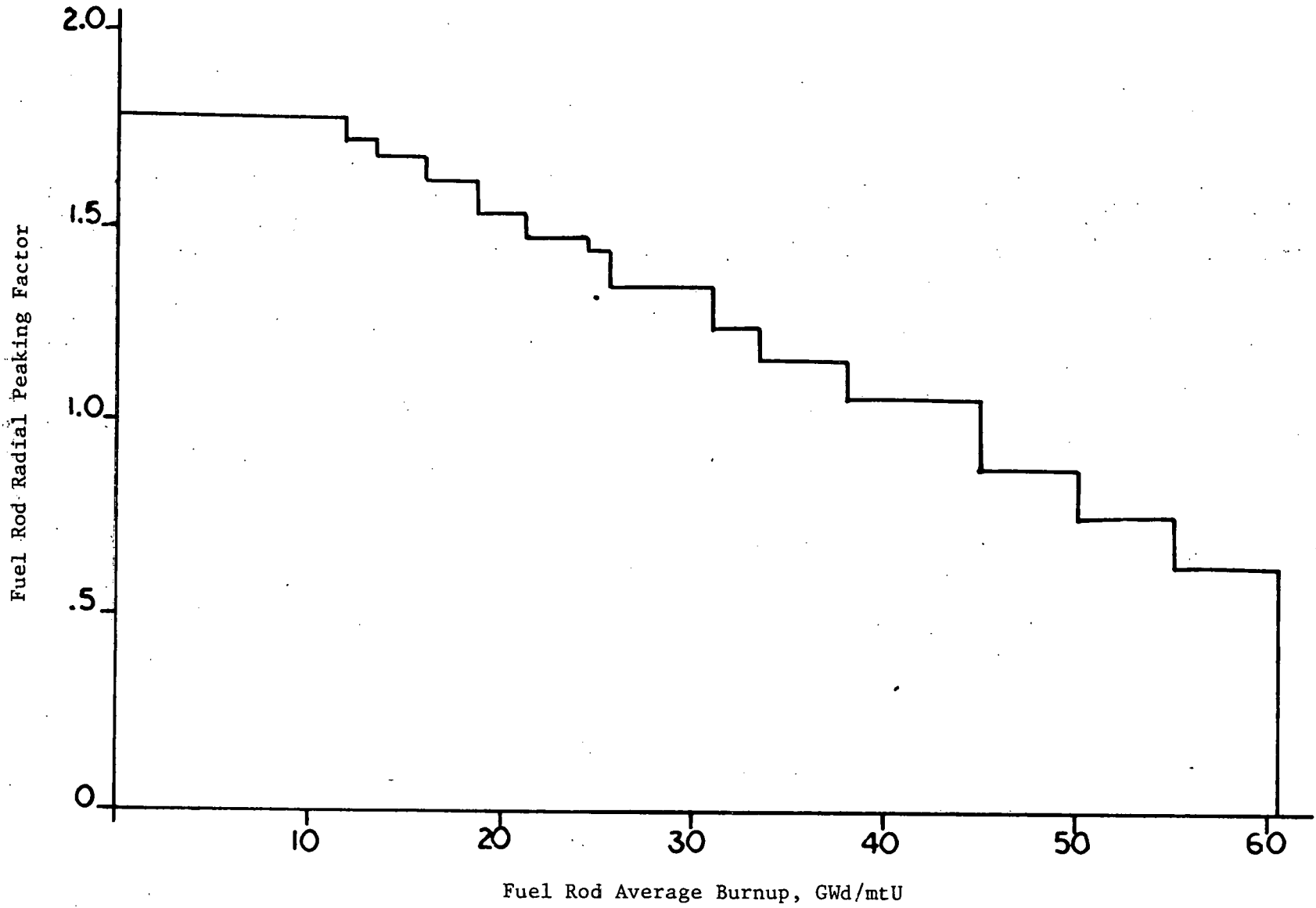


Figure 6-2. Fuel Rod Radial Peaking Factor Power History

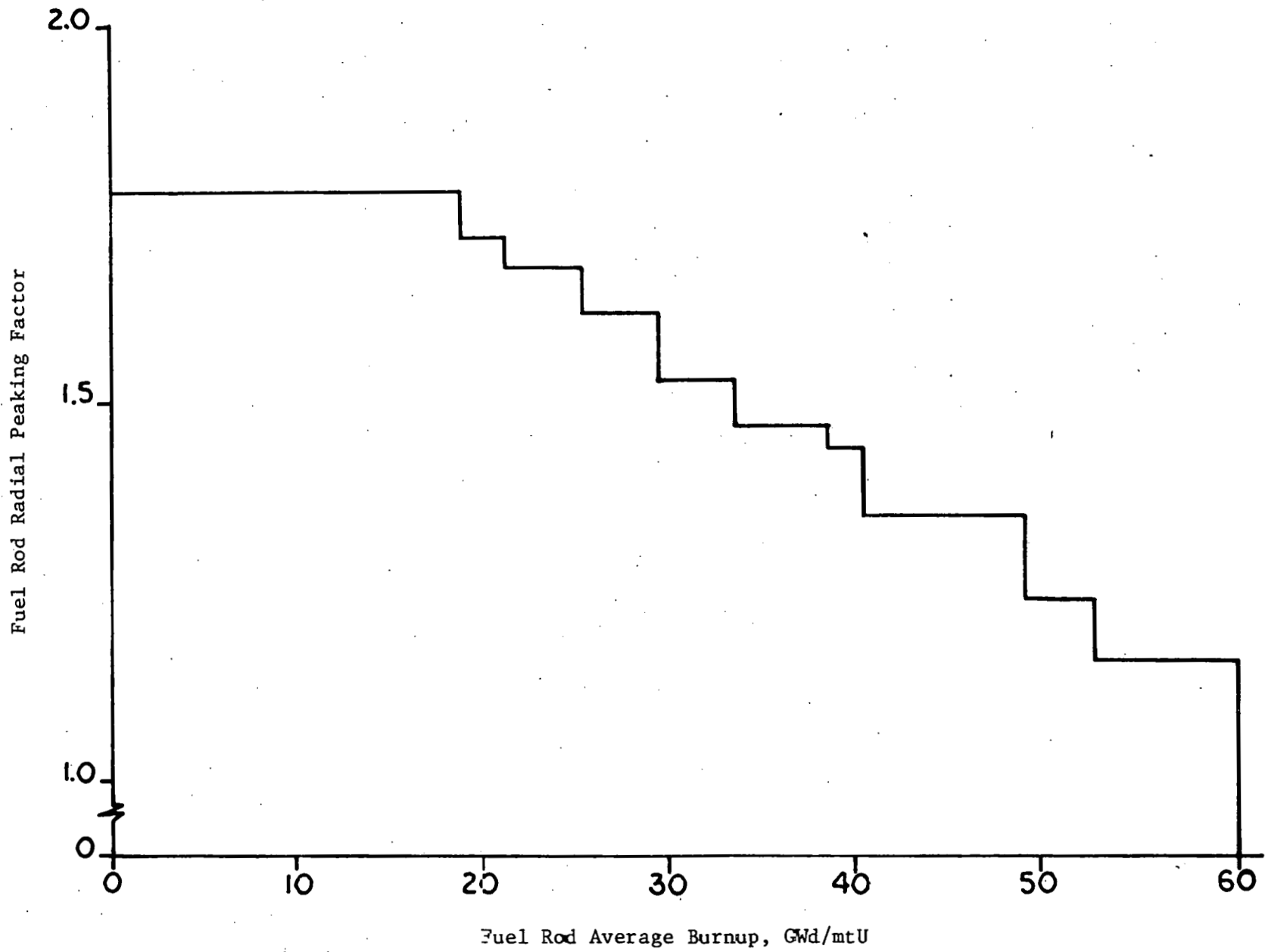
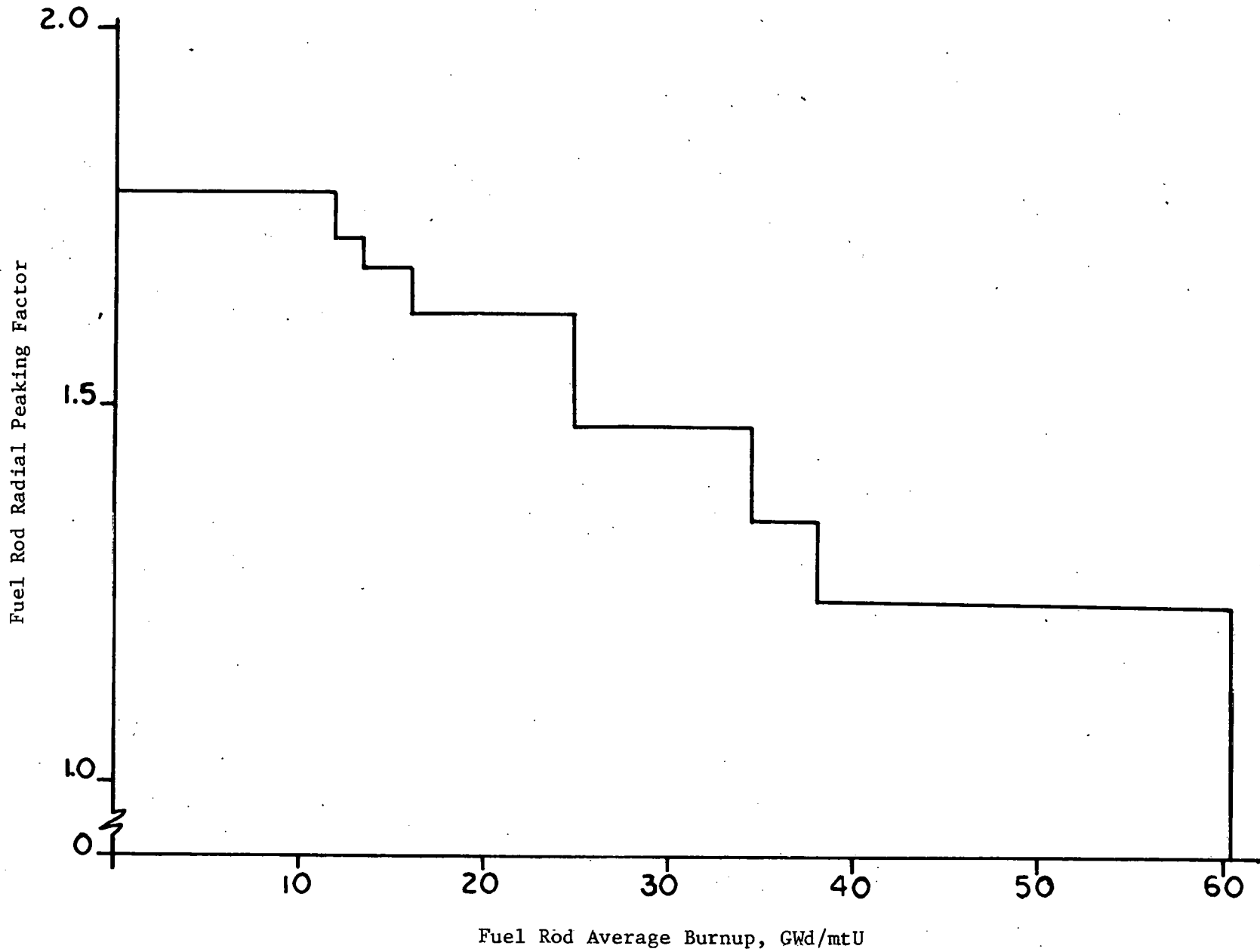


Figure 6-3. Fuel Rod Radial Peaking Factor Power History



6-15

Babcock & Wilcox

Figure 6-4. EOL Internal Rod Pressure Vs Fuel Densification

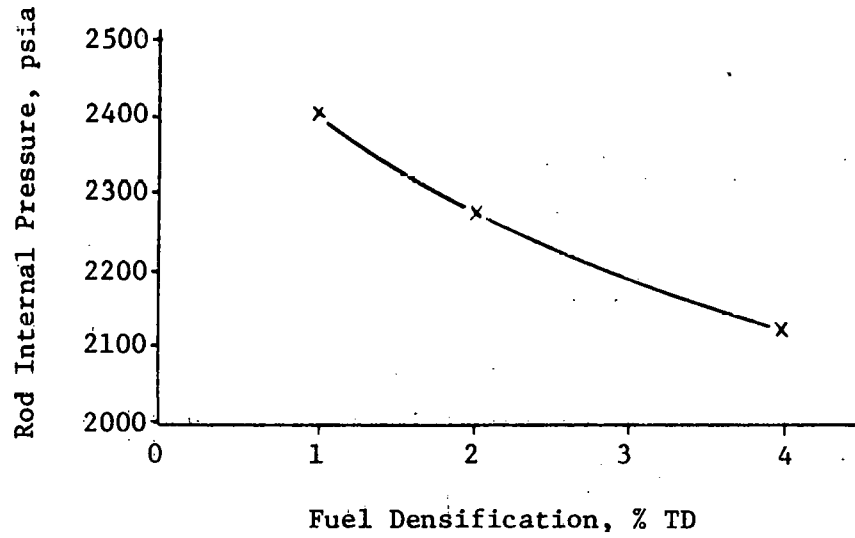


Figure 6-5. EOL Internal Rod Pressure Vs Initial Rod Pressure

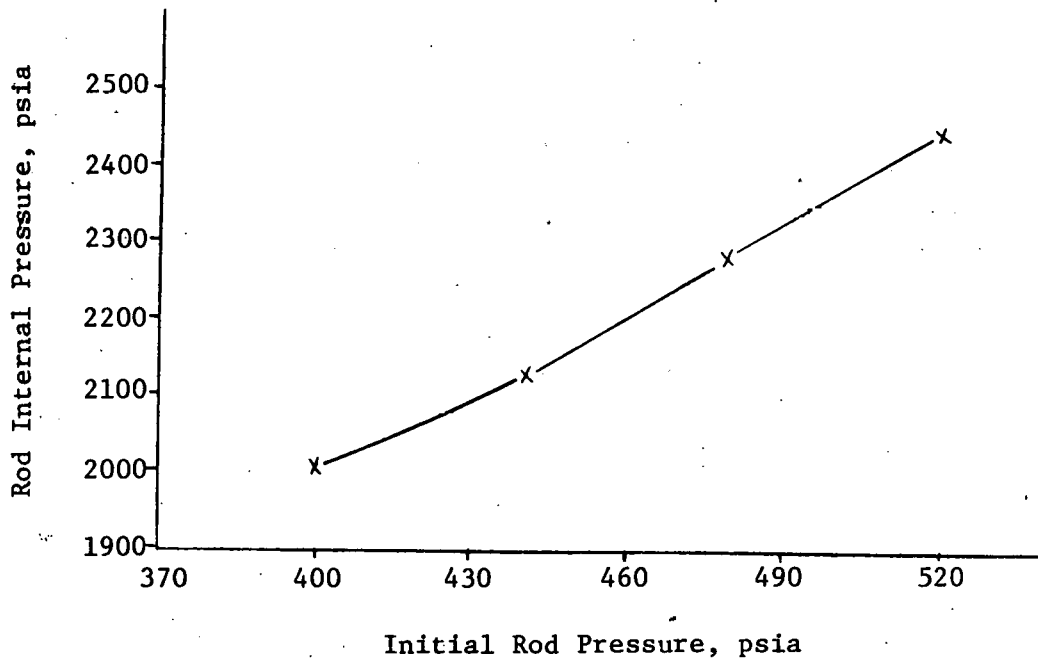


Figure 6-6. EOL Internal Rod Pressure Vs Fuel Pellet Outside Diameter

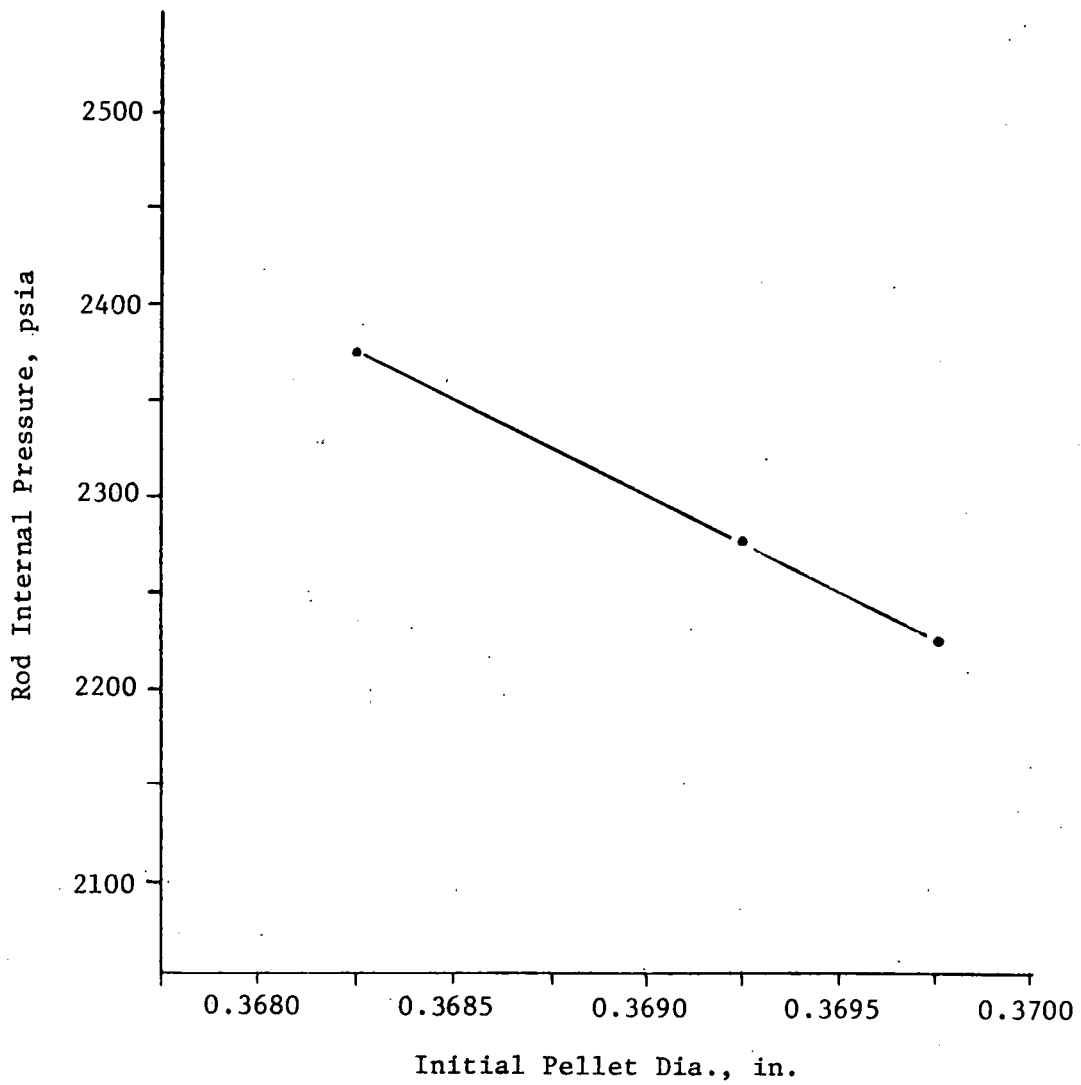


Figure 6-7. EOL Internal Rod Pressure Vs Rod Plenum Volume

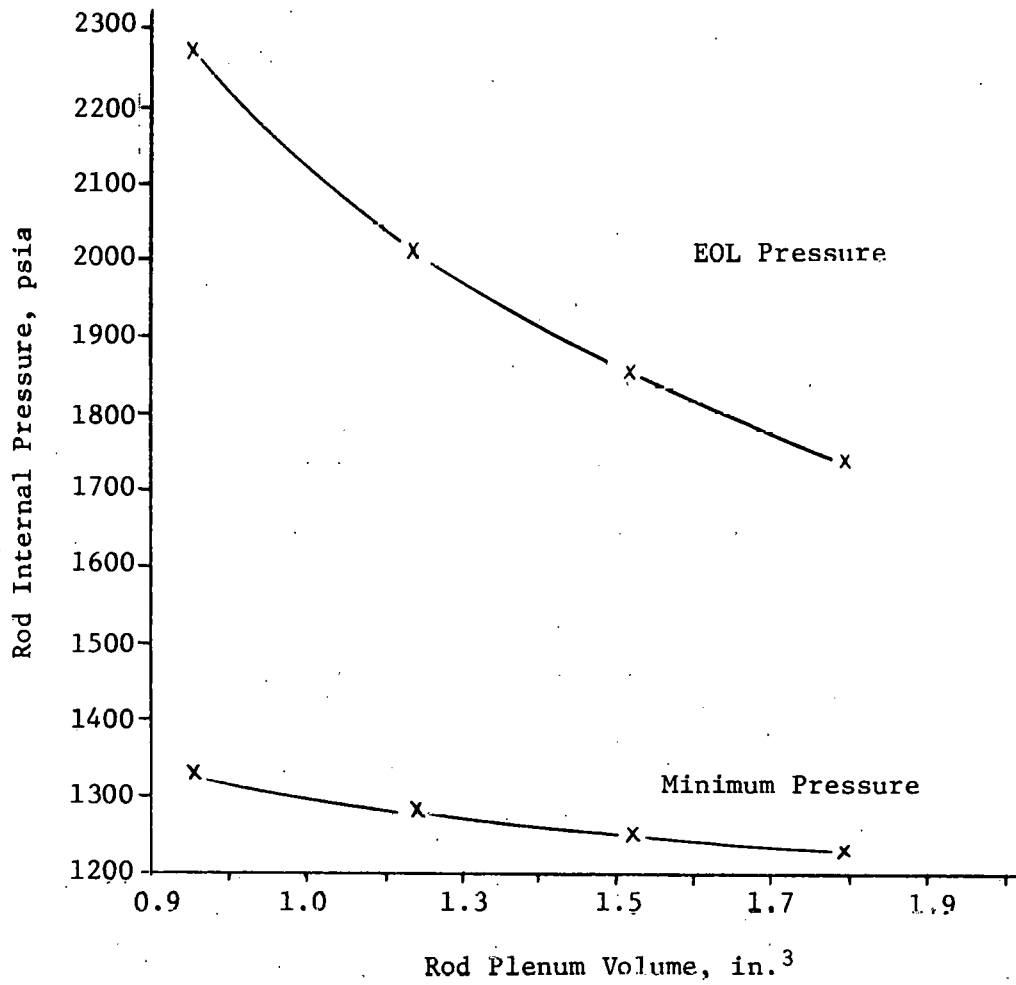


Figure 6-8. Maximum Fuel Temperature Vs Burnup

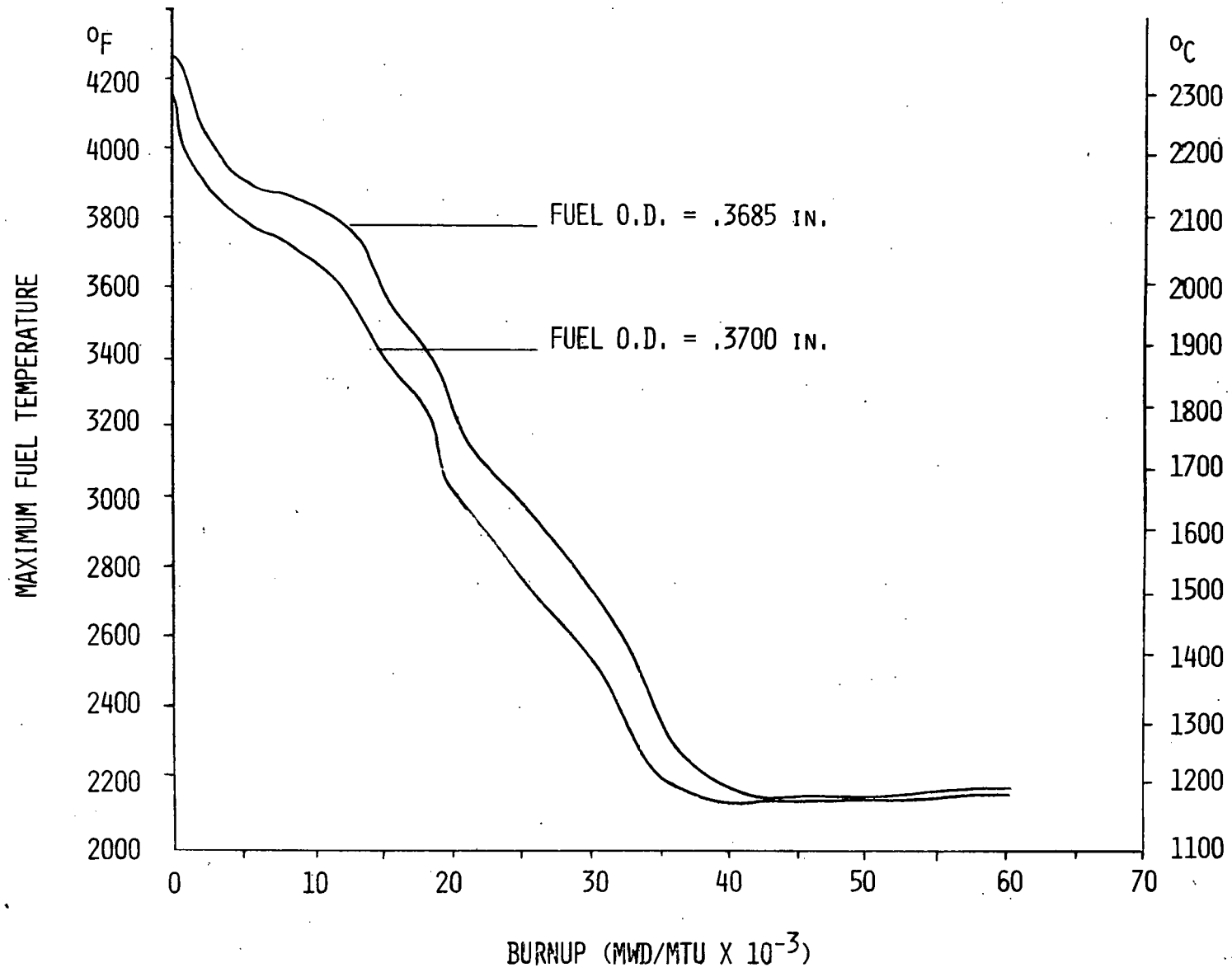


Figure 6-9. Maximum Fuel Temperature Vs Burnup

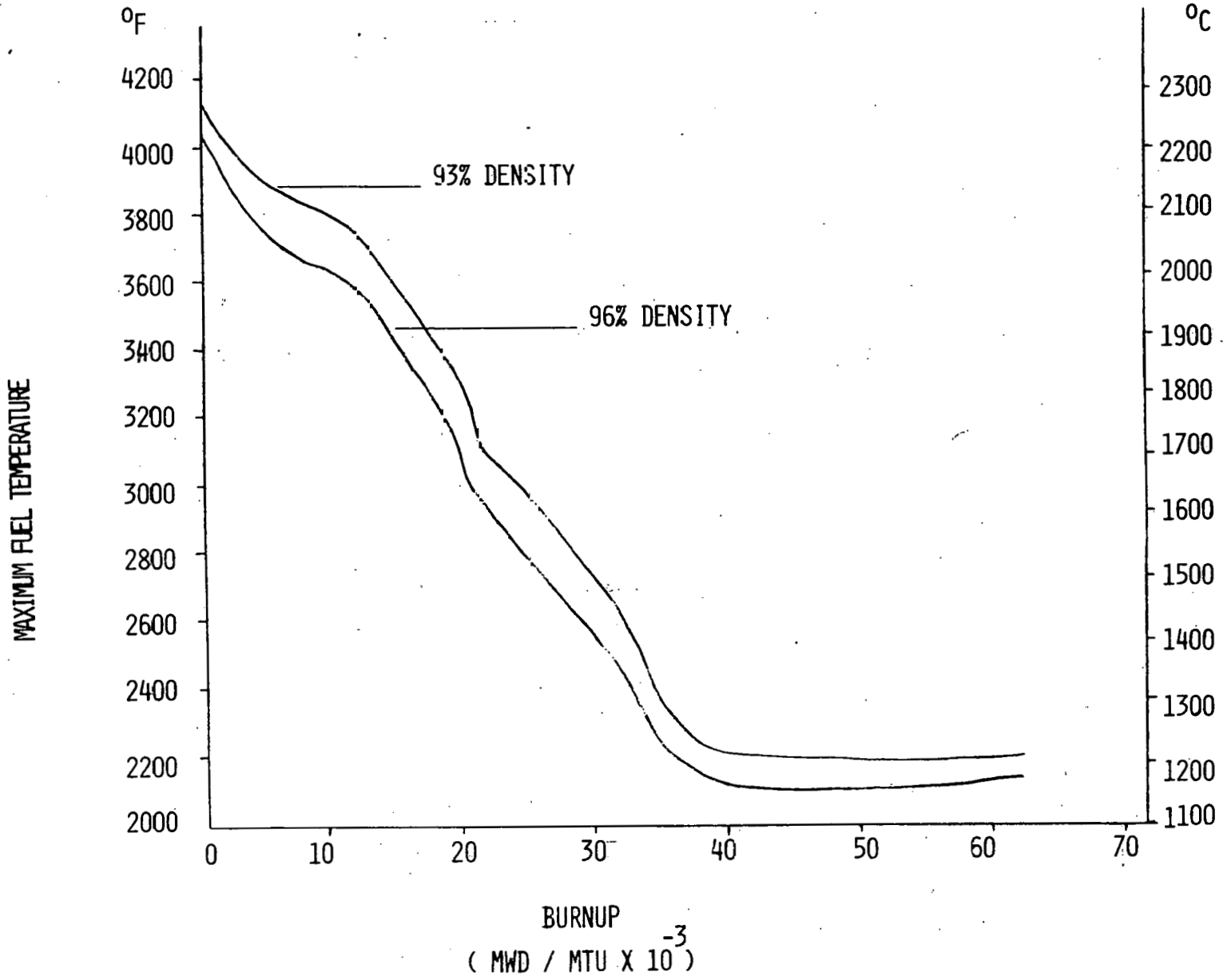


Figure 6-10. Maximum Fuel Temperature Vs Burnup

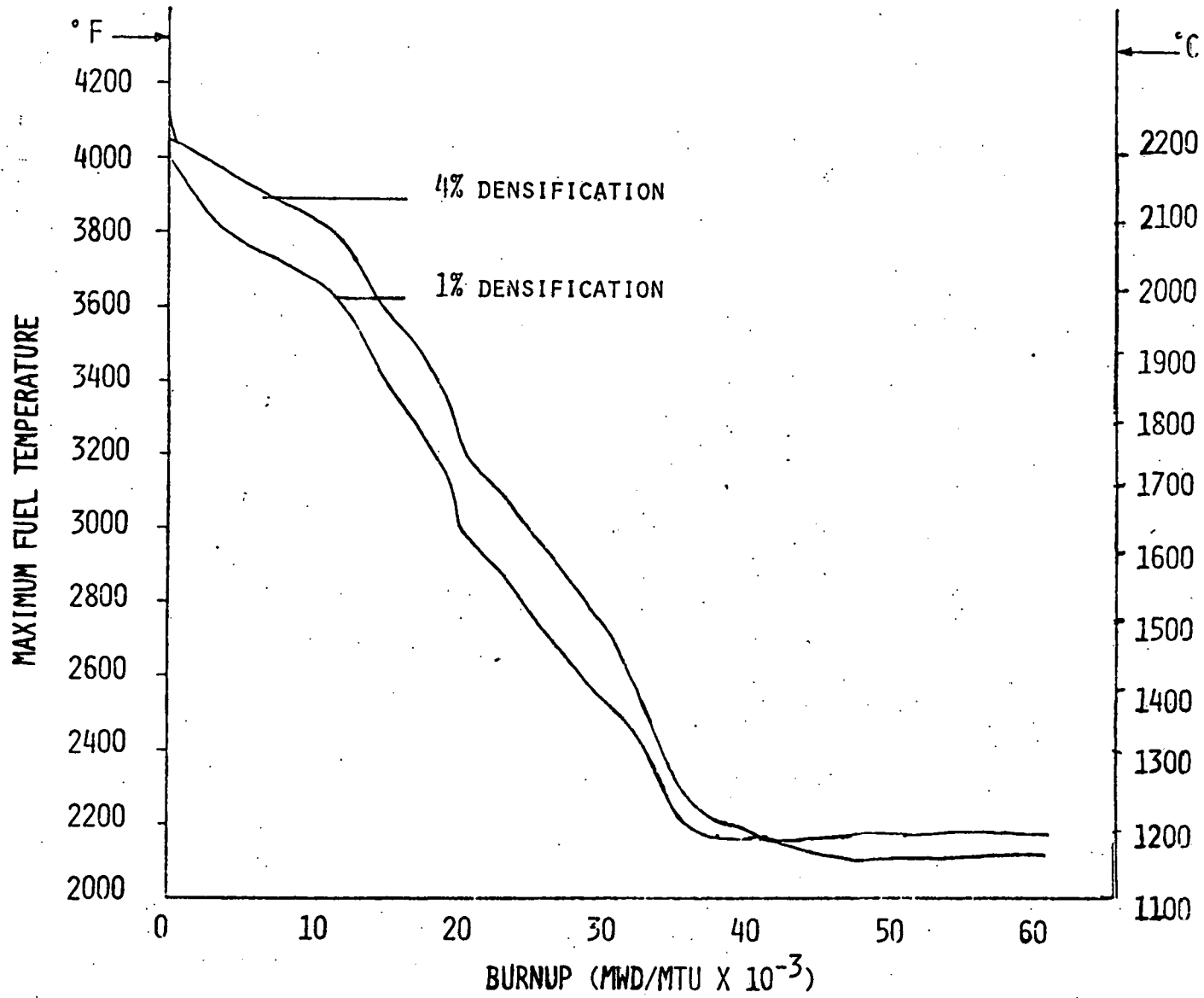


Figure 6-11. Creep Ovality Vs Cladding Wall Thickness

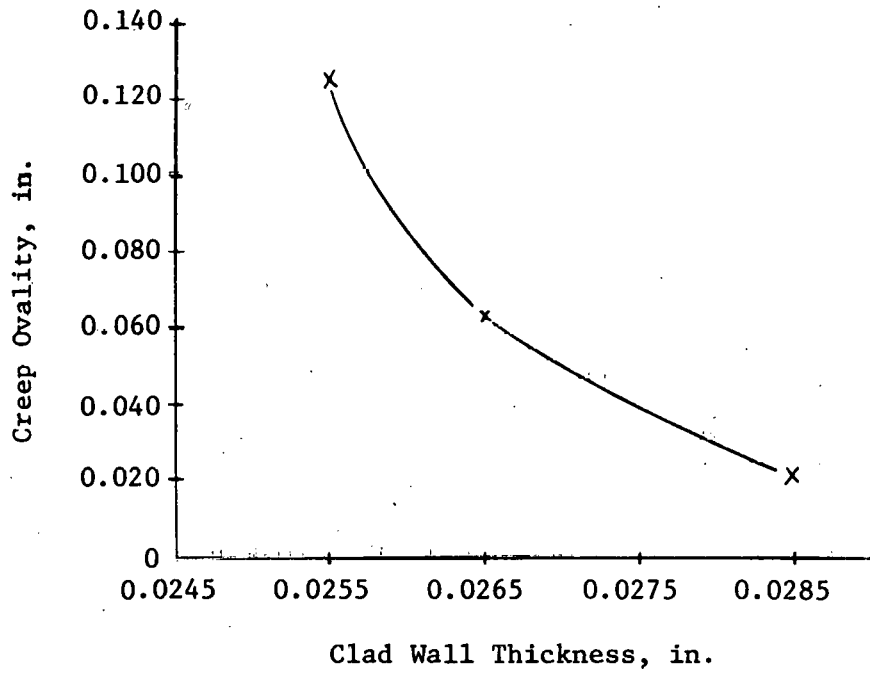


Figure 6-12. Creep Ovality Vs Fuel Rod Plenum Volume

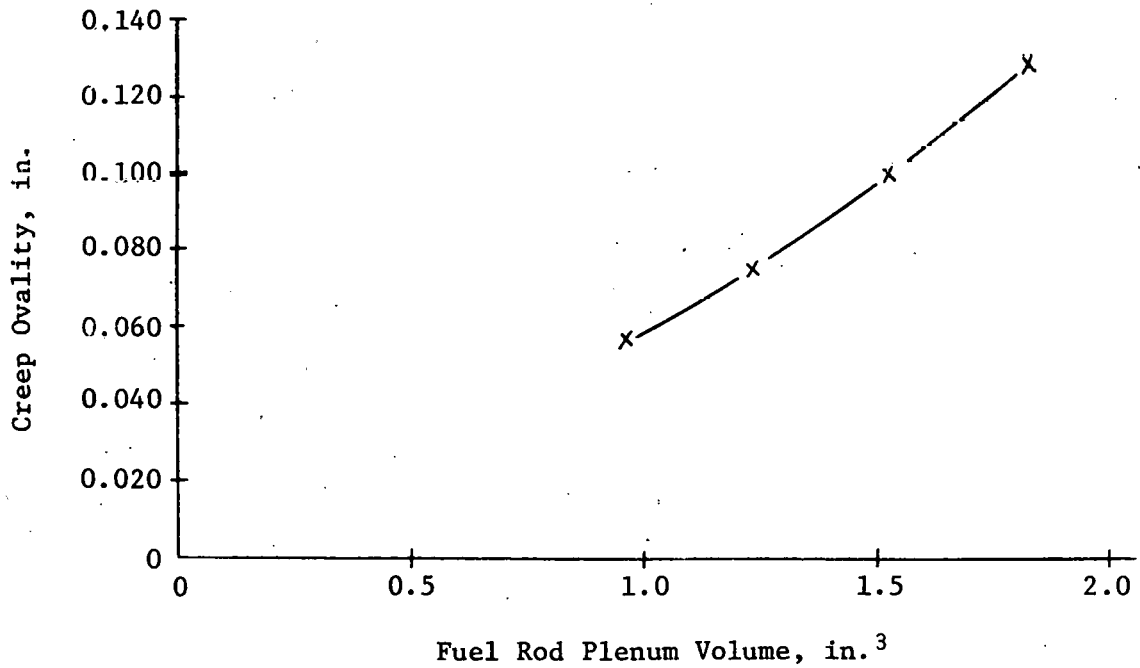


Figure 6-13. Creep Ovality Vs Fuel Rod Initial Pressure

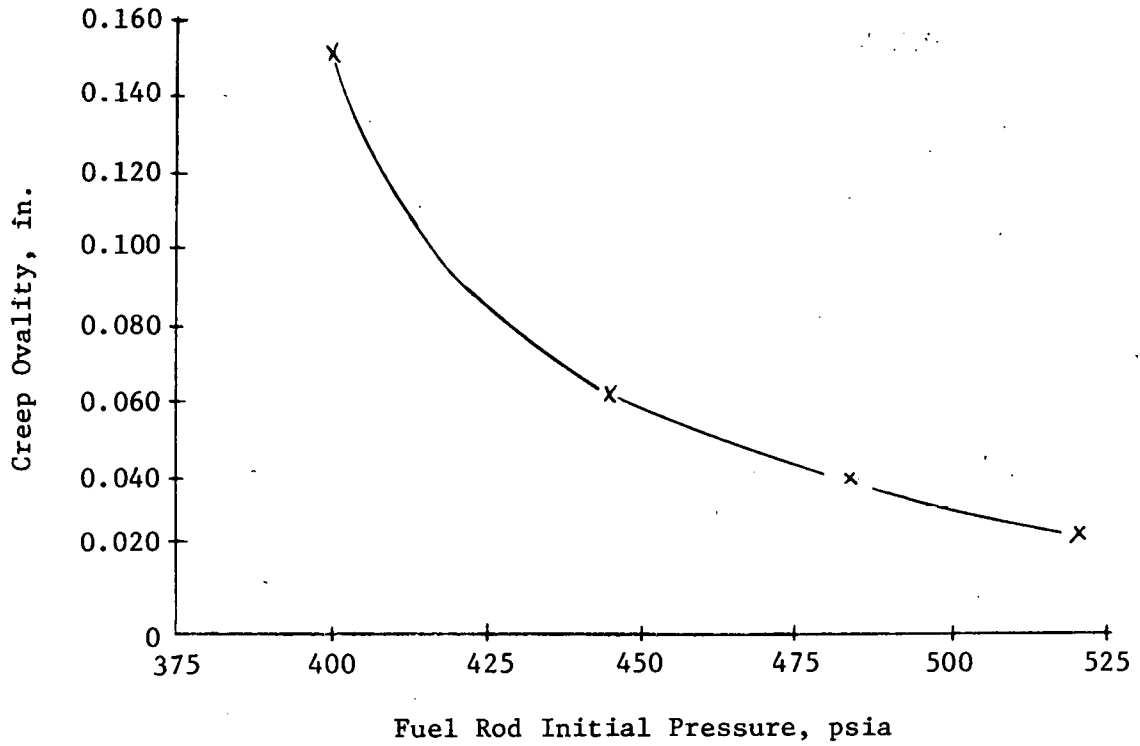


Figure 6-14. Creep Ovality Vs Fuel
Densification

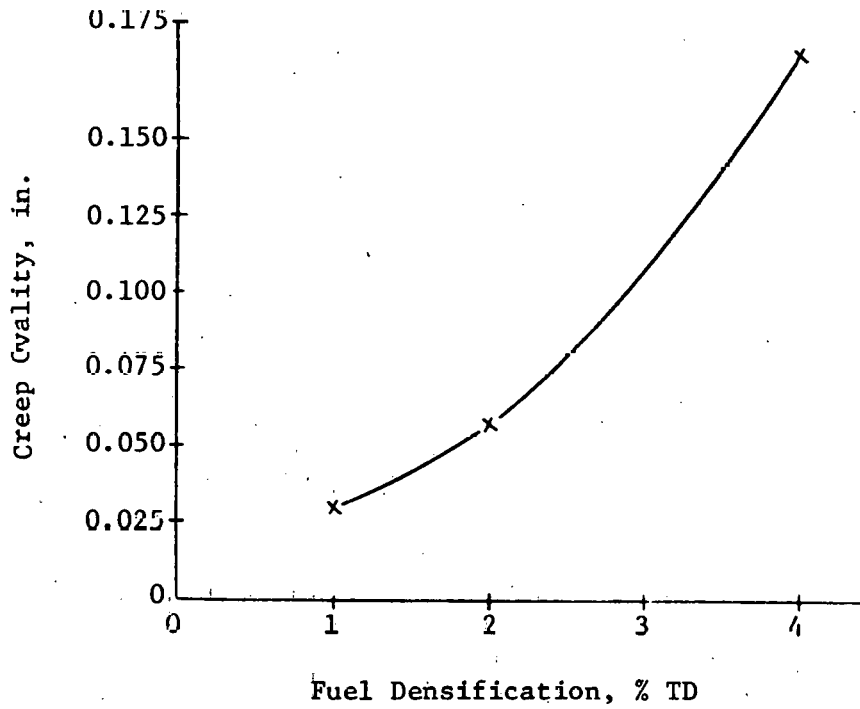


Figure 6-15. Creep Ovality Vs Burnup

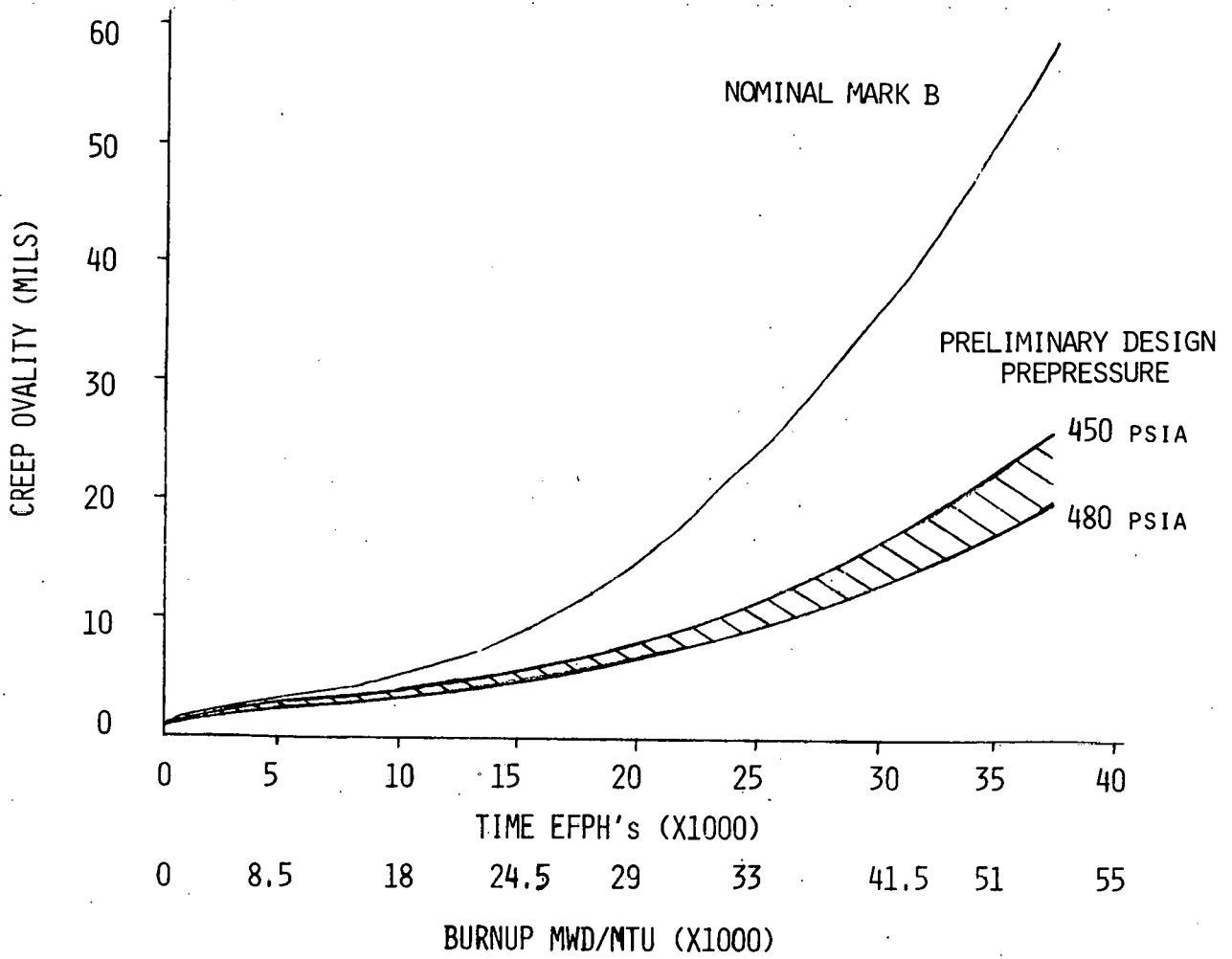


Figure 6-16. EOL Creep Ovality as a Function of Wall Thickness and Prepressure

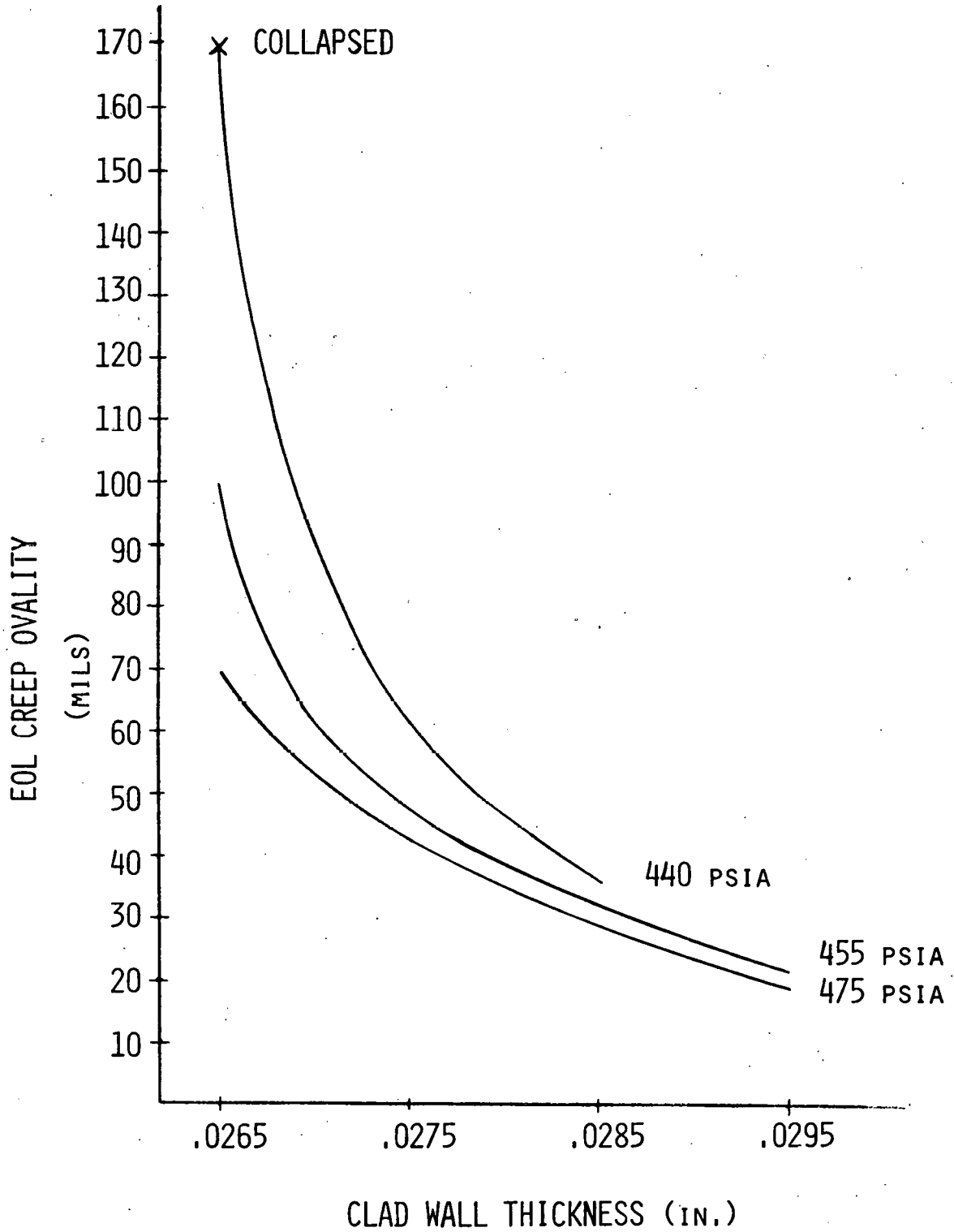


Figure 6-17. EOL Internal Rod Pressure Vs Burnup

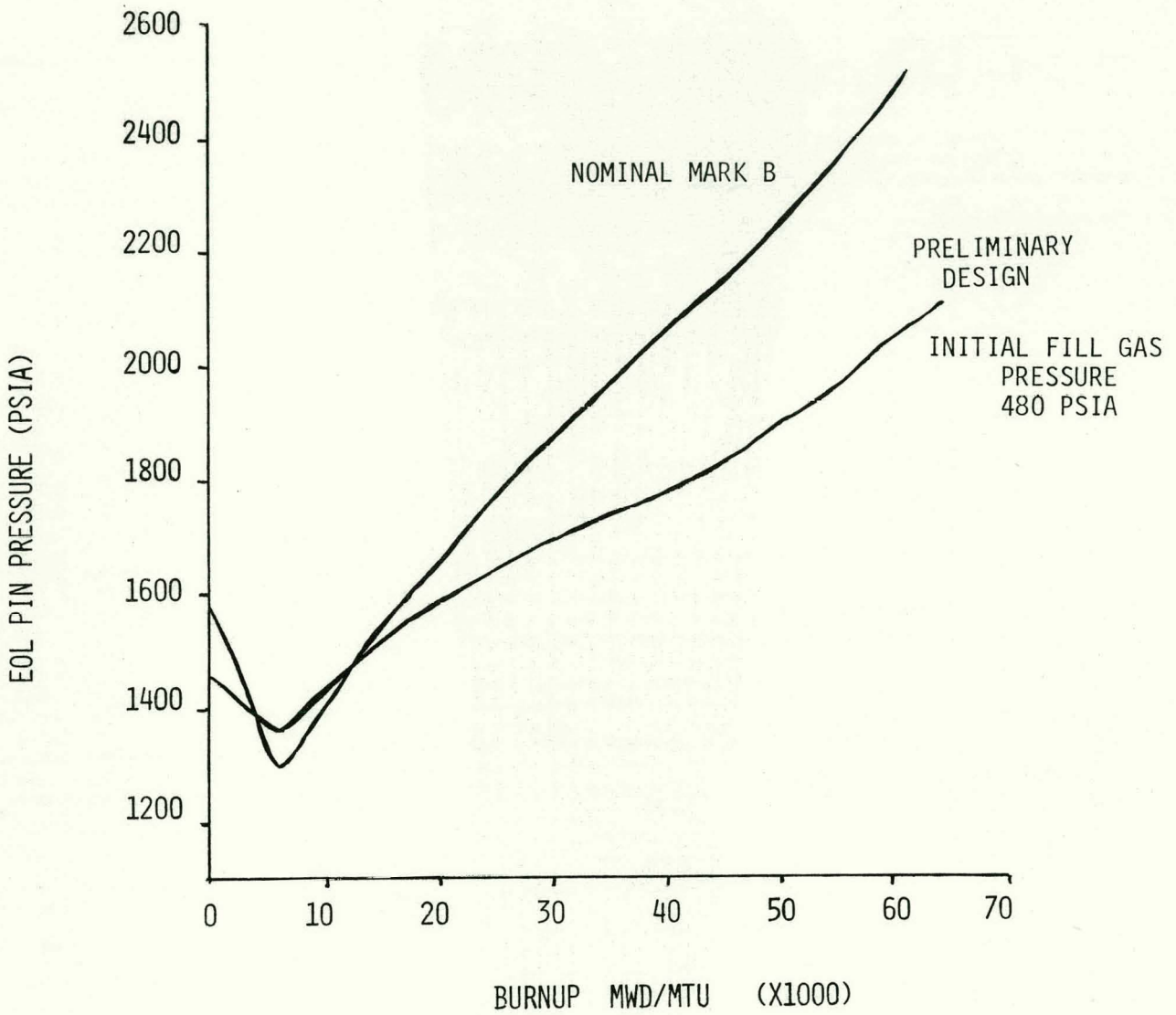


Figure 6-18.
Mark B Fuel Assembly

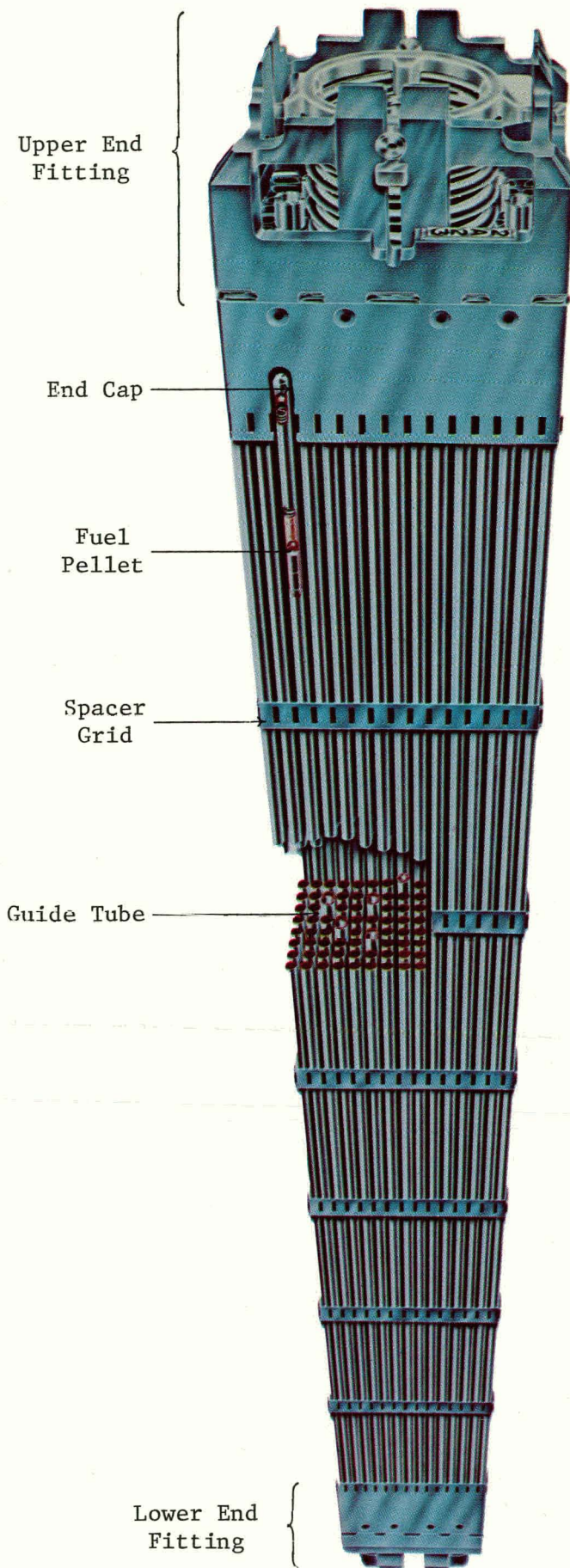
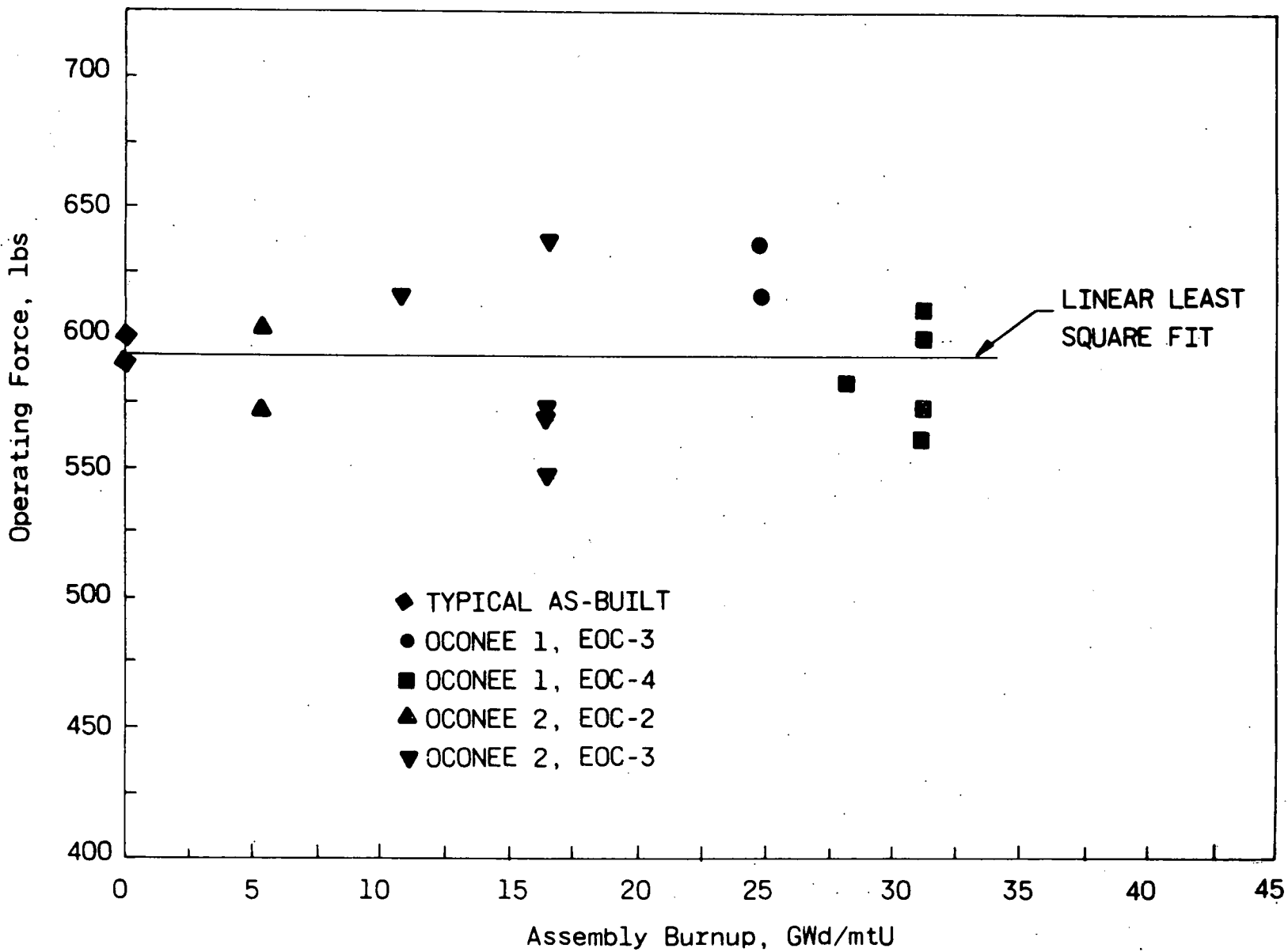


Figure 6-19. Holddown Spring Net Operating Force



6-29

6-29

Babcock & Wilcox

Figure 6-20. Fuel Assembly Growth as Function of Assembly Average Fluence

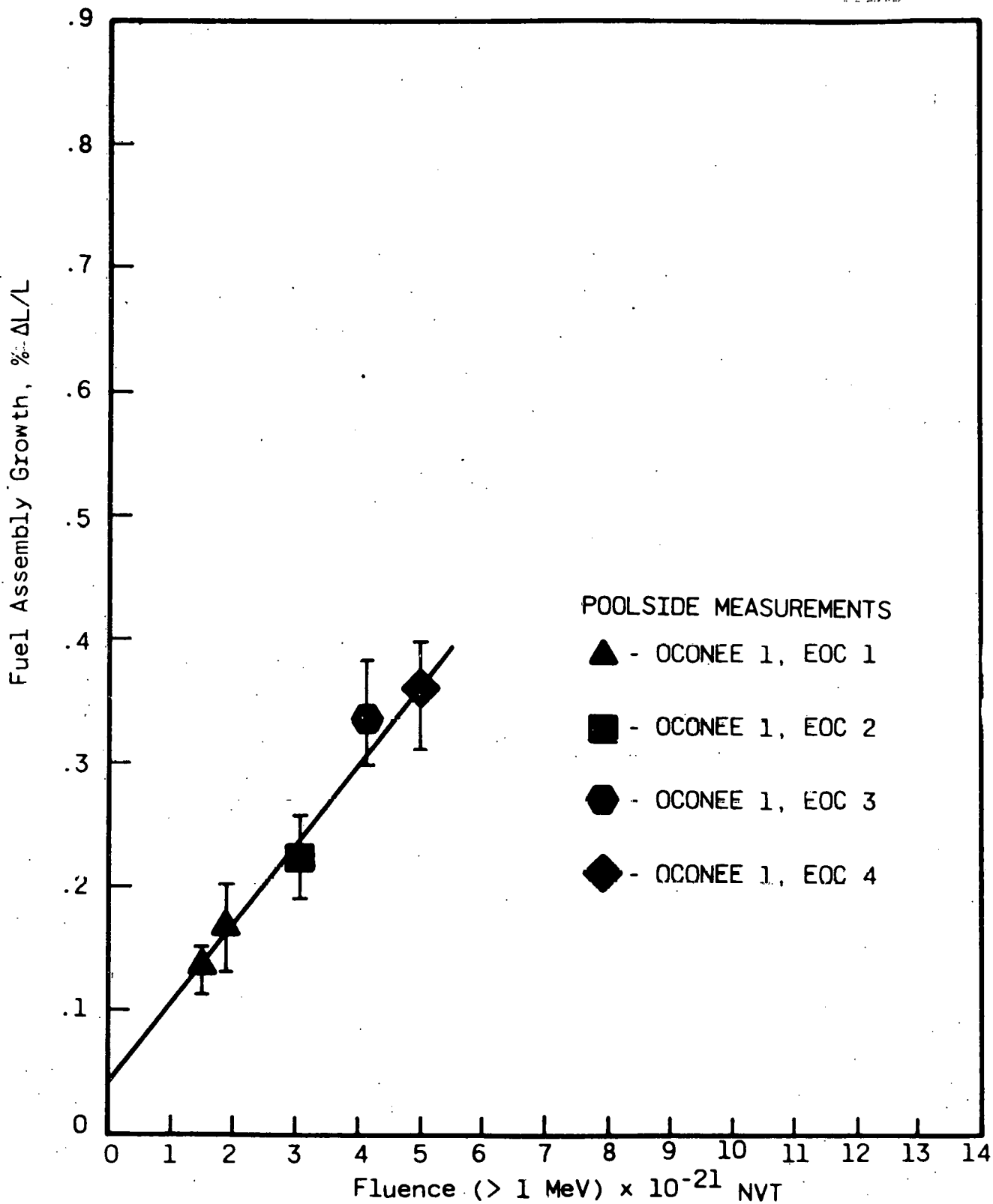
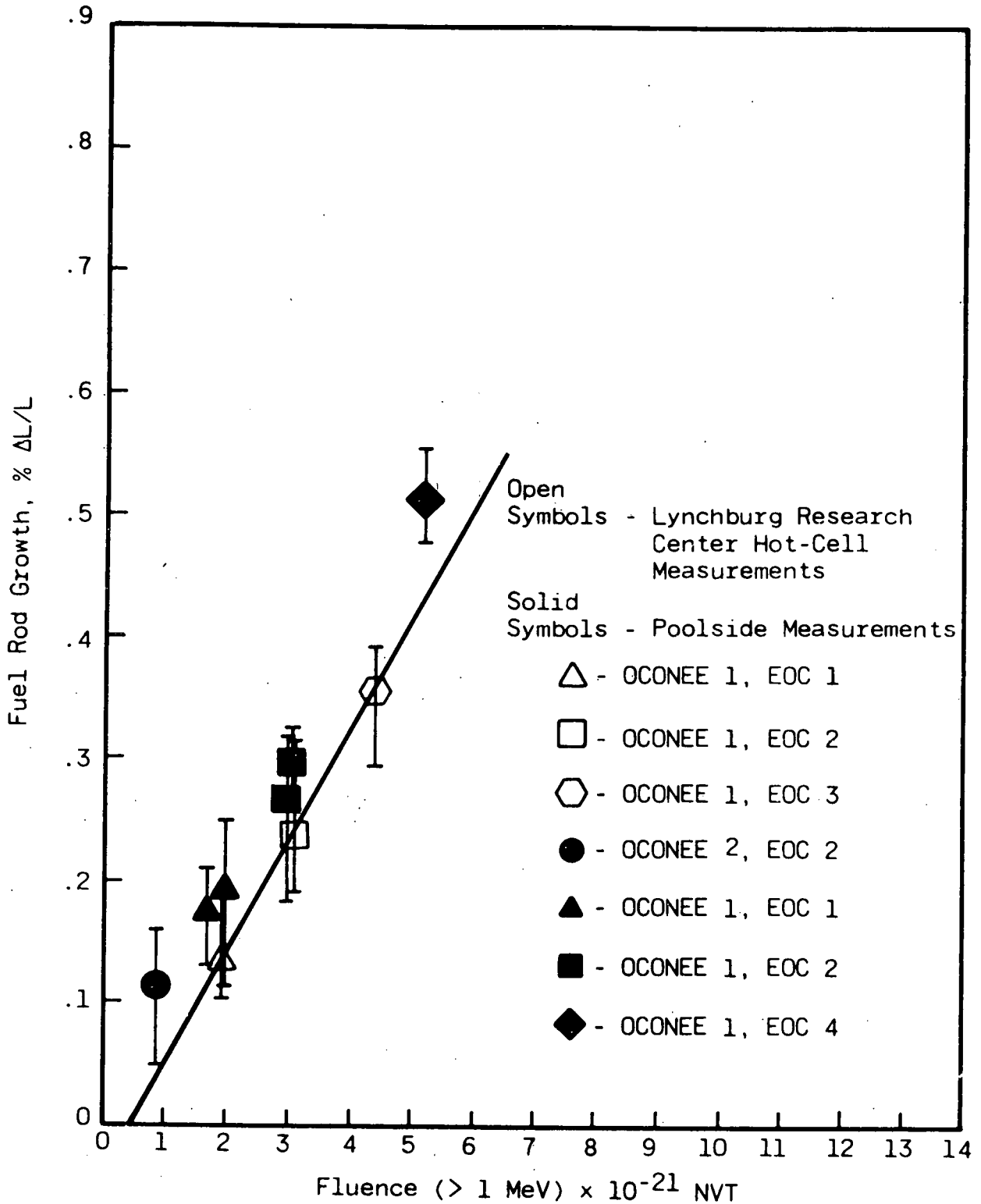


Figure 6-21. Fuel Rod Growth as Function of Assembly Average Fluence



7. PROGRESS TO DATE — TASK 3, "ENGINEERING AND DESIGN OF IMPROVED POOLSIDE EXAMINATION EQUIPMENT"

7.1. Introduction

The nondestructive evaluation of the physical effects of irradiation on fuel assemblies provides invaluable fuel performance data for design verification and benchmarking of analytical models for predicting fuel behavior. Special equipment is being designed for these nondestructive measurements of the important performance characteristics of lead-test assemblies to be irradiated in the Arkansas Nuclear One, Unit 1 (ANO-1) reactor. These measurements will be performed at the reactor site using the water of either the reactor pool or the spent fuel storage pool to provide shielding for the operators. Highly specialized, remotely operated equipment is being designed to acquire accurate inspection results.

7.2. Examination Scope

The following inspections are deemed to be most important in tracking the performance of lead-test assembly designs:

1. Visual examination.
2. Fuel column length and gap formation.
3. Fuel rod localized bow.
4. Fuel assembly bow and twist.
5. Fuel rod diameter.
6. Fuel rod and assembly length.
7. Grid spring relaxation.
8. Holddown spring relaxation.
9. Crud deposition characteristics.

These inspections, which address the changes in appearance, mechanical properties, and physical dimensions that occur as a consequence of irradiation, are based on the experience of the nuclear industry at large and that of B&W at the Duke Power Company's Oconee Nuclear Station since 1974.

7.3. Design Guidelines

The ground rules for the development of the post irradiation examination (PIE) system are given below.

1. Applicable regulatory body requirements shall be met.
2. Requirements for facility modifications to accommodate the system shall be minimized.
3. The system shall have the capability to perform all of the tests listed.
4. The system shall be based on proven technology.
5. The largest structural component shall measure less than 16 × 7 × 5 feet.
6. The heaviest structural component shall weigh less than 2.5 tons.
7. The system shall have independent fuel handling capability.
8. The data output shall be computer-compatible.
9. The system design shall consider ease of repair and availability of components.
10. The system design should provide high throughput (several simultaneous test operations are desirable.)
11. Interference with normal site operations should be minimized.
12. The system should be capable of being removed and reinstalled.

7.4. Results and Discussion

7.4.1. Operating Location Selection

The selection of an operating location for the inspection system that met the guidelines given in section 7.3. involved consideration of many factors. As various locations were considered, the most frequently encountered constraint was interference with some aspect of reactor operations. Few (if any) reactor sites incorporated space in the original plant design for a PIE equipment system, and little room is available for retrofitting without some interference.

The program requirement that fuel inspections be performed on fuel scheduled for further irradiation (and therefore during refueling outage periods) makes it impractical to install the system in the reactor pool or in the spent fuel storage pool because of mechanical interference with the fuel handling mechanisms. The lack of space around the fuel storage racks further excluded consideration of the spent fuel storage area. The one underwater space accessible to fuel and unused during refueling periods was the cask loading pit,

an area 46 ft deep and adjacent to the ANO-1 spent fuel pool (as shown in Figure 7-1).

Other considerations in selection of the inspection area were as follows:

1. The fuel handling mechanism should be capable of loading and unloading assemblies either from the inspection equipment or from one or more storage positions accessible to both mechanisms.
2. The fuel handling mechanism should not interfere mechanically with inspection equipment during fuel transfer operations.
3. Ample space for several instrument racks and an operating crew of four to six persons should be available immediately adjacent to the underwater inspection location.
4. The necessary services — electrical power, compressed air, etc. — must be available.
5. The impact of the PIE system on site operations (load limits on structures, radiation levels in adjacent areas, etc.) should be minimized.

7.4.2. System Description

As depicted in Figure 7-2, a free-standing underwater structure bearing on the load pads in the bottom of the cask loading pit was selected for the PIE system. To facilitate its movement, the structure will be modular. A base structure will mate to the existing load pads and will support the remainder of the underwater components. The fuel racks and support structure will be remotely attachable to the base structure. The support structure will house a removable measurement frame which contains the dimensioning equipment and will support and position the removable gamma scan station components. It will also provide mounting points for the underwater illumination required for visual examinations and other visually monitored operations.

Two other structures located above the water level will work in conjunction with the underwater components. The fuel transfer assembly provides the capability for vertical and horizontal movement of fuel assemblies from the time they are deposited in the fuel storage rack until they are removed by the plant fuel handling mechanism. It consists of two hoists attached to their separate bridge and carriage structures, which are mounted on a movable gantry frame. Thus, transfers between the fuel rack and the measurement positions can be made as needed. When the fuel handling machine must travel over the cask loading pit, as is the case whenever fuel is delivered to or removed from the PIE system, the fuel transfer assembly may be rolled out of the way.

A semi-fixed work platform is also located over the underwater structure, but at such a level that it does not interfere with the movement of the fuel handling mechanism. The work platform serves as a mounting structure for the dimensional measuring head vertical drive unit and as a support for fuel grapples and other underwater tooling, as well as an operator's support when manually controlled underwater manipulations are required.

Two transfer hoists operating from a common support structure will move an assembly to any of the three test stations. Three assemblies may be subjected to different examinations simultaneously. The visual station requires the use of a hoist to provide vertical translation of the fuel past the periscope; the gamma scan station uses the other hoist in a similar fashion. The measurement station holds the fuel assembly in a fixed position, but it must be loaded by one of the hoists with the assembly to be inspected before both of the other stations are put to use. Accordingly, it cannot be unloaded until one of the hoists is free. However, the time required for the battery of tests performed in the measurement station negates the inconvenience of not having a third hoist. The delays in unloading that station because of a wait to complete a gamma scan or a visual exam are expected to be small. The complexity and added expense of a three-hoist system that would provide absolute independence of the three test stations were not considered to be justifiable.

A commercially available underwater periscope mounted in the northeast corner of the cask loading pit and associated lighting completes the list of system components installed in fixed locations. A portable underwater TV camera is also installed for making videotape records of fuel appearance and operations monitoring.

The system arrangement shown in Figure 7-2 is expected to be representative of the final design. The details of components as to size, shape, and construction are expected to change as the design phase progresses and available commercial components are selected to meet performance criteria.

The capability of the inspection system must be compatible with the type and quantity of intended operations. A time phasing study was performed listing the planned operations to find out whether the intended measurements could be obtained in the time available. As illustrated in Figure 7-3, approximately 36 hours was projected for examination of four fuel assemblies. The locations at which the various tests are to be performed are tabulated in Table 7-1.

The current system arrangement with an independent fuel assembly transfer device, interim fuel storage rack, three separate operating stations for gamma scanning, physical measurements, and visual examinations, plus associated support structures provides a very flexible system in terms of allowing three parallel operations with little or no interaction between them. Independent fuel handling capability (once the four fuel assemblies are placed in the PIE equipment storage racks) minimizes dependence on ANO-1 station equipment that may be in use for other purposes.

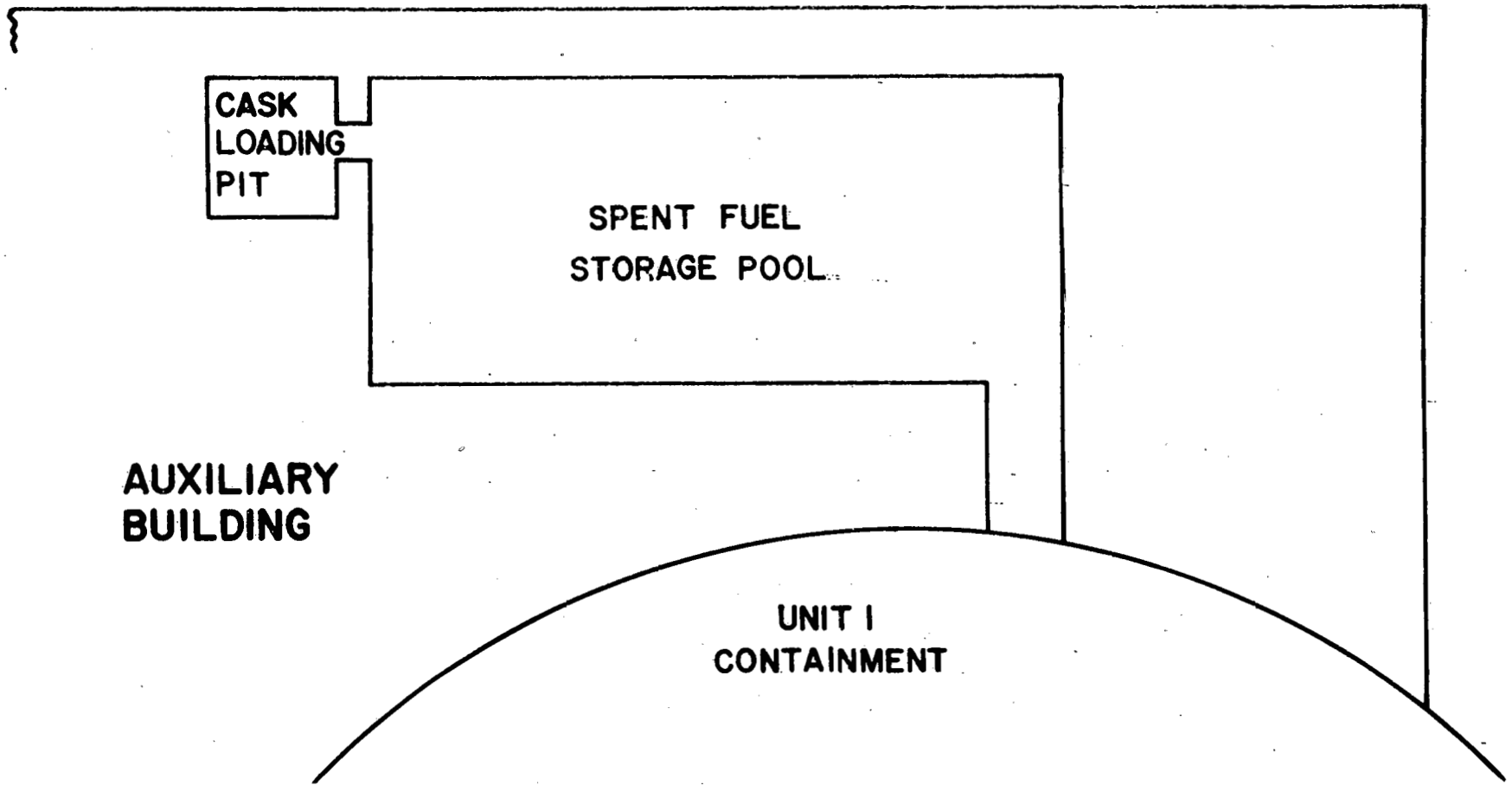
Table 7-1. PIE System Test Capabilities

<u>Location</u>	<u>Test capability</u>
Visual station	Visual examination
	Photography
	Video tape recording
	Fuel assembly length ^(a)
	Fuel rod length ^(a)
	Grid axial position
Gamma scan station	Axial fission product distribution ^(b)
	Fuel stack height ^(a)
	Fuel gap location
Measurement station	Fuel rod diameter
	Fuel rod ovality
	Assembly bow and twist
	Rod spacing measurements
	Holddown spring measurements
	Grid spring relaxation

(a) Using fuel hoist vertical position readout.

(b) Corner rods only.

Figure 7-1. Cask Loading Pit Area in Auxiliary Building



7-6

Babcock & Wilcox

SCALE: 1"=13'

Figure 7-2. PIE System Arrangement in Cask Loading Pit

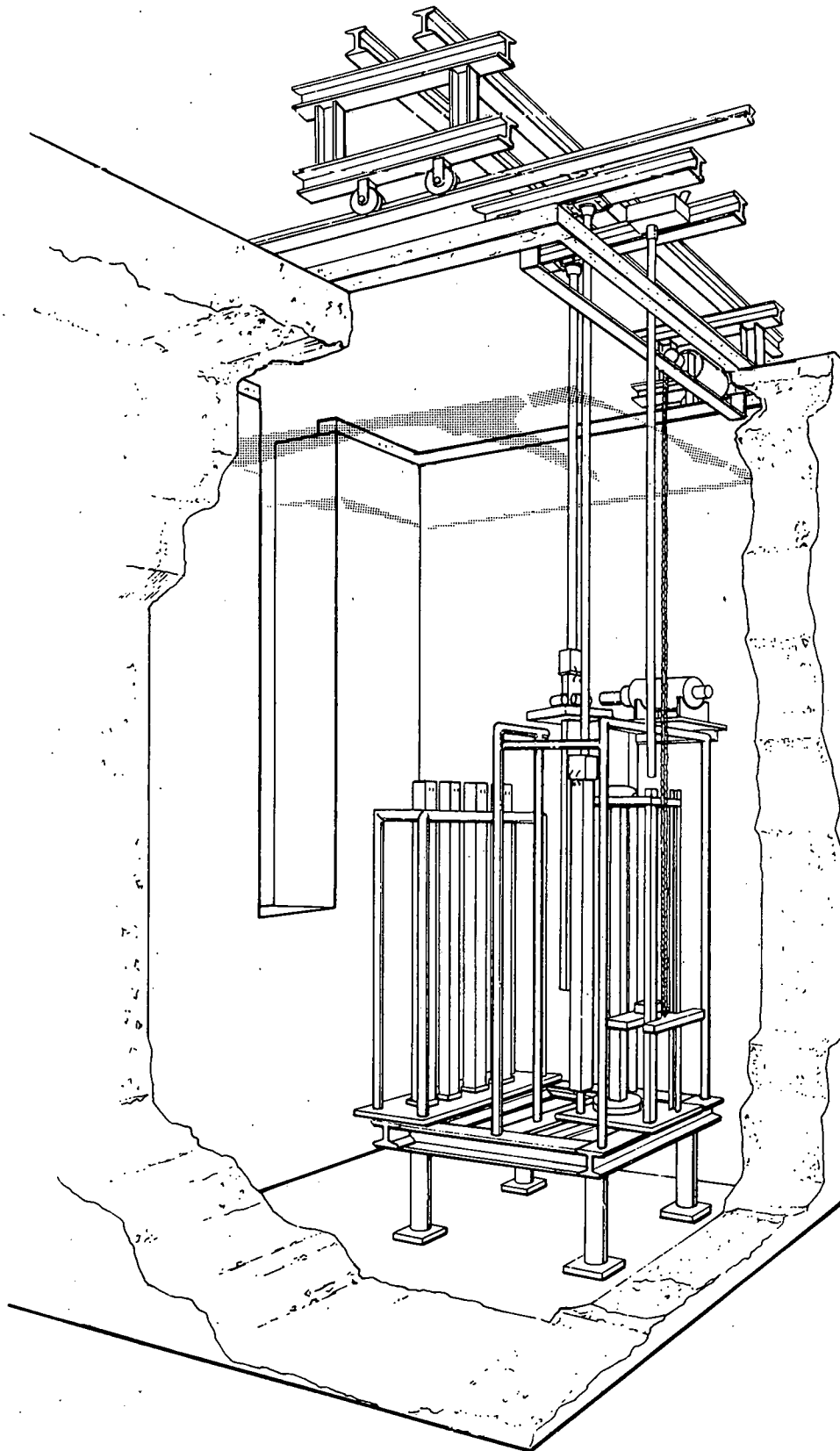
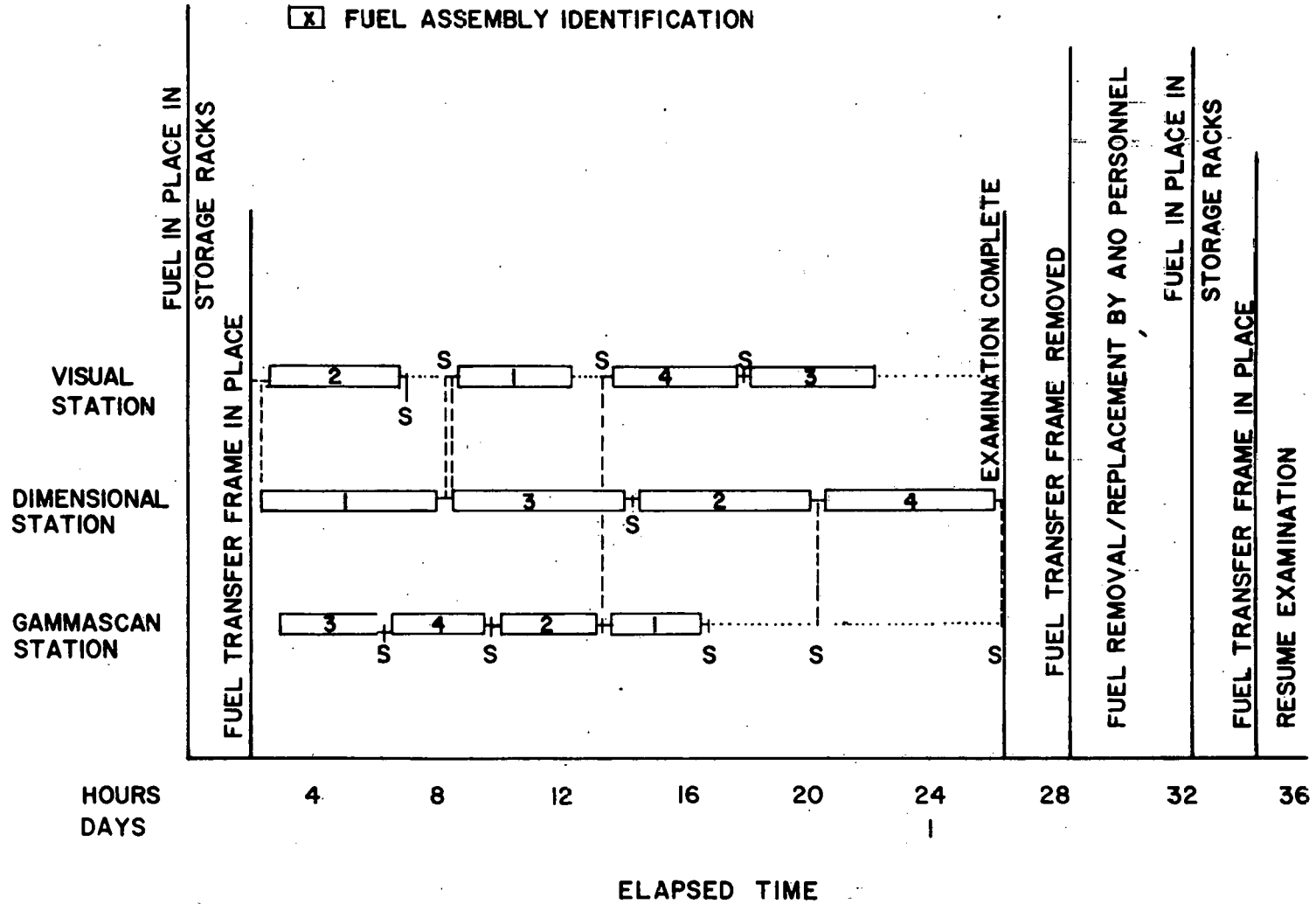


Figure 7-3. PIE Operations Flow Plan

LEGEND

- IDLE STATION
- EXAMINATION IN PROGRESS
- S TRANSFER TO/FROM STORAGE STATION
- ⊗ FUEL ASSEMBLY IDENTIFICATION



8. REFERENCES

- ¹ Babcock & Wilcox's Version of PDQ07 -- User's Manual, BAW-10117, Babcock & Wilcox, Lynchburg, Virginia, June 1976.
- ² FLAM3 -- A Three-Dimensional Nodal Code for Calculating Core Reactivity and Power Distributions, BAW-10124, Babcock & Wilcox, Lynchburg, Virginia, November 1975.
- ³ NULIF -- Neutron Spectrum Generator, Few Group Constant Calculator, and Fuel Depletion Code, BAW-10015, Babcock & Wilcox, Lynchburg, Virginia, June 1976.
- ⁴ T. A. Coleman, et al., Qualification of the B&W Mark B Fuel Assembly for High Burnup -- First Semi-Annual Progress Report, July-December 1978, BAW-1546-1, Babcock & Wilcox, Lynchburg, Virginia, August 1979.
- ⁵ TACO2 -- Fuel Pin Performance Analysis, BAW-10141, Babcock & Wilcox, Lynchburg, Virginia, August 1979.
- ⁶ Program to Determine In-Reactor Performance of B&W Fuel -- Cladding Creep Collapse, BAW-10084, Rev. 2, Babcock & Wilcox, Lynchburg, Virginia, October 1978.

APPENDIX A

Description of Fuel Cycle Study

Feed batch size: 36 assemblies
Cycle length: 292 EFPD
Power level: 2772 MWt
Control mode: Feed and bleed

Introduction

The fuel management plan described in detail in this appendix was chosen to provide fuel cycle data at burnups of 48,500 MWd/mtU with an annual fuel cycle. This fuel management plan loads 36 fresh fuel assemblies per cycle and, thus, represents a five-batch reload for a 177 fuel assembly core. As indicated in section 5.1.3, this fuel cycle provided a 17.3% fuel utilization improvement relative to the base case.

1. Fuel Shuffle Pattern

These cycles employed the LBP shuffle scheme, whereby the fresh assemblies with LBP are loaded in the interior of the core in a broken checkerboard pattern. To adequately control power peaking, it was necessary to establish a fuel loading pattern that spread out the 36 fresh assemblies so that any fresh assembly could have no more than one other fresh assembly diagonally adjacent to it. This fresh fuel pattern was used in all six cycles. Once-burned fuel was loaded on the periphery. Table A-1 outlines the fuel inventory plan for the 36-FA feed core.

Cycle 4, the first transition cycle, was shuffled from Rancho Seco cycle 3 at 300 EFPD. This cycle required the reinsertion of 29 twice-burned assemblies from cycle 2. The cycle 4 fuel loading pattern and LBP concentrations are shown in Figure A-1. Cycle 4 was depleted to 267 EFPD and shuffled to the next cycle.

Cycles 5, 6, and 7, which can be thought of as the approach to equilibrium cycles, used the same fresh fuel pattern as cycle 4. The fuel shuffle and LBP concentrations for cycles 5, 6, and 7 are presented in Figures A-2, A-3, and A-4, respectively.

In cycle 8 an equilibrium fuel loading pattern was established for five-batch refueling. The fuel shuffle pattern and LBP concentrations for cycles 8 and 9 are given in Figures A-5 and A-6.

2. Cycle Lifetime and Uranium Utilization

The cycle lengths attained were 267, 268, 298, 320, 290, and 290 EFPD for cycles 4 through 9. These cycles were run to the same EOL effective multiplication factor (k_{eff}) utilizing a constant feed batch size and enrichment. A cycle 10 length of 299 EFPD was estimated from a beginning of cycle 10 case using the equilibrium shuffle pattern and the same LBP loading as cycle 9. When all transition effects die out, the projected equilibrium cycle length is 297 EFPD compared to a target value of 292 EFPD.

Thus, the initial equilibrium cycle enrichment estimate of 4.02 wt % ^{235}U for the 36-FA feed was reasonably accurate, although the detailed fuel management evaluation gave a cycle length that was slightly greater than estimated. An equilibrium feed enrichment of 3.96 wt % ^{235}U is projected for 292-EFPD cycles based on the results from this study. The equilibrium uranium utilization would be 13.76 MWy/2000 U_3O_8 , a 17.3% improvement over the three-batch annual cycle base case using the LBP shuffle scheme.

3. Core Power Distribution

The maximum allowable radial peak for these studies, 1:651, is based on the design radial peak for the Oconee-class plants. All of the 36-FA feed fuel cycles met this criterion for radial peaking, as shown below. Power distributions at beginning, middle, and end of cycle for each cycle are given in Figures A-7 through A-12.

<u>Cycle</u>	<u>Maximum calculated peak</u>	<u>Percent margin</u>
4	1.559	5.6
5	1.508	8.7
6	1.517	8.1
7	1.494	9.5
8	1.498	9.3
9	1.491	9.7

4. Burnup Distribution

The burnup accumulated by each batch of fuel during each cycle and the discharge batch average burnups are given in Table A-2 for the 36-FA feed case. The maximum assembly discharge burnup was 51,553 Mwd/mtU at EOC 9.

5. Control Rod Worths

The hot zero power (HZP) control rod pattern worth was run with the PDQ code for BOL and EOL for all cycles. These worths are listed in Table A-3 along with the maximum stuck rod worth for cycles 4 and 9.

A two-dimensional FLAME model was used at BOL and EOL of each cycle to identify the maximum stuck rod. Then the PDQ pattern worths and power deficits, along with the FLAME maximum stuck rod worth, were used to calculate a shutdown margin for each cycle. The cycles with the lowest EOC shutdown margins were selected for full-core PDQ stuck rod worth calculations and the shutdown margins recalculated. The resultant shutdown margins are given in Table A-3.

Table A-1. Fuel Inventory Plan, 36-FA Feed

<u>E</u>	<u>Batch</u>	<u>Cycle</u>							
		<u>2</u>	<u>3</u>	<u>4</u>	<u>5</u>	<u>6</u>	<u>7</u>	<u>8</u>	<u>9</u>
2.01	1					13	33		
2.67	2	61	5	29	1				
3.00	3	60	60						
3.19	4	56	56	56	48				
3.04	5		56	56	56	56			
4.02	6			56	36	36	36	33	
4.02	7				36	36	36	36	33
4.02	8					36	36	36	36
4.02	9						36	36	36
4.02	10							36	36
4.02	11								36

Table A-2. Fuel Burnup Distribution

Batch No.	Initial enrich't	No. of assemblies	MWd/mtU by cycle									Batch average burnup
			Cycle 1	Cycle 2	Cycle 3	Cycle 4	Cycle 5	Cycle 6	Cycle 7	Cycle 8	Cycle 9	
1A	2.01	10	17589	--	--	--	--	--	--	--	--	17589
1B	2.01	13	14763	--	--	--	--	--	8347	--	--	23111
1C	2.01	33	16430	--	--	--	--	--	--	9043	--	25473
2A	2.67	26	17980	9114	--	--	--	--	--	--	--	27094
2B	2.67	5	16419	9159	9233	--	--	--	--	--	--	34811
2C	2.67	29	17376	9155	--	8183	--	--	--	--	--	34714
2D	2.67	1	16419	9159	--	--	--	7315	--	--	--	32893
3	3.00	60	12850	9716	9523	--	--	--	--	--	--	32089
4A	3.19	8	--	13030	10752	9653	--	--	--	--	--	33435
4B	3.19	48	--	9123	11595	8881	8371	--	--	--	--	37969
5	3.04	56	--	--	9528	7405	8863	9332	--	--	--	35128
6A	4.02	3	--	--	--	12748	7849	11118	11814	--	--	43529
6B	4.02	33	--	--	--	12203	7239	10938	11034	8444	--	49857
7A	4.02	3	--	--	--	--	12549	8478	11987	10638	--	43652
7B	4.02	33	--	--	--	--	12025	7696	11772	9963	8439	49896
8A	4.02	3	--	--	--	--	--	13554	8487	10531	10694	43266
8B	4.02	33	--	--	--	--	--	13220	7751	10493	9977	(41441)
9A	4.02	3	--	--	--	--	--	--	14784	7619	10409	(32812)
9B	4.02	33	--	--	--	--	--	--	14101	6986	10445	(31532)
10A	4.02	3	--	--	--	--	--	--	--	13398	8004	(21402)
10B	4.02	33	--	--	--	--	--	--	--	12822	7285	(20107)
11A	4.02	3	--	--	--	--	--	--	--	--	13439	(13439)
11B	4.02	33	--	--	--	--	--	--	--	--	12892	(12892)
Core			15542	9506	10134	9019	9053	10066	10809	9796	9863	
(Not discharged)												

A-5

Table A-3. Control Rod Worths

	Cycle					
	4	5	6	7	8	9
HZP control rod worths, % $\Delta\rho$						
BOC	7.31	6.84	7.03	7.07	6.94	6.84
EOC	7.93	7.55	7.78	7.87	7.64	7.55
Max stuck rod worth, % $\Delta\rho$						
BOC	1.82	--	--	--	--	1.38
EOC	1.81	--	--	--	--	1.41
Shutdown margin, % $\Delta\rho$						
BOC	1.90	--	--	--	--	1.83
EOC	1.26	--	--	--	--	1.28

Figure A-1. Cycle 4 Core Loading Plan

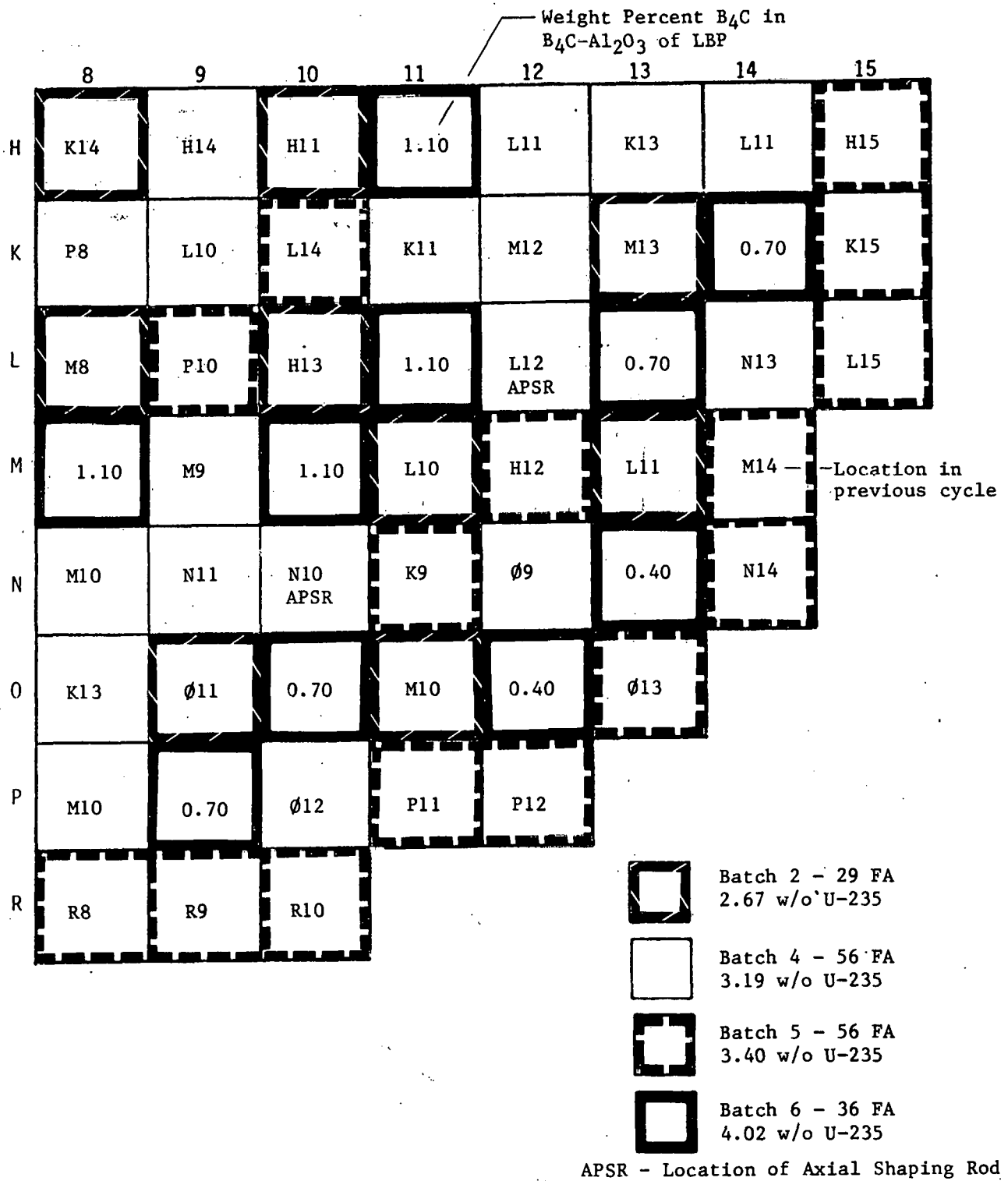


Figure A-2. Cycle 5 Core Loading Plan

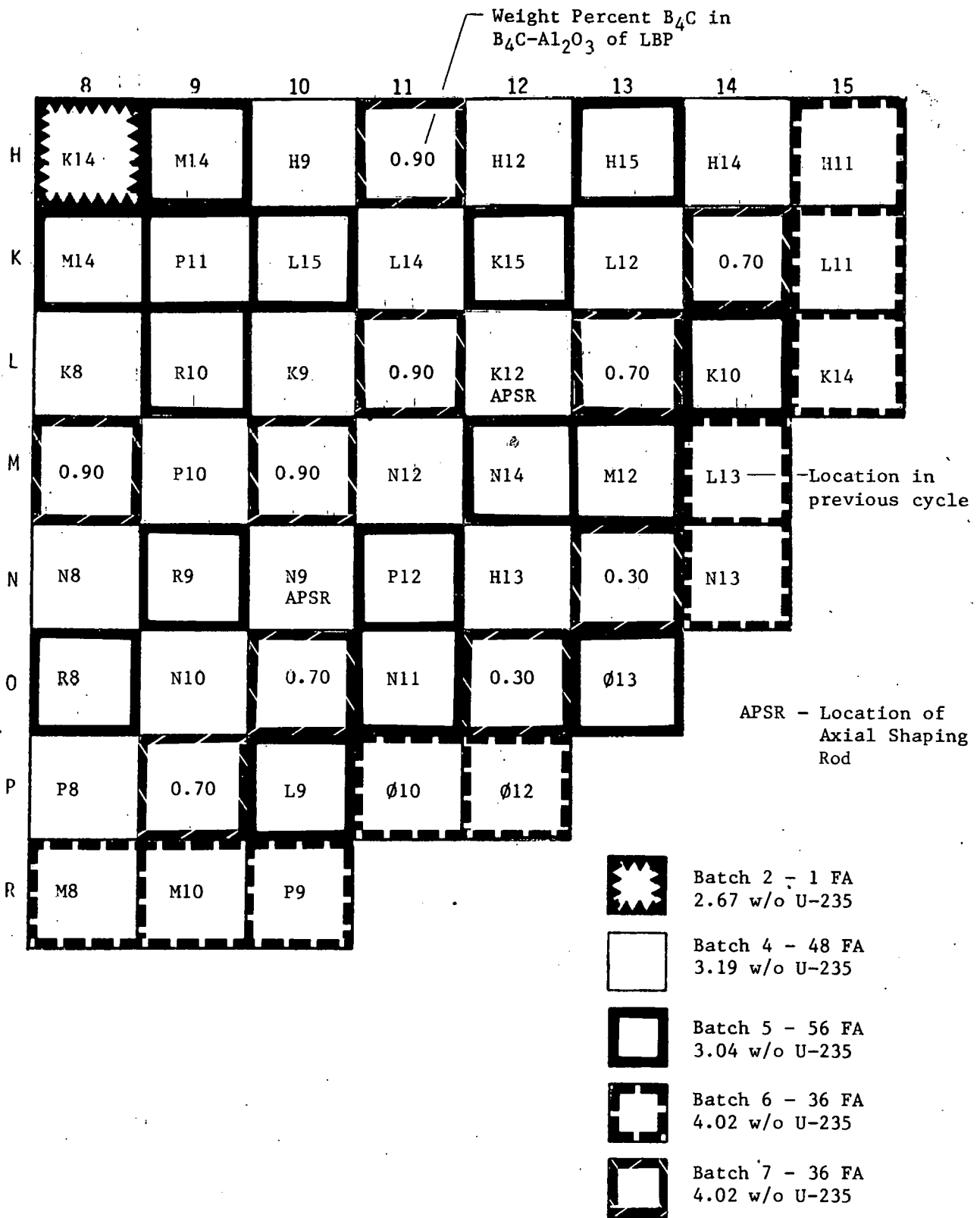


Figure A-3. Cycle 6 Core Loading Plan

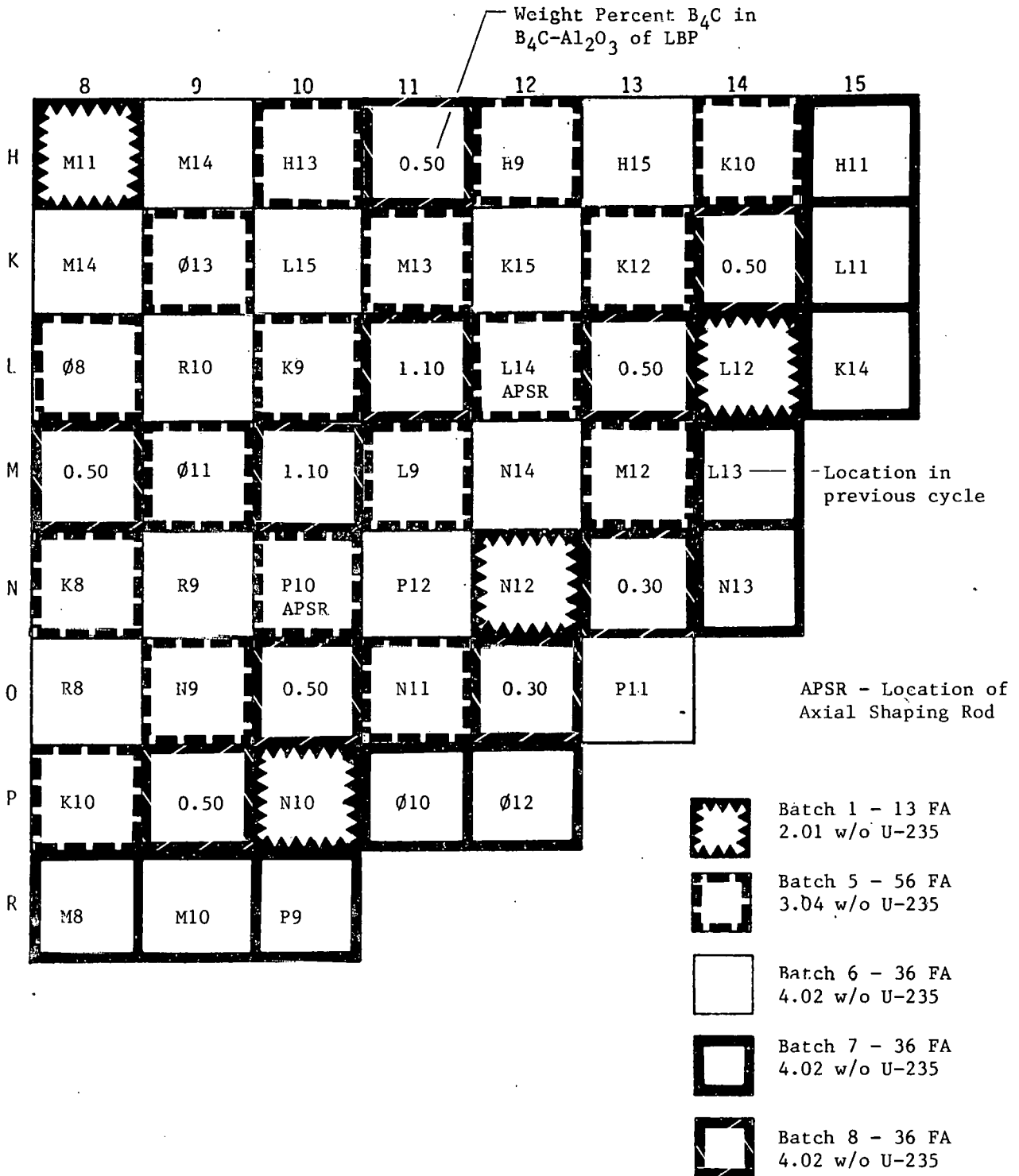
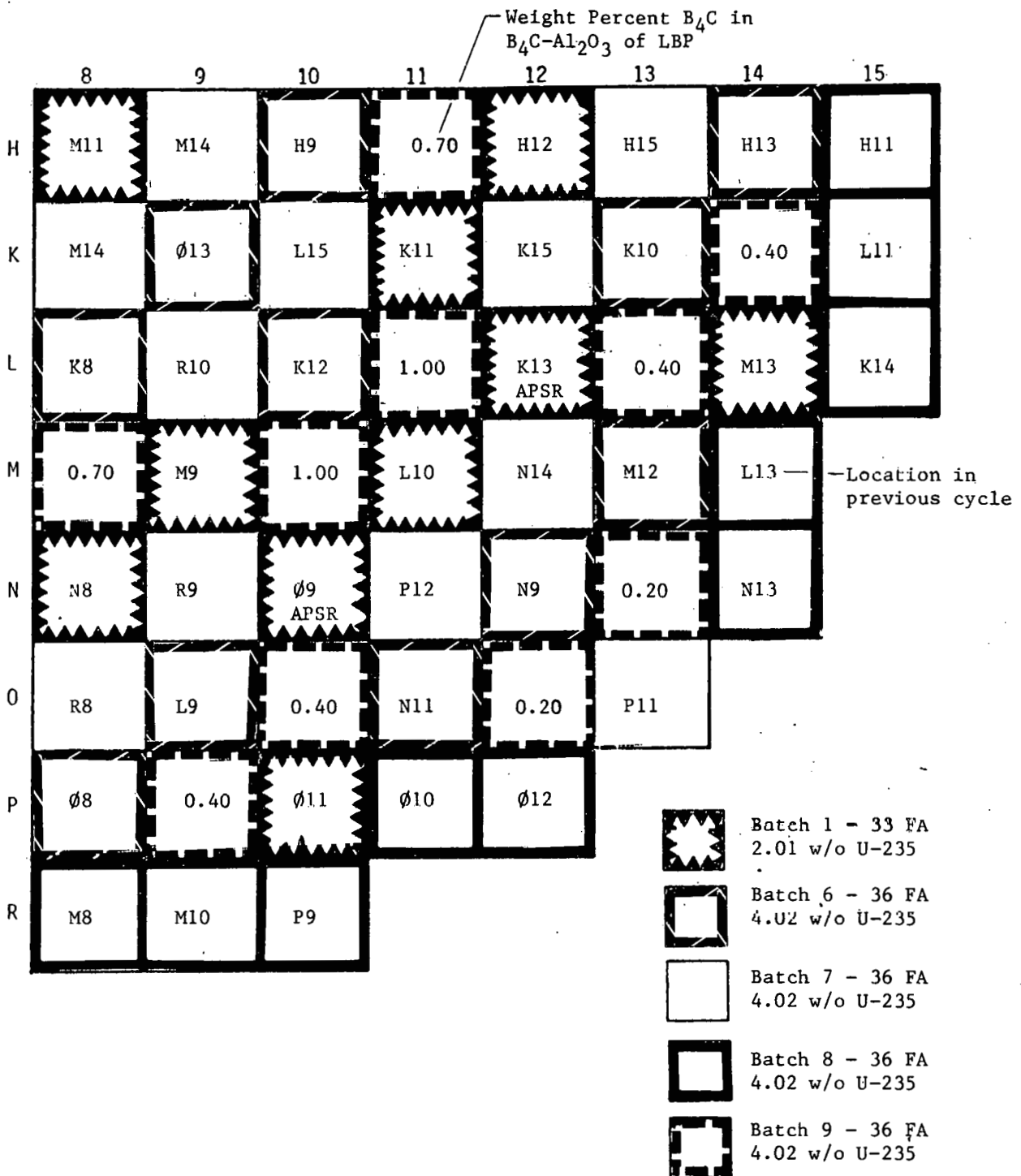
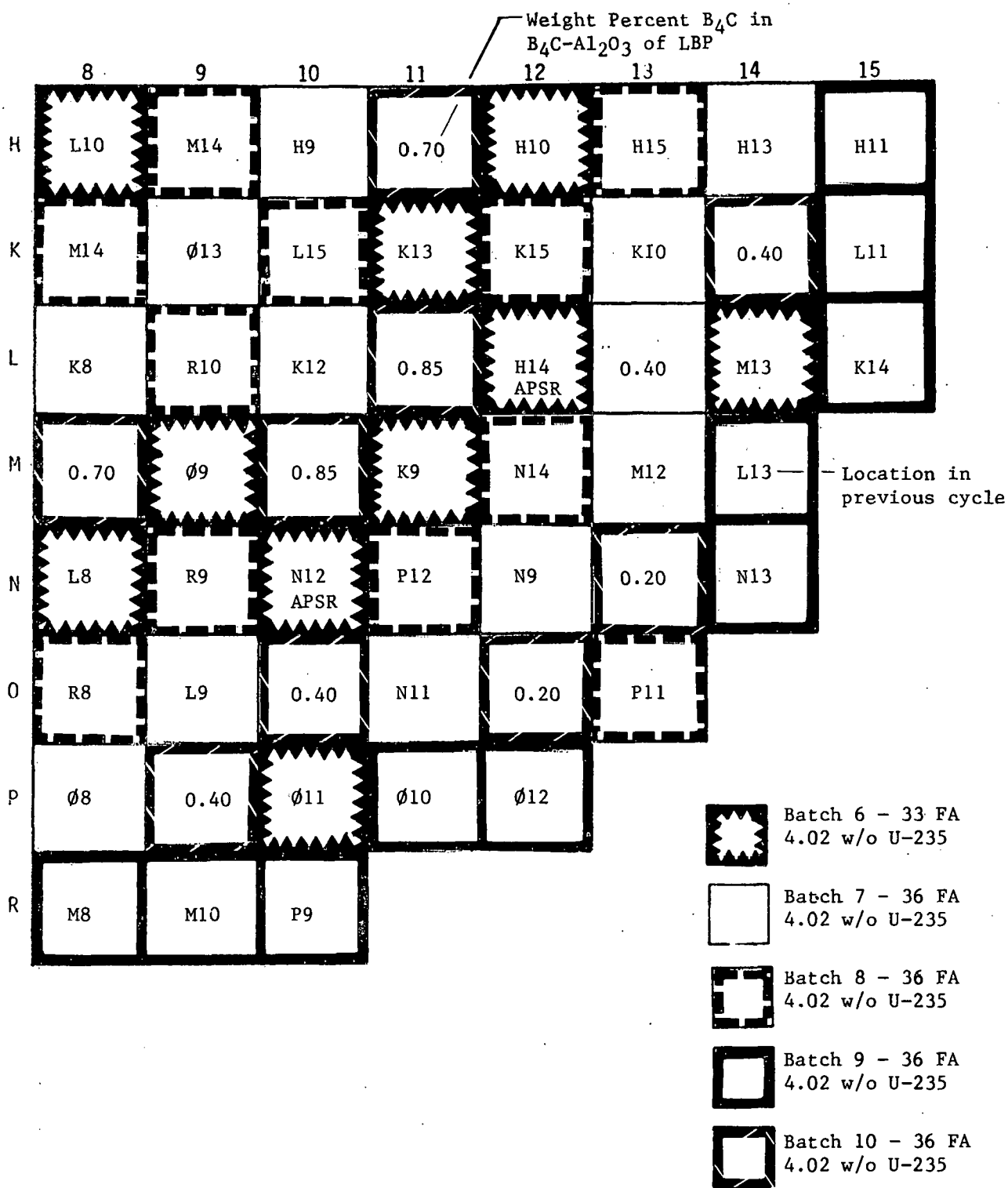


Figure A-4. Cycle 7 Core Loading Plan



APSR - Location of Axial Shaping Rod

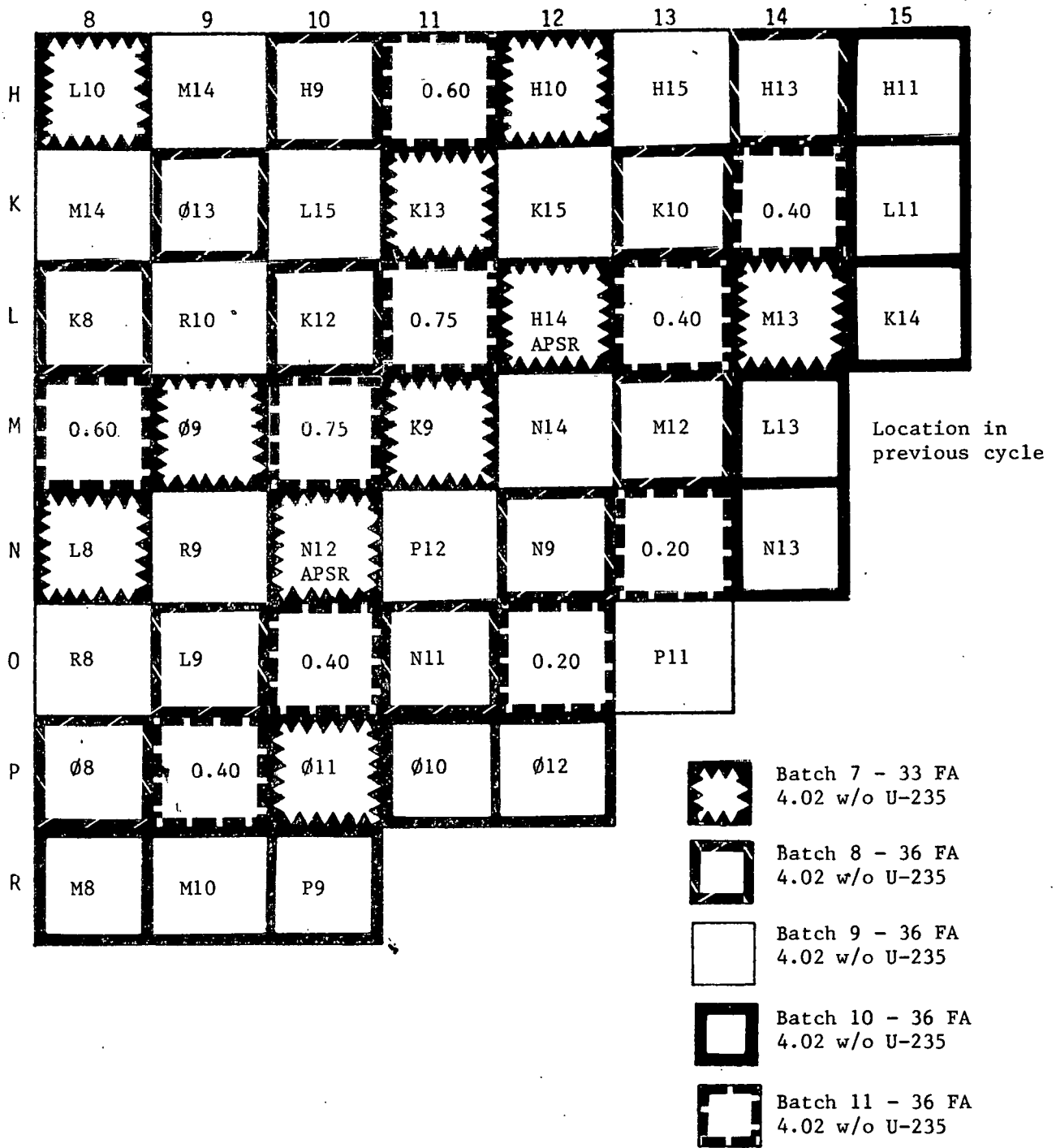
Figure A-5. Cycle 8 Core Loading Plan



APSR - Location of Axial Shaping Rod

Figure A-6. Cycle 9 Core Loading Plan

Weight Percent B_4C in
 $B_4C-Al_2O_3$ of LBP



APSR - Location of Axial Shaping Rod

Figure A-7. Cycle 4, Core Power Distribution — 36-FA Feed

	8	9	10	11	12	13	14	15
H	0.701	0.850	0.837	1.427	1.032	0.975	1.003	0.749
	0.760	0.895	0.866	1.429	1.030	0.986	1.004	0.775
	0.799	0.925	0.888	1.428	1.030	0.989	0.998	0.787
K		0.908	1.118	1.079	1.038	0.918	1.361	0.742
		0.936	1.113	1.068	1.036	0.929	1.355	0.767
		0.956	1.115	1.066	1.033	0.933	1.336	0.778
L			0.955	1.427	0.962	1.406	0.961	0.547
			0.964	1.423	0.950	1.386	0.960	0.589
			0.975	1.420	0.945	1.362	0.956	0.613
M				0.945	1.124	0.883	0.765	
				0.945	1.092	0.881	0.787	
				0.951	1.076	0.881	0.800	
N					1.092	1.297	0.599	
					1.045	1.244	0.621	
					1.023	1.213	0.637	
O						0.767	Beginning of Cycle	
						0.758	Middle of Cycle	
						0.756	End of Cycle	

Figure A-8. Cycle 5, Core Power Distribution - 36-FA Feed

	8	9	10	11	12	13	14	15
H	0.769	0.935	0.934	1.386	0.856	0.956	0.869	0.865
	0.805	0.955	0.945	1.397	0.885	0.982	0.888	0.876
	0.832	0.971	0.957	1.397	0.901	0.993	0.896	0.884
K		0.990	1.110	0.997	0.997	0.906	1.326	0.860
		0.996	1.103	1.004	1.013	0.920	1.329	0.868
		1.005	1.101	1.009	1.019	0.926	1.317	0.874
L			0.982	1.390	0.847	1.382	0.896	0.636
			0.988	1.395	0.857	1.368	0.899	0.667
			0.993	1.390	0.862	1.348	0.899	0.687
M				0.933	1.073	0.984	0.943	
				0.939	1.055	0.961	0.930	
				0.945	1.046	0.951	0.929	
N					0.925	1.281	0.715	
					0.905	1.221	0.713	
					0.899	1.188	0.720	
O						0.652	Beginning of Cycle	
						0.653	Middle of Cycle	
						0.659	End of Cycle	

Figure A-9. Cycle 6, Core Power Distribution - 36-FA Feed

	8	9	10	11	12	13	14	15
H	0.761	1.066	0.932	1.397	0.908	1.156	0.973	0.869
	0.804	1.070	0.944	1.385	0.919	1.129	0.958	0.863
	0.837	1.079	0.953	1.359	0.927	1.112	0.948	0.867
K		0.934	1.187	0.874	1.112	0.968	1.367	0.840
		0.948	1.173	0.896	1.104	0.963	1.332	0.839
		0.962	1.167	0.912	1.098	0.958	1.296	0.844
L			0.963	1.337	0.804	1.375	0.778	0.592
			0.978	1.358	0.818	1.350	0.797	0.628
			0.992	1.370	0.830	1.316	0.808	0.657
M				1.006	1.189	0.937	0.869	
				1.010	1.162	0.934	0.882	
				1.015	1.145	0.931	0.894	
N					0.895	1.227	0.662	
					0.902	1.200	0.682	
					0.905	1.175	0.702	
O						0.673	Beginning of Cycle	
						0.689	Middle of Cycle	
						0.702	End of Cycle	

Figure A-10. Cycle 7, Core Power Distribution - 36-FA Feed

	8	9	10	11	12	13	14	15
H	0.971	1.103	1.043	1.380	0.821	1.131	0.989	0.785
	0.818	1.085	1.037	1.398	0.865	1.116	0.977	0.801
	0.849	1.086	1.035	1.381	0.889	1.102	0.968	0.819
K		1.061	1.231	0.870	1.101	1.063	1.326	0.766
		1.043	1.204	0.912	1.110	1.048	1.301	0.785
		1.042	1.188	0.933	1.106	1.033	1.265	0.803
L			1.099	1.349	0.776	1.384	0.730	0.531
			1.094	1.379	0.806	1.351	0.760	0.578
			1.089	1.380	0.824	1.305	0.779	0.619
M				0.869	1.175	1.015	0.825	
				0.903	1.144	0.986	0.836	
				0.925	1.129	0.976	0.856	
N					1.048	1.252	0.642	
					1.003	1.180	0.649	
					0.988	1.146	0.673	
O						0.679	Beginning of Cycle	
						0.671	Middle of Cycle	
						0.685	End of Cycle	

Figure A-11. Cycle 8, Core Power Distribution - 36-FA Feed

	8	9	10	11	12	13	14	15
H	0.774	1.043	1.019	1.357	0.844	1.098	0.969	0.766
	0.806	1.051	1.024	1.374	0.872	1.096	0.973	0.799
	0.836	1.063	1.028	1.368	0.889	1.089	0.969	0.819
K		1.028	1.197	0.924	1.069	1.046	1.313	0.747
		1.030	1.182	0.943	1.076	1.039	1.304	0.780
		1.037	1.174	0.953	1.078	1.028	1.278	0.799
L			1.094	1.369	0.817	1.373	0.755	0.517
			1.086	1.377	0.825	1.342	0.776	0.570
			1.082	1.372	0.831	1.307	0.788	0.607
M				0.971	1.174	1.019	0.814	
				0.969	1.136	0.990	0.828	
				0.972	1.120	0.980	0.846	
N					1.058	1.282	0.652	
					1.010	1.209	0.661	
					0.994	1.175	0.681	
O						0.687	Beginning of Cycle	
						0.681	Middle of Cycle	
						0.690	End of Cycle	

Figure A-12. Cycle 9, Core Power Distribution - 36-FA Feed

	8	9	10	11	12	13	14	15
H	0.740	1.007	0.994	1.341	0.828	1.085	0.982	0.814
	0.786	1.032	1.010	1.363	0.860	1.084	0.980	0.835
	0.821	1.050	1.018	1.354	0.878	1.080	0.974	0.850
K		0.984	1.173	0.980	1.045	1.038	1.328	0.790
		1.002	1.169	0.932	1.058	1.031	1.310	0.812
		1.016	1.164	0.942	1.061	1.022	1.282	0.827
L			1.089	1.363	0.804	1.367	0.766	0.545
			1.086	1.372	0.815	1.335	0.783	0.593
			1.079	1.361	0.822	1.302	0.794	0.629
M				0.969	1.167	1.025	0.846	
				0.968	1.129	0.993	0.853	
				0.970	1.114	0.982	0.869	
N					1.065	1.287	0.670	
					1.014	1.209	0.675	
					0.997	1.175	0.694	
O						0.691	Beginning of Cycle	
						0.682	Middle of Cycle	
						0.691	End of Cycle	

APPENDIX B

Description of Fuel Cycle Study

Feed batch size:	60 assemblies
Cycle length:	497 EFPD
Power level:	2568 MWt
Control mode:	Rodded

Introduction

The fuel management plan described in detail in this appendix was chosen to provide fuel cycle data at burnups of 45,838 MWd/mtU with an approximately 18-month cycle. This fuel management plan loads 60 fresh fuel assemblies per cycle and, thus, represents a three-batch reload for a 177 fuel assembly core. As indicated in section 5.1.3, this fuel cycle provided a 6.7% fuel utilization improvement relative to the base case and also offers the increased availability potential of an 18-month cycle.

1. Fuel Shuffle Patterns

These cycles employed the LBP shuffle scheme, whereby the fresh fuel assemblies with LBP are loaded in the interior of the core in an approximate checkerboard pattern. For a 60-FA feed, eight fresh FAs were located on the core periphery along with once-burned fuel to achieve a flatter core power distribution. Table B-1 describes the fuel inventory plan utilized.

Cycle 5, the first transition cycle, was initiated by shuffling of the fuel isotopics from ANO-1 cycle 4 at 387 EFPD. Sixty-four once-burned and fifty-three twice-burned assemblies from cycle 4 were used in cycle 5. The cycle 5 fuel loading pattern and LBP concentrations are shown in Figure B-1. Cycle 5 was depleted to 469 EFPD and shuffled to the next cycle.

Cycles 5, 6, and 7, which are approaching an equilibrium cycle, all utilize the same fresh fuel loading pattern. The fuel shuffle patterns and LBP concentrations used in these cycles are given in Figures B-2 and B-3, respectively.

2. Cycle Lifetime and Uranium Utilization

The cycle lifetimes attained were 466, 466, 510, and 505 EFPD for cycles 5 through 8. These cycles were run to the same EOL effective multiplication factor (k_{eff}) using a constant feed batch size and enrichment. When all transition effects die out, the projected equilibrium cycle length is 507 EFPD compared to a target value of 497 EFPD. Thus, the initial equilibrium cycle estimate of 4.106 wt % ^{235}U for the 60-FA feed was reasonably accurate, although the detailed fuel management evaluation gave a cycle length slightly greater than estimated. An equilibrium feed enrichment of 4.085 wt % ^{235}U is projected for 497 EFPD cycles based on the results from this study. The equilibrium uranium utilization would be 12.52 MWy/2000 lb U_3O_8 , a 6.7% improvement over the three-batch annual cycle base case using the LBP shuffle scheme.

3. Core Power Distribution

The maximum allowable radial peak for these studies was a 1.651 and is based on the design radial peak for the Oconee class plants. All of the 60 feed fuel cycles met this criterion for radial peaking as shown below. Power distributions at beginning, middle, and end of cycle for each cycle are given in Figures B-4, B-5, B-6, and B-7.

<u>Cycle</u>	<u>Maximum calculated peak</u>	<u>Percent margin</u>
5	1.638	0.8
6	1.644	0.4
7	1.579	4.4
8	1.576	4.5

4. Burnup Distribution

The burnup accumulated by each batch of fuel during each cycle and the discharge batch average burnups are given in Table B-2 for the 60-FA feed case. The maximum assembly discharge burnup was 55,713 MWd/mtU at EOC 8.

5. Control Rod Worths

The hot zero power (HZP) control rod pattern worth was run with PDQ for BOL and EOL for all cycles. These worths are listed in Table B-3 along with the maximum stuck rod worth for cycles 5 and 8.

A two-dimensional FLAME model was used at beginning and end of each cycle to identify the stuck rod of maximum worth. Then the PDQ pattern worths and power deficits, along with the FLAME maximum stuck rod worth, were used to calculate a shutdown margin for each cycle. The cycles with the lowest EOC shutdown margin were selected for full-core PDQ stuck rod worth calculations and the shutdown margins recalculated. The resultant margins are given in Table B-3.

Table B-1. Fuel Inventory Plan - 60-FA

<u>Batch</u>	<u>Enrichment</u>	<u>Cycle</u>							
		<u>1</u>	<u>2</u>	<u>3</u>	<u>4</u>	<u>5</u>	<u>6</u>	<u>7</u>	<u>8</u>
1	2.06	56		5	1				
2	2.75	61	61						
3	3.05	60	60	60					
4	2.64		56	56	56				
5	3.01			56	56	53			
6	3.19				64	64	57		
7	4.106					60	60	57	
8	4.106						60	60	57
9	4.106							60	60
10	4.106								60

Table B-2. Fuel Burnup Distribution

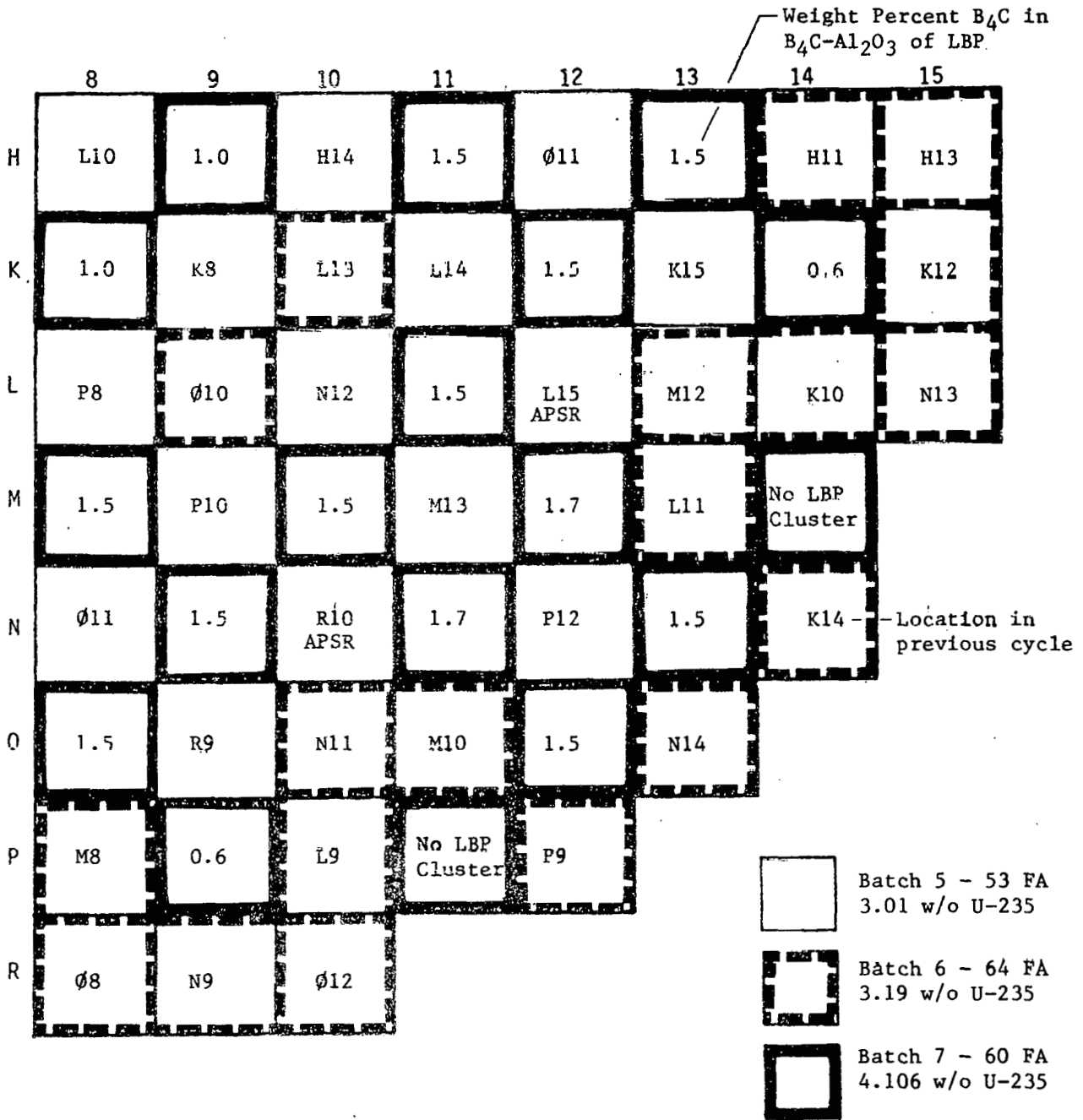
Batch No.	Initial enrich't	No. of assemblies	Mwd/mtU by cycle									Batch average burnup
			Cycle 1	Cycle 2	Cycle 3	Cycle 4	Cycle 5	Cycle 6	Cycle 7	Cycle 8	Cycle 9	
1A	2.06	50	17203	--	--	--	--	--	--	--	--	17203
1B	2.06	5	13438	--	6420	--	--	--	--	--	--	19858
1C	2.06	1	14854	--	--	10129	--	--	--	--	--	24983
2	2.75	61	17926	8221	--	--	--	--	--	--	--	26147
3	3.05	60	12231	9517	8403	--	--	--	--	--	--	30151
4	2.64	56	--	7752	9852	10678	--	--	--	--	--	28282
5A	3.01	3	--	--	12264	15768	--	--	--	--	--	28032
5B	3.01	53	--	--	8458	9745	14421	--	--	--	--	32624
6A	3.19	7	--	--	--	16610	15369	--	--	--	--	31979
6B	3.19	57	--	--	--	15012	10523	13815	--	--	--	39350
7A	4.11	3	--	--	--	--	20855	16347	--	--	--	37202
7B	4.11	57	--	--	--	--	18366	10986	16146	--	--	45498
8A	4.11	3	--	--	--	--	--	21148	17625	--	--	38773
8B	4.11	57	--	--	--	--	--	18508	11431	16065	--	46004
9A	4.11	3	--	--	--	--	--	--	19880	17035	--	36915
9B	4.11	57	--	--	--	--	--	--	20003	11083	--	(31086)
10A	4.11	3	--	--	--	--	--	--	--	22428	--	(22428)
10B	4.11	57	--	--	--	--	--	--	--	19847	--	(19847)
Core			15647	8512	8887	12112	14583	14583	15959	15803		
(Not discharged)												

B-4

Table B-3. Control Rod Worths

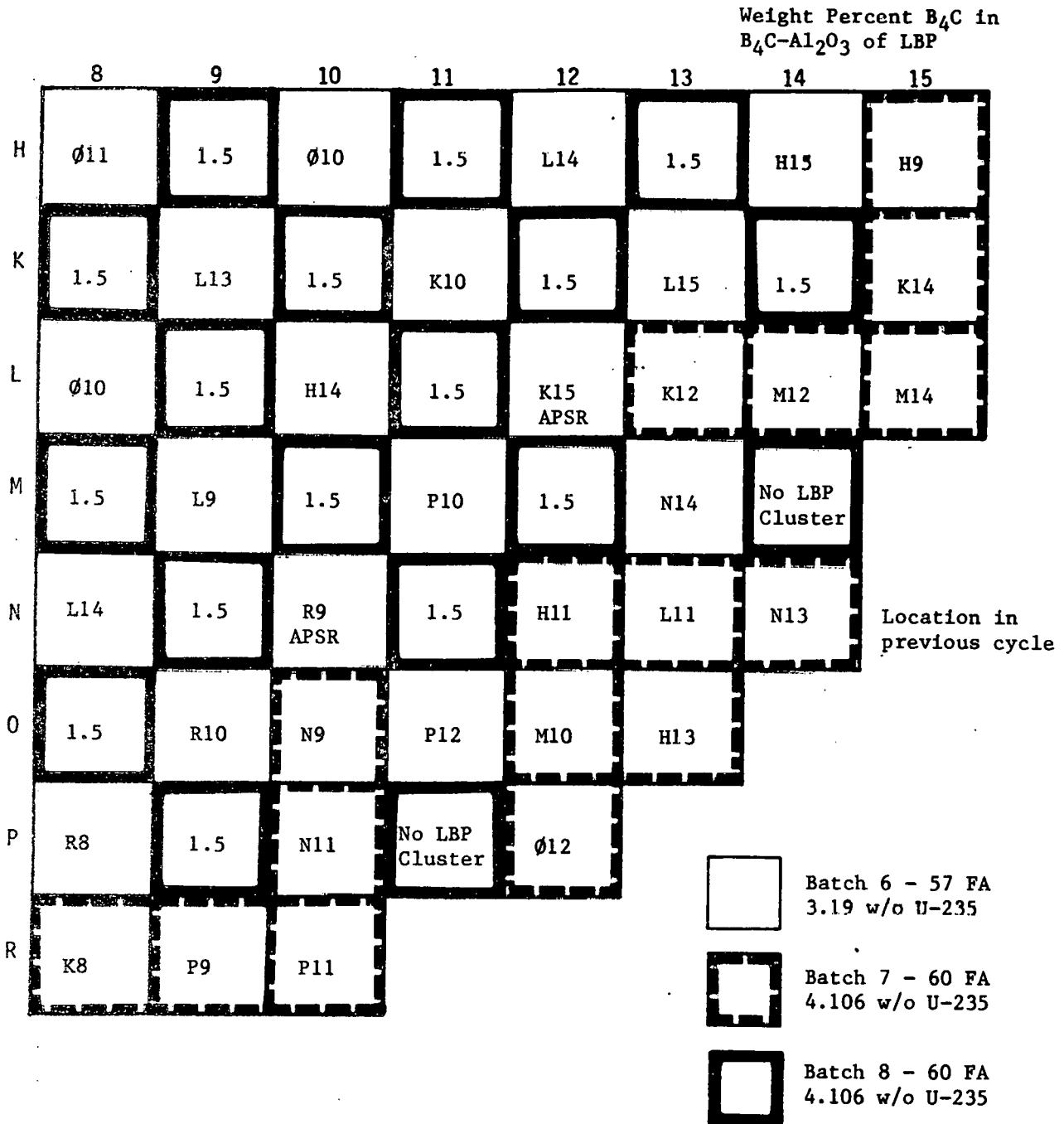
	Cycle			
	5	6	7	8
H2P control rod worths, %Δρ				
BOC (groups 1-6)	7.47	7.21	7.06	7.14
EOC (groups 1-7)	8.87	8.74	8.68	8.76
Max stuck rod worth, %Δρ				
BOC	1.26	--	--	0.85
EOC	1.90	--	--	1.85
Shutdown margin, %Δρ				
BOC	2.67	--	--	2.49
EOC	1.80	--	--	1.51

Figure B-1. Cycle 5 Core Loading Plan



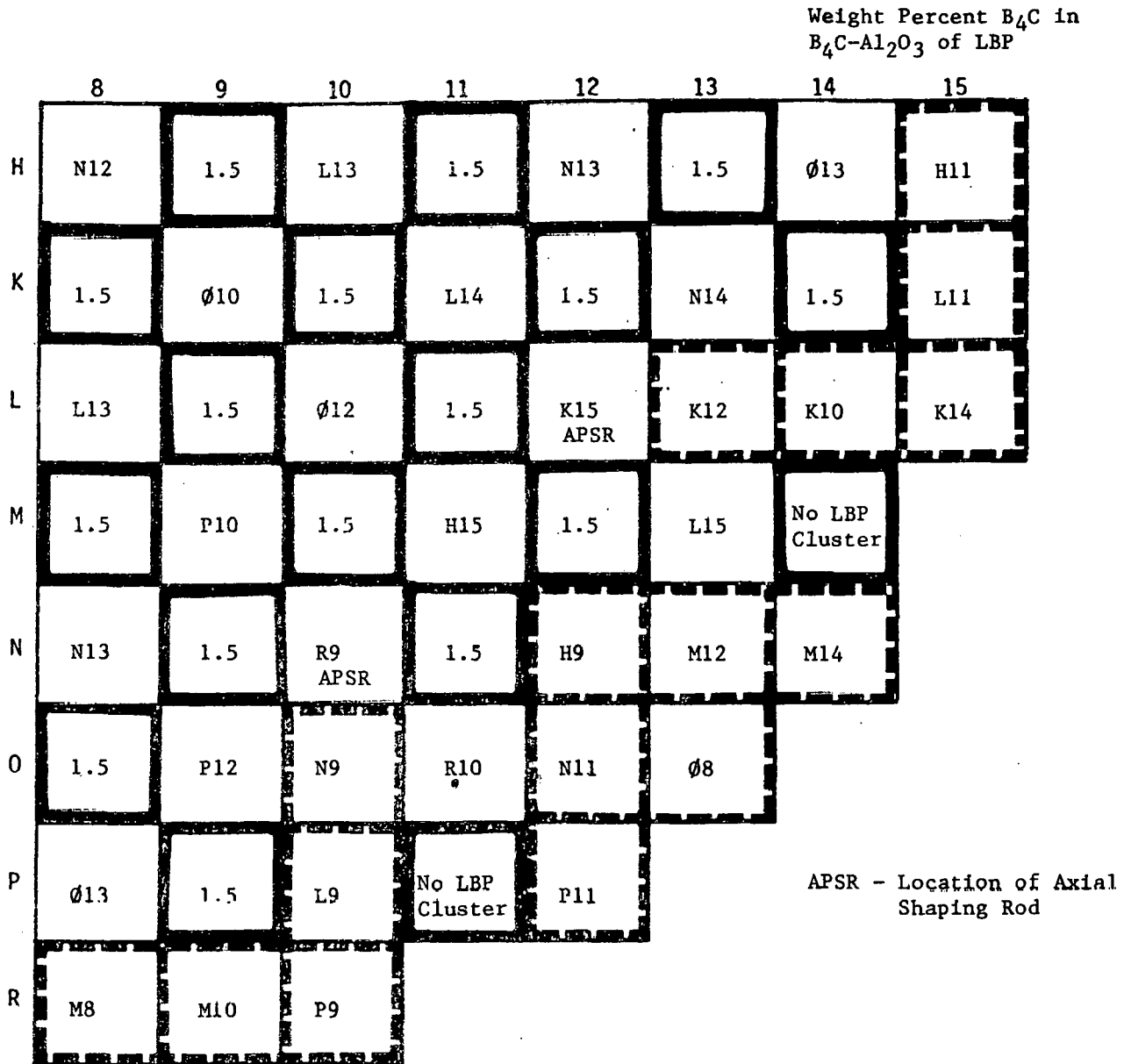
APSR - Location of Axial Shaping Rod

Figure B-2. Cycle 6 Core Loading Plan



APSR- Location of Axial Shaping Rod

Figure B-3. Core Loading Plan For Cycles 7 and 8






	Cycle 7	Cycle 8
	Batch 7 - 57 FA 4.106 w/o U-235	Batch 8 - 57 FA 4.106 w/o U-235
	Batch 8 - 60 FA 4.106 w/o U-235	Batch 9 - 60 FA 4.106 w/o U-235
	Batch 9 - 60 FA 4.106 w/o U-235	Batch 10 - 60 FA 4.106 w/o U-235

Figure B-4. Cycle 5 Core Power Distribution - 60-FA Feed, Rodded

	8	9	10	11	12	13	14	15
H	1.048	1.462	1.036	1.460	1.126	1.355	0.570	0.389
	1.016	1.406	1.009	1.440	1.104	1.361	0.618	0.475
	0.925	1.276	0.965	1.342	1.047	1.455	1.198	0.703
K		1.012	1.033	1.083	1.469	1.104	1.071	0.433
		0.988	1.011	1.066	1.447	1.080	1.108	0.511
		0.960	1.057	1.041	1.349	1.080	1.270	0.650
L			0.595	1.307	1.022	1.097	0.853	0.393
			0.633	1.324	1.004	1.050	0.854	0.456
			1.104	1.374	0.934	0.968	0.842	0.509
M				1.052	1.447	1.111	1.056	
				1.050	1.426	1.055	1.005	
				1.012	1.272	0.927	0.907	
N					1.194	1.121	0.497	
					1.152	1.146	0.536	
					0.997	1.023	0.501	
O						0.536	Beginning of Cycle	
						0.595	Middle of Cycle	
						0.552	End of Cycle	

Figure B-5. Cycle 6 Core Power Distribution - 60-FA Feed, Rodded

	8	9	10	11	12	13	14	15
H	0.988	1.383	0.977	1.401	1.037	1.293	0.507	0.460
	1.025	1.471	1.054	1.443	1.017	1.446	1.096	0.732
	0.980	1.378	1.009	1.371	1.000	1.408	1.088	0.760
K		0.958	1.290	0.971	1.396	1.077	1.042	0.553
		1.071	1.551	1.041	1.362	1.049	1.252	0.716
		1.019	1.449	1.006	1.319	1.048	1.254	0.750
L			0.674	1.279	0.952	1.181	1.000	0.504
			1.337	1.456	0.879	0.971	0.870	0.530
			1.248	1.386	0.876	0.994	0.907	0.579
M				0.998	1.389	0.965	1.102	
				0.966	1.176	0.739	0.795	
				0.959	1.185	0.788	0.864	
N					1.237	0.969	0.572	
					0.901	0.697	0.432	
					0.943	0.762	0.497	
O						0.565	Beginning of Cycle	
						0.431	Middle of Cycle	
						0.496	End of Cycle	

Figure B-6. Cycle 7 Core Power Distribution - 60-FA Feed, Rodded

	8	9	10	11	12	13	14	15
H	1.033	1.337	1.028	1.406	1.149	1.243	0.503	0.386
	1.105	1.449	1.082	1.452	1.135	1.280	0.563	0.479
	0.993	1.317	1.018	1.323	1.050	1.376	1.132	0.738
K		0.996	1.264	1.079	1.408	1.111	0.941	0.451
		1.067	1.357	1.091	1.405	1.086	1.011	0.533
		1.027	1.388	1.044	1.288	1.085	1.227	0.708
L			0.697	1.323	1.099	1.170	0.918	0.425
			0.747	1.337	1.043	1.085	0.892	0.479
			1.242	1.351	0.945	0.995	0.895	0.557
M				1.198	1.428	1.087	1.026	
				1.135	1.349	0.993	0.937	
				1.052	1.177	0.874	0.857	
N					1.210	0.927	0.533	
					1.090	0.861	0.530	
					0.929	0.758	0.501	
O						0.527	Beginning of Cycle	
						0.532	Middle of Cycle	
						0.497	End of Cycle	

Figure B-7. Cycle 8 Core Power Distribution - 60-FA Feed, Rodded

	8	9	10	11	12	13	14	15
H	1.060	1.392	1.067	1.457	1.169	1.273	0.511	0.379
	1.031	1.408	1.069	1.408	1.079	1.428	1.142	0.689
	0.981	1.317	1.017	1.332	1.051	1.389	1.137	0.724
K		1.034	1.315	1.113	1.436	1.126	0.947	0.438
		1.080	1.493	1.096	1.347	1.099	1.223	0.652
		1.023	1.392	1.050	1.299	1.095	1.233	0.693
L			0.711	1.343	1.072	1.140	0.899	0.417
			1.325	1.437	0.946	0.962	0.845	0.498
			1.235	1.360	0.934	0.987	0.891	0.553
M				1.198	1.399	1.062	1.005	
				1.081	1.180	0.828	0.786	
				1.060	1.184	0.880	0.863	
N					1.158	0.866	0.507	
					0.880	0.674	0.427	
					0.925	0.744	0.498	
O						0.492	Beginning of Cycle	
						0.419	Middle of Cycle	
						0.489	End of Cycle	

APPENDIX C

Description of Fuel Cycle Study

Feed batch size: 60 assemblies
Cycle length: 460 EFPD
Power level: 2772 MWt
Control mode: Feed and bleed

Introduction

The fuel management plan described in detail in this appendix was chosen to provide fuel cycle data at burnups of 45,838 MWd/mtU with an approximately 18-month cycle. This fuel management plan loads 60 fresh fuel assemblies per cycle and, thus, represents a three-batch reload for a 177 fuel assembly core. As indicated in section 5.1.3, this fuel cycle provided a 6.9% fuel utilization improvement relative to the base case and also offers the increased availability potential of an 18-month cycle.

1. Fuel Shuffle Patterns

These cycles employed the LBP shuffle scheme, whereby the fresh fuel assemblies with LBP are loaded in the interior of core in an approximate checkerboard pattern. For the 60-FA feed, eight fresh fuel assemblies were located on the core periphery along with once burned fuel to achieve a flatter core power distribution. Table C-1 gives the fuel inventory plan used.

Cycle 5, the first transition cycle, was initiated by shuffling the fuel isotopics from ANO-1 cycle 4 at 387 EFPD. Sixty-four once-burned and fifty-three twice-burned assemblies from cycle 4 were used in cycle 5. The cycle 5 fuel loading pattern is shown in Figure C-1, which gives the LBP concentrations for cycle 5. Cycle 5 was depleted to 430 EFPD and shuffled to the next cycle.

Cycle 5, 6, and 7, which are approaching an equilibrium cycle, all utilize the same fresh fuel loading pattern. The fuel shuffle pattern and LBP concentrations used in these cycles are given in Figures C-2 and C-3, respectively.

2. Cycle Lifetime and Uranium Utilization

The cycle lifetimes attained were 430, 427, 474, and 476 EFPD for cycles 5 through 8. These cycles were run to the same EOL effective multiplication factor (k_{eff}) using a constant feed batch size and enrichment. When all transition effects die out, the projected equilibrium cycle length is 463 EFPD compared to a target value of 460 EFPD. Thus, the initial equilibrium cycle estimate of 4.106 wt % ^{235}U for the 60-FA feed was reasonably accurate, although the detailed fuel management evaluation gave a cycle that was slightly greater than estimated. An equilibrium feed enrichment of 4.079 wt % ^{235}U is projected for 460 EFPD cycles based on the results from this study. The equilibrium uranium utilization would be 12.54 MWy/2000 lb U_3O_8 , a 6.9% improvement over the three-batch annual cycle base case using the LBP shuffle scheme.

3. Core Power Distribution

The maximum allowable radial peak for these studies, 1.651, is based on the design radial peak for the Oconee-class plants. All of the 60-FA feed fuel cycles met this criterion for radial peaking as shown below. Power distributions at the beginning, middle, and end of cycle are given in Figures C-4 through C-7 for each cycle.

<u>Cycle</u>	<u>Maximum calculated peak</u>	<u>Percent margin</u>
5	1.566	5.2
6	1.548	6.2
7	1.510	8.5
8	1.577	4.5

4. Burnup Distribution

The burnup accumulated by each batch of fuel during each cycle and the discharge batch average burnups are given in Table C-2 for the 60-FA feed case. The maximum assembly discharge burnup was 54,506 MWd/mtU at EOC 8.

5. Control Rod Worths

The hot zero power (HZP) control rod pattern with was run with PDQ for BOL and EOL for all cycles. These worths are listed in Table C-3 along with the maximum stuck rod worth for cycles 5 and 8.

A two-dimensional FLAME model was used at the BOL and EOL of each cycle to identify the maximum stuck rod. Then the PDQ pattern worths and power deficits, along with the FLAME maximum stuck rod worth, were used to calculate a shutdown margin for each cycle. The cycles with the lowest EOC shutdown margin were selected for full-core PDQ stuck rod worth calculations and the shutdown margins recalculated. The resultant shutdown margins are given in Table C-3.

Table C-1. Fuel Inventory Plan - 60-FA Feed,
Feed and Bleed

<u>Batch</u>	<u>Enrichment</u>	<u>Cycle</u>							
		<u>1</u>	<u>2</u>	<u>3</u>	<u>4</u>	<u>5</u>	<u>6</u>	<u>7</u>	<u>8</u>
1	2.06	56		5	1				
2	2.75	61	61						
3	3.05	60	60	60					
4	2.64		56	56	56				
5	3.01			56	56	53			
6	3.19				64	64	57		
7	4.106					60	60	57	
8	4.106						60	60	57
9	4.106							60	60
10	4.106								60

Table C-2. Fuel Burnup Distribution

Batch No.	Initial enrich't	No. of assemblies	Mwd/mtU by cycle									Batch average burnup
			Cycle 1	Cycle 2	Cycle 3	Cycle 4	Cycle 5	Cycle 6	Cycle 7	Cycle 8	Cycle 9	
1A	2.06	50	17203	--	--	--	--	--	--	--	--	17203
1B	2.06	5	13438	--	6420	--	--	--	--	--	--	19858
1C	2.06	1	14854	--	--	10129	--	--	--	--	--	24983
2	2.75	61	17926	8221	--	--	--	--	--	--	--	26147
3	3.05	60	12231	9517	8403	--	--	--	--	--	--	30151
4	2.64	56	--	7752	9852	10678	--	--	--	--	--	28282
5A	3.01	3	--	--	12264	15768	--	--	--	--	--	28032
5B	3.01	53	--	--	8458	9745	14447	--	--	--	--	32650
6A	3.19	7	--	--	--	16610	14573	--	--	--	--	31183
6B	3.19	57	--	--	--	15012	10714	13967	--	--	--	39693
7A	4.11	3	--	--	--	--	20141	15261	--	--	--	35402
7B	4.11	57	--	--	--	--	18158	10626	16722	--	--	45506
8A	4.11	3	--	--	--	--	--	20670	16627	--	--	37297
8B	4.11	57	--	--	--	--	--	18285	11086	16921	--	46292
9A	4.11	3	--	--	--	--	--	--	22106	16223	--	38329
9B	4.11	57	--	--	--	--	--	--	19875	10852	--	(30727)
10A	4.11	3	--	--	--	--	--	--	--	22572	--	(22572)
10B	4.11	57	--	--	--	--	--	--	--	20161	--	(20161)
Core			15647	8512	8887	12112	14542	14418	16012	16094		
(Not discharged)												

C-5

Table C-3. Control Rod Worths

	Cycle			
	5	6	7	8
HZP control rod worths, % $\Delta\rho$				
BOC	8.07	7.86	7.82	7.96
EOC	8.66	8.58	8.52	8.61
Max stuck rod worth, % $\Delta\rho$				
BOC	1.52	--	--	0.74
EOC	1.94	--	--	1.21
Shutdown margin, % $\Delta\rho$				
BOC	3.48	--	--	3.55
EOC	1.59	--	--	2.20

Figure C-1. Cycle 5 Core Loading Plan

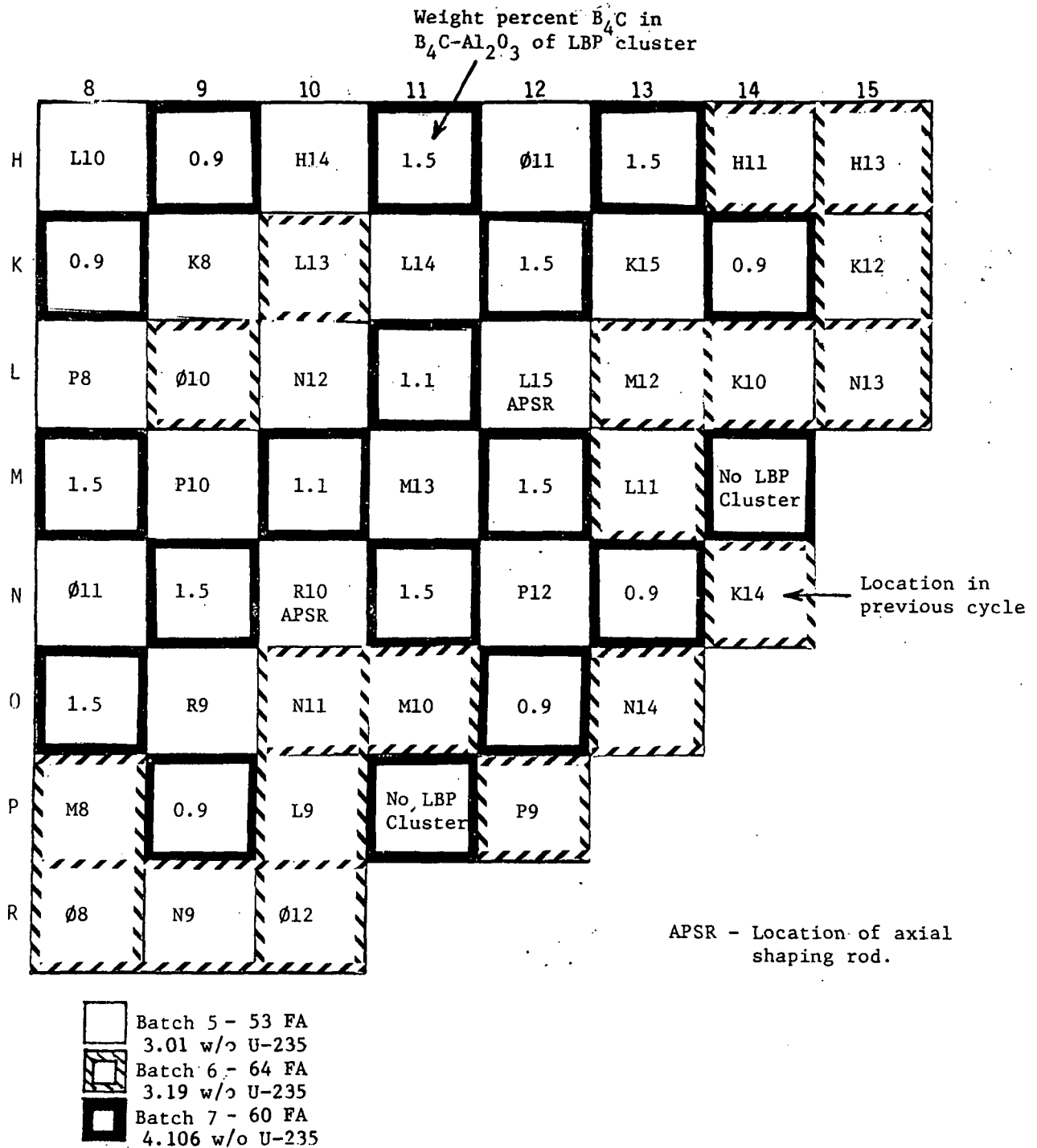
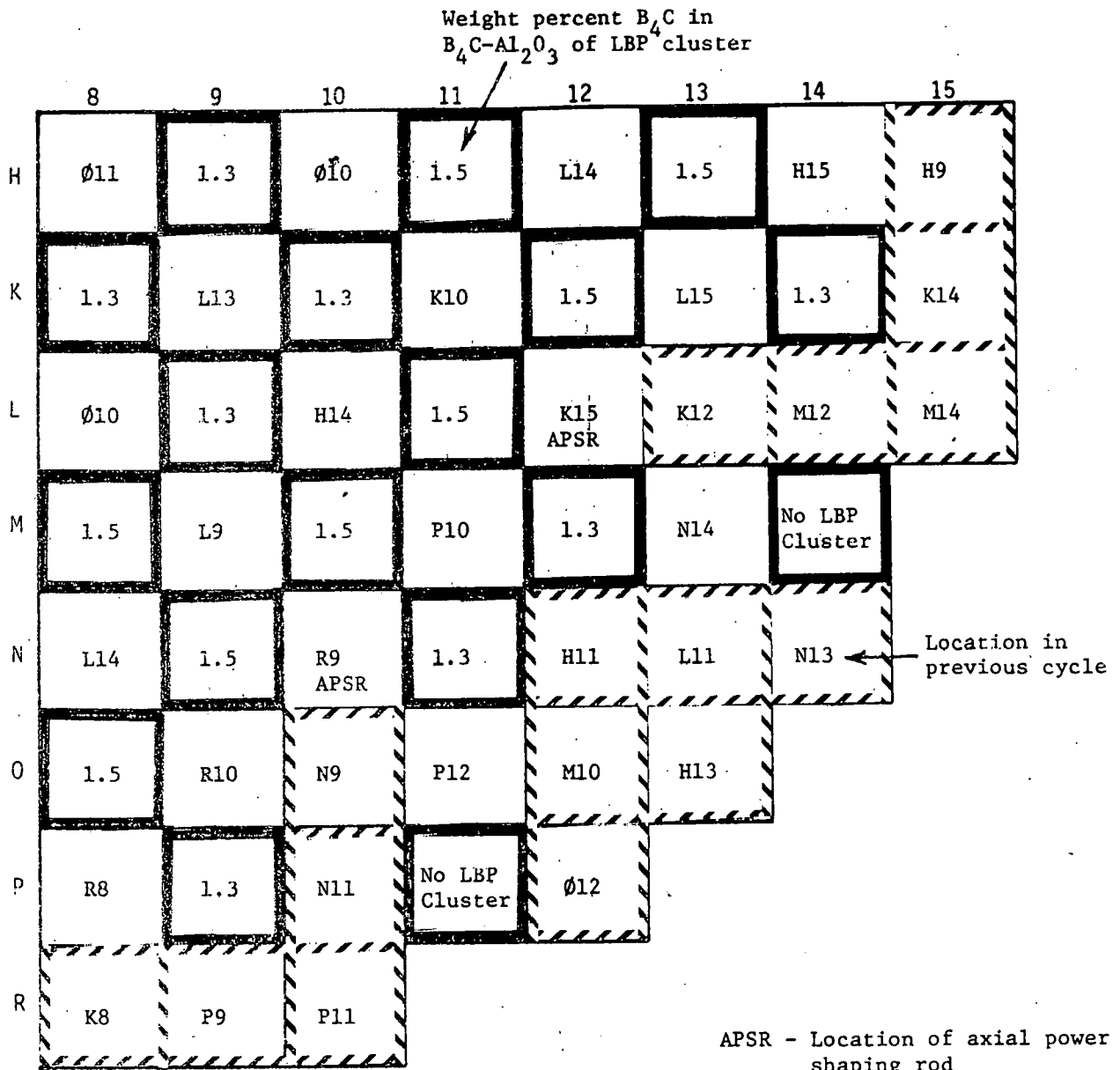





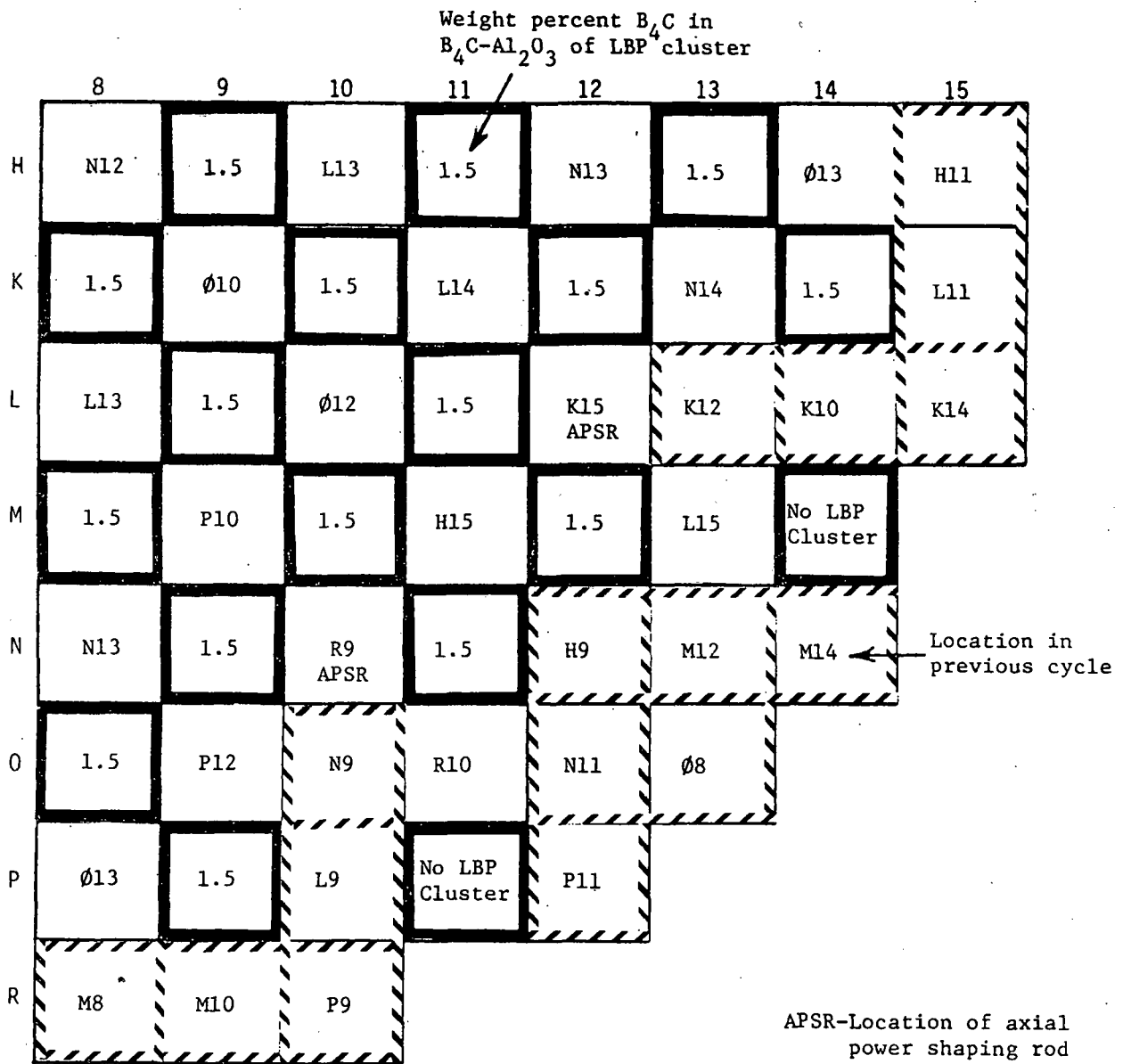
Figure C-2. Cycle 6 Core Loading Plan



-  Batch 6 - 57 FA
3.19 w/o U-235
-  Batch 7 - 60 FA
4.106 w/o U-235
-  Batch 8 - 60 FA
4.106 w/o U-235







APSR - Location of axial power
shaping rod

Figure C-3. Core Loading Plan For Cycles 7 and 8



Cycle 7

Cycle 8

	Batch 7 - 57 FA
	4.106 w/o U-235
	Batch 8 - 60 FA
	4.106 w/o U-235
	Batch 9 - 60 FA
	4.106 w/o U-235

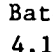
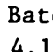
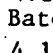
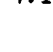


	Batch 8 - 57 FA
	4.106 w/o U-235
	Batch 9 - 60 FA
	4.106 w/o U-235
	Batch 10 - 60 FA
	4.106 w/o U-235

Figure C-4. Cycle 5 Core Power Distribution - 60 Feed, Feed and Bleed

	8	9	10	11	12	13	14	15
H	1.007	1.430	1.021	1.417	1.082	1.413	0.962	0.481
	0.964	1.348	0.978	1.385	1.066	1.414	0.987	0.565
	0.940	1.283	0.961	1.345	1.048	1.383	0.999	0.622
K		1.016	1.102	1.091	1.416	1.084	1.116	0.462
		0.970	1.044	1.054	1.395	1.072	1.169	0.545
		0.950	1.019	1.029	1.355	1.060	1.188	0.602
L			0.998	1.437	0.986	1.019	0.792	0.370
			0.969	1.390	0.970	1.000	0.823	0.445
			0.952	1.328	0.953	1.000	0.855	0.506
M				1.066	1.383	1.019	0.946	
				1.043	1.365	0.994	0.942	
				1.021	1.337	0.997	0.974	
N					1.116	1.069	0.449	
					1.091	1.103	0.502	
					1.079	1.124	0.551	
O						0.497	Beginning of Cycle	
						0.563	Middle of Cycle	
						0.612	End of Cycle	

Figure C-5. Cycle 6 Core Power Distribution — 60 Feed, Feed and Bleed

	8	9	10	11	12	13	14	15
H	1.026	1.439	1.016	1.386	1.023	1.380	0.875	0.589
	1.056	1.479	1.044	1.416	1.025	1.368	0.882	0.621
	0.977	1.348	0.988	1.357	1.008	1.353	0.918	0.694
K		1.025	1.414	0.977	1.354	1.093	1.162	0.617
		1.054	1.450	0.999	1.355	1.063	1.159	0.641
		0.986	1.353	0.976	1.326	1.045	1.199	0.710
L			0.992	1.329	0.902	1.124	0.973	0.505
			1.016	1.351	0.989	1.071	0.933	0.526
			0.983	1.322	0.896	1.050	0.946	0.595
M				0.973	1.278	0.862	0.977	
				0.977	1.266	0.843	0.927	
				0.973	1.262	0.865	0.947	
N					1.095	0.814	0.484	
					1.052	0.804	0.497	
					1.046	0.843	0.560	
O						0.464	Beginning of Cycle	
						0.487	Middle of Cycle	
						0.556	End of Cycle	

Figure C-6. Cycle 7 Core Power Distribution - 60 Feed, Feed and Bleed

	8	9	10	11	12	13	14	15
H	1.101	1.406	1.102	1.417	1.132	1.303	0.845	0.479
	1.081	1.406	1.077	1.404	1.100	1.330	0.905	0.573
	1.003	1.292	1.005	1.306	1.052	1.313	0.960	0.666
K		1.099	1.423	1.131	1.368	1.116	1.001	1.481
		1.077	1.410	1.093	1.354	1.092	1.082	0.567
		1.002	1.300	1.027	1.289	1.083	1.155	0.660
L			1.163	1.404	1.033	1.091	0.844	0.393
			1.118	1.377	0.992	1.041	0.854	0.460
			1.042	1.291	0.961	1.045	0.910	0.549
M				1.156	1.295	0.973	0.892	
				1.101	1.269	0.938	0.871	
				1.055	1.249	0.966	0.935	
N					1.071	0.810	0.460	
					1.021	0.807	0.494	
					1.032	0.864	0.574	
O						0.444	Beginning of Cycle	
						0.485	Middle of Cycle	
						0.565	End of Cycle	

Figure C-7. Cycle 8 Core Power Distribution - 60 Feed, Feed and Bleed

	8	9	10	11	12	13	14	15
H	1.131	1.470	1.152	1.477	1.189	1.350	0.860	0.467
	1.073	1.418	1.089	1.425	1.129	1.357	0.917	0.561
	0.993	1.298	1.009	1.319	1.071	1.330	0.967	0.651
K		1.151	1.486	1.162	1.407	1.147	1.006	0.463
		1.088	1.429	1.099	1.371	1.114	1.089	0.552
		1.006	1.311	1.029	1.303	1.099	1.162	0.642
L			1.220	1.435	1.012	1.052	0.811	0.382
			1.142	1.389	0.977	1.023	0.841	0.458
			1.059	1.304	0.952	1.031	0.899	0.546
M				1.162	1.258	0.913	0.849	
				1.109	1.260	0.915	0.867	
				1.066	1.254	0.951	0.934	
N					1.008	0.739	0.426	
					0.998	0.776	0.485	
					1.021	0.843	0.567	
O						0.404	Beginning of Cycle	
						0.469	Middle of Cycle	
						0.552	End of Cycle	

APPENDIX D

Description of Fuel Cycle Study

Feed batch size: 68 assemblies
Cycle length: 460 EFPD
Power level: 2772 MWt
Control mode: Feed and bleed

Introduction

The fuel management plan described in detail in this appendix was chosen to provide fuel cycle data at burnups of 40,448 MWd/mtU with an approximately 18-month cycle. This fuel management plan loads 68 fresh fuel assemblies per cycle. As indicated in section 5.1.3, this fuel cycle provided a 3.4% fuel utilization improvement relative to the base case and also offers the increased availability potential of an 18-month cycle.

1. Fuel Shuffle Patterns

These cycles employed the LBP shuffle scheme, whereby the fresh fuel assemblies with LBP are loaded in the interior of the core in an approximate checkerboard pattern. For the first cycle of the 68-FA feed, eight fresh fuel assemblies were located on the core periphery. In the subsequent cycles of the 68-FA feed case, no fresh fuel assemblies were situated on the core periphery and the equilibrium loading pattern was established. Table D-1 gives the fuel inventory plan utilized.

Cycle 5, the first transition cycle, was initiated by shuffling the fuel isotopes from ANO-1 cycle 4 at 387 EFPD. Sixty-four once-burned and forty-five twice-burned assemblies from cycle 4 were utilized in cycle 5. The cycle 5 fuel loading pattern and LBP concentrations are shown in Figure D-1. Cycle 5 was depleted to 450 EFPD and shuffled to the next cycle.

Cycles 5, 6, and 7, which are approaching an equilibrium cycle, all use the same fresh fuel loading pattern. The fuel loading pattern and LBP concentrations used in these cycles are given in Figures D-2 and D-3, respectively.

2. Cycle Lifetimes and Uranium Utilization

The cycle lifetimes attained were 450, 453, 476, and 469 EFPD for cycles 5 through 8. These cycles were run to the same EOL effective multiplication factor (k_{eff}) using a constant feed batch size and enrichment. When all transition effects die out, the projected equilibrium cycle length is 469 EFPD compared to a target value of 460 EFPD. Thus, the initial equilibrium cycle estimate of 3.803 wt % ^{235}U for the 68-FA feed was reasonably accurate, although the detailed fuel management evaluation gave a cycle length that was slightly greater than estimated. An equilibrium feed enrichment of 3.738 wt % ^{235}U is projected for 460 EFPD cycles based on the results from this study. The equilibrium uranium utilization would be 12.13 MWy/2000 lb U_3O_8 , a 3.4% improvement over the three-batch annual cycle base case using the LBP shuffle scheme.

3. Core Power Distributions

The maximum allowable radial peak for these studies, 1.651, is based on the design radial peak for the Oconee-class plants. All of the 68-FA feed fuel cycles met this criterion for radial peaking, as shown below. Power distributions at the beginning, middle, and end of cycle for each cycle are given in Figures D-4 through D-7.

<u>Cycle</u>	<u>Maximum calculated peak</u>	<u>Percent margin</u>
5	1.535	7.0
6	1.547	6.3
7	1.596	3.3
8	1.570	4.9

4. Burnup Distributions

The burnup accumulated by each batch of fuel during each cycle and the discharge batch average burnups are given in Table D-2 for the 68-FA feed case. The maximum assembly discharge burnup was 49,967 MWd/mtU at EOC 8.

5. Control Rod Worths

The hot zero power (HZP) control rod pattern worth was run with PDQ for BOL and EOL for all cycles. These worths are listed in Table D-3 along with the maximum stuck rod worth for cycles 5 and 8.

A two-dimensional FLAME model was used at the BOL and EOL of each cycle to identify the stuck rod of maximum worth. Then the PDQ pattern worths and power deficits, along with the FLAME maximum stuck rod worth, were used to calculate a shutdown margin for each cycle. The cycles with the lowest EOC shutdown margin were selected for full-core PDQ stuck rod worth calculations and the shutdown margin recalculated. The resultant margins are given in Table D-3.

Table D-1. Fuel Inventory Plan -- 68-FA Feed

<u>Batch</u>	<u>Enrichment</u>	<u>Cycle</u>							
		<u>1</u>	<u>2</u>	<u>3</u>	<u>4</u>	<u>5</u>	<u>6</u>	<u>7</u>	<u>8</u>
1	2.06	56		5	1				
2	2.75	61	61						
3	3.05	60	60	60					
4	2.64		56	56	56				
5	3.01			56	56	45	4		
6	3.19				64	64	37		
7	3.803					68	68	41	
8	3.803						68	68	41
9	3.803							68	68
10	3.803								68

Table D-2. Fuel Burnup Distribution

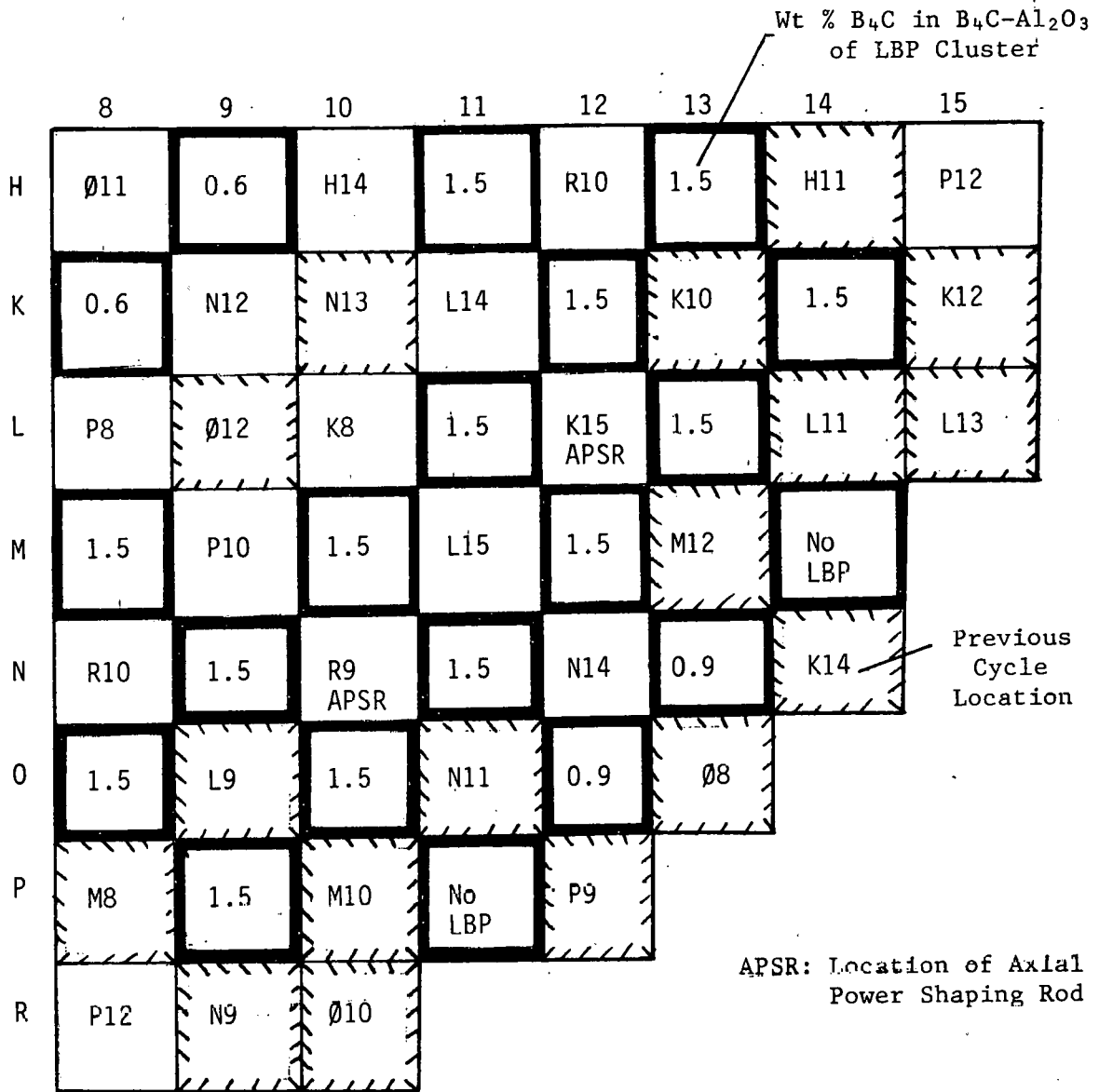
Batch No.	Initial enrich't	No. of assemblies	Mwd/mtU by cycle									Batch-average burnup
			Cycle 1	Cycle 2	Cycle 3	Cycle 4	Cycle 5	Cycle 6	Cycle 7	Cycle 8	Cycle 9	
1A	2.06	50	17203	--	--	--	--	--	--	--	--	17203
1B	2.06	5	13438	--	6420	--	--	--	--	--	--	19858
1C	2.06	1	14854	--	--	10129	--	--	--	--	--	24983
2	2.75	61	17926	8221	--	--	--	--	--	--	--	26147
3	3.05	60	12231	9517	8403	--	--	--	--	--	--	30151
4	2.64	56	--	7752	9852	10678	--	--	--	--	--	28282
5A	3.01	11	--	--	10470	14109	--	--	--	--	--	24579
5B	3.01	41	--	--	8362	9395	15723	--	--	--	--	33480
5C	3.01	4	--	--	6764	5856	7777	15692	--	--	--	36089
6A	3.19	27	--	--	--	16186	15259	--	--	--	--	31485
6B	3.19	37	--	--	--	14448	9385	15527	--	--	--	39360
7A	3.80	27	--	--	--	--	20355	15610	--	--	--	35965
7B	3.80	41	--	--	--	--	17193	8478	17752	--	--	43423
8A	3.80	27	--	--	--	--	--	20422	15741	--	--	36163
8B	3.80	41	--	--	--	--	--	18311	8225	17328	--	43864
9A	3.80	27	--	--	--	--	--	--	21867	15386	--	37253
9B	3.80	41	--	--	--	--	--	--	18672	8188	--	(26860)
10A	3.80	27	--	--	--	--	--	--	--	21526	--	(21526)
10B	3.80	41	--	--	--	--	--	--	--	18570	--	(18570)
Core			15647	8512	8887	12112	15201	15302	16079	15843		
(Not discharged)												

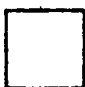
D-4

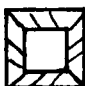
Table D-3. Control Rod Worths

	<u>Cycle</u>			
	<u>5</u>	<u>6</u>	<u>7</u>	<u>8</u>
HZP control rod worths, % $\Delta\rho$				
BOC	8.30	8.18	8.32	8.08
EOC	8.77	8.71	8.66	8.59
Max stuck rod worth, % $\Delta\rho$				
BOC	1.33	--	--	1.34
EOC	1.66	--	--	1.72
Shutdown margin, % $\Delta\rho$				
BOC	3.34	--	--	3.13
EOC	1.94	--	--	1.70

Figure D-1. Cycle 5 Core Loading Plan



 Batch 5 - 45 FA,
3.01 wt % ²³⁵U

 Batch 6 - 64 FA,
3.19 wt % ²³⁵U


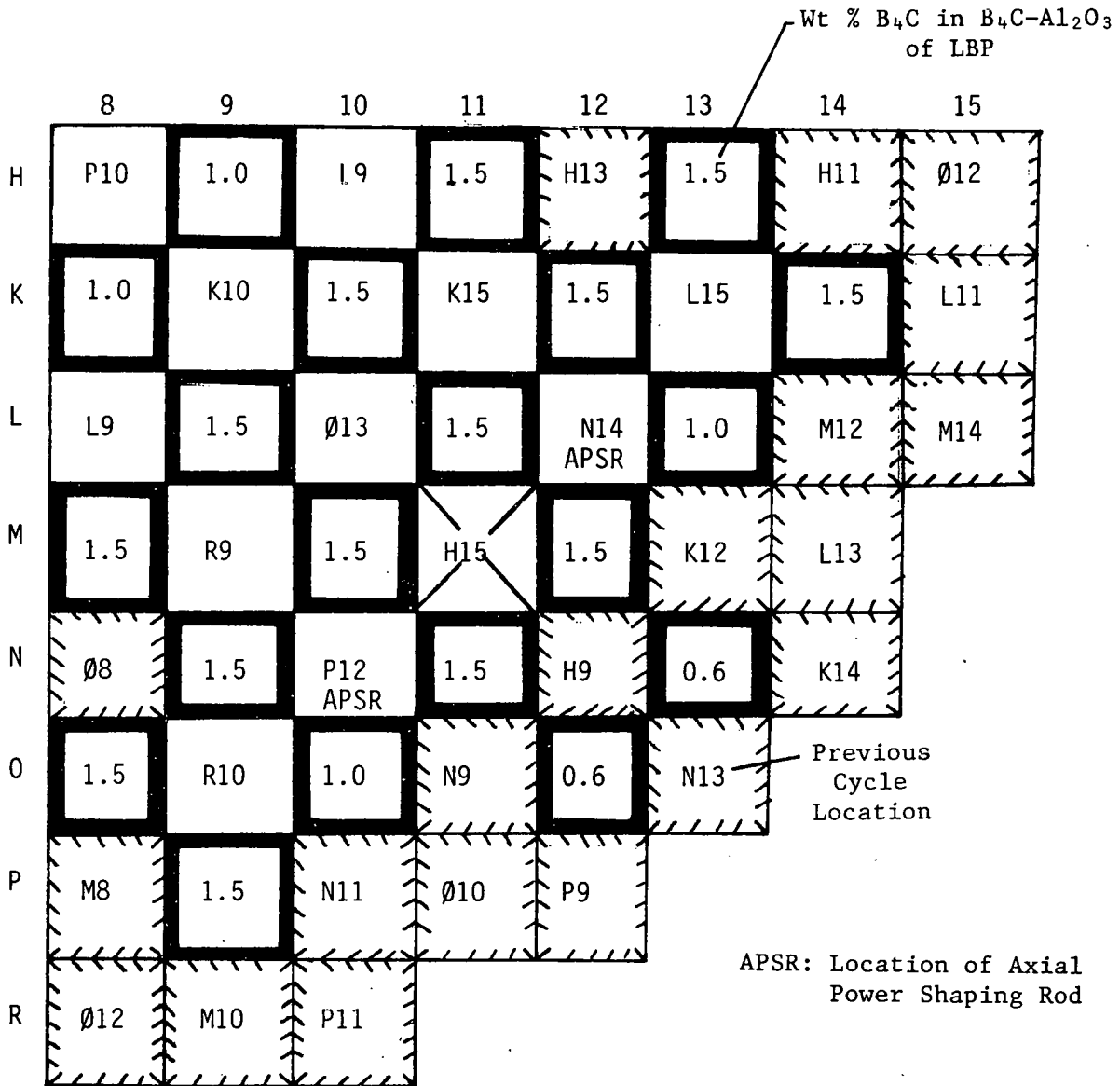

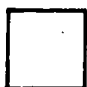
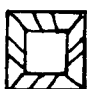
 Batch 7 - 68 FA,
3.802 wt % ²³⁵U

Figure D-2. Cycle 6 Core Loading Plan



 Batch 5 - 4 FA,
3.01 wt % ²³⁵U

 Batch 6 - 37 FA,
3.19 wt % ²³⁵U

 Batch 7 - 68 FA,
3.803 wt % ²³⁵U


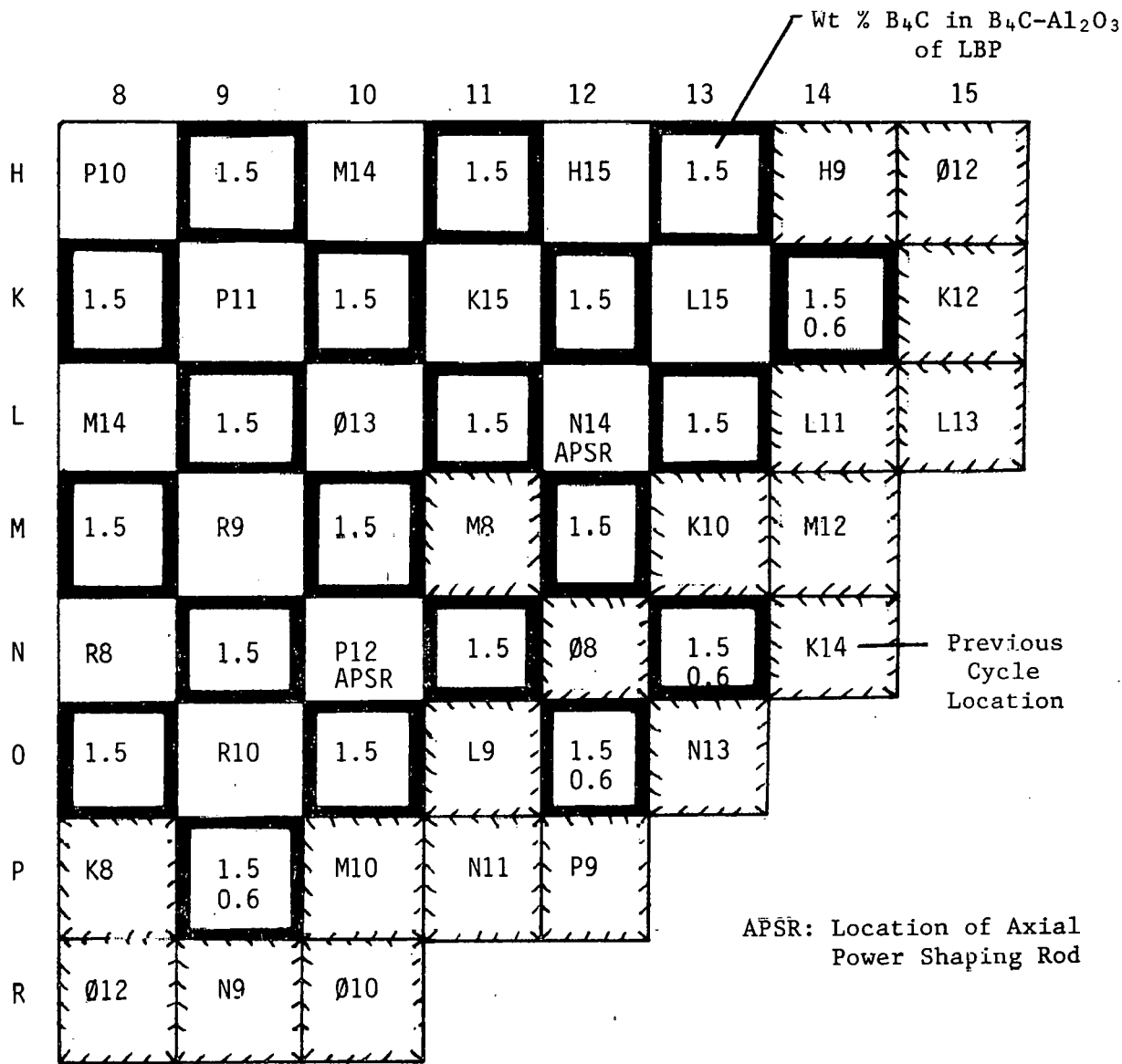
 Batch 8 - 68 FA,
3.803 wt % ²³⁵U

Figure D-3. Cycle 7 and Cycle 8 Core Loading Plan



Cycle 7

Cycle 8

Batch 7 - 41 FA,
3.803 wt % ²³⁵U

Batch 8 - 41 FA,
3.803 wt % ²³⁵U

Batch 8 - 68 FA,
3.803 wt % ²³⁵U

Batch 9 - 68 FA,
3.803 wt % ²³⁵U

Batch 9 - 68 FA,
3.803 wt % ²³⁵U

Batch 10 - 68 FA,
3.803 wt % ²³⁵U

Figure D-4. Cycle 5 Core Power Distribution - 68-FA Feed

	8	9	10	11	12	13	14	15
H	1.081	1.410	1.032	1.364	1.182	1.356	0.902	0.422
	0.947	1.238	0.939	1.316	1.133	1.375	0.958	0.526
	0.928	1.187	0.931	1.279	1.093	1.340	0.989	0.604
K		1.017	1.176	1.089	1.394	1.164	0.999	0.421
		0.909	1.052	1.033	1.374	1.137	1.103	0.519
		0.902	1.030	1.011	1.320	1.112	1.157	0.595
L			1.035	1.349	1.047	1.256	0.805	0.333
			0.973	1.323	1.023	1.283	0.848	0.413
			0.962	1.281	0.993	1.268	0.881	0.479
M				1.140	1.348	1.065	0.917	
				1.103	1.347	1.042	0.925	
				1.068	1.302	1.027	0.948	
N					1.087	0.992	0.434	
					1.075	1.048	0.491	
					1.054	1.063	0.537	
O						0.485	Beginning of Cycle	
						0.553	Middle of Cycle	
						0.599	End of Cycle	

Figure D-5. Cycle 6 Core Power Distribution — 68-FA Feed

	8	9	10	11	12	13	14	15
H	0.977	1.321	1.000	1.415	1.361	1.347	0.988	0.540
	0.988	1.340	1.004	1.390	1.240	1.335	0.992	0.607
	0.945	1.256	0.971	1.317	1.172	1.314	1.028	0.687
K		0.985	1.321	1.100	1.378	1.054	1.017	0.483
		0.997	1.345	1.069	1.350	1.031	1.081	0.553
		0.962	1.287	1.030	1.298	1.029	1.145	0.632
L			1.062	1.326	0.958	1.237	0.810	0.371
			1.054	1.328	0.939	1.228	0.832	0.440
			1.021	1.282	0.925	1.214	0.878	0.518
M				1.044	1.326	1.060	0.621	
				1.022	1.293	1.003	0.649	
				1.005	1.264	1.001	0.702	
N					1.215	1.050	0.452	
					1.109	1.024	0.485	
					1.081	1.031	0.537	
O						0.602	Beginning of Cycle	
						0.610	Middle of Cycle	
						0.649	End of Cycle	

Figure D-6. Cycle 7 Core Power Distribution - 68-FA Feed

	8	9	10	11	12	13	14	15
H	1.132	1.435	1.212	1.461	1.226	1.292	0.916	0.481
	1.044	1.351	1.103	1.380	1.145	1.313	0.964	0.578
	0.967	1.236	1.014	1.270	1.080	1.291	1.010	0.670
K		1.210	1.479	1.213	1.380	1.118	0.948	0.428
		1.099	1.379	1.112	1.342	1.102	1.054	0.523
		1.009	1.257	1.031	1.271	1.090	1.132	0.614
L			1.293	1.453	1.076	1.155	0.730	0.309
			1.158	1.365	1.022	1.199	0.801	0.394
			1.060	1.264	0.984	1.217	0.870	0.481
M				1.342	1.308	0.953	0.530	
				1.204	1.292	0.971	0.610	
				1.126	1.267	1.007	0.695	
N					1.083	0.827	0.361	
					1.064	0.926	0.445	
					1.082	1.032	0.539	
O						0.466	Beginning of Cycle	
						0.553	Middle of Cycle	
						0.653	End of Cycle	

Figure D-7. Cycle 8 Core Power Distribution - 68-FA Feed

	8	9	10	11	12	13	14	15
H	1.100	1.393	1.175	1.419	1.190	1.272	0.938	0.516
	1.055	1.361	1.108	1.380	1.137	1.297	0.958	0.590
	1.001	1.278	1.044	1.302	1.094	1.286	0.987	0.667
K		1.176	1.443	1.179	1.339	1.065	1.019	0.448
		1.107	1.388	1.110	1.329	1.056	1.078	0.522
		1.041	1.296	1.054	1.284	1.055	1.111	0.596
L			1.280	1.429	1.064	1.133	0.725	0.316
			1.173	1.368	1.020	1.178	0.780	0.390
			1.096	1.291	0.996	1.205	0.839	0.467
M				1.319	1.315	0.958	0.535	
				1.195	1.291	0.956	0.599	
				1.133	1.268	0.982	0.674	
N					1.134	0.946	0.392	
					1.076	0.983	0.455	
					1.070	1.024	0.528	
O						0.544	Beginning of Cycle	
						0.593	Middle of Cycle	
						0.656	End of Cycle	

APPENDIX E

Description of Fuel Cycle Study

Feed batch size: 80 assemblies
Cycle length: 460 EFPD
Power level: 2772 MWt
Control mode: Feed and bleed

Introduction

The fuel management plan described in detail in this appendix was chosen to provide fuel cycle data at burnups of 34,382 MWd/mtU with an approximately 18-month cycle. This fuel management plan loads 80 fresh fuel assemblies per cycle and, thus, represents a two-batch reload for a 177 fuel assembly core. As indicated in section 5.1.3, this fuel cycle yielded a 4.2% fuel utilization loss relative to the base case.

1. Fuel Shuffle Patterns

These cycles employed the LBP shuffle scheme, whereby the fresh assemblies with LBP are loaded in the interior of the core in a checkerboard pattern. For the 80-FA feed, 17 fresh fuel assemblies were located on the core periphery along with once-burned fuel. Table E-1 outlines the fuel inventory plan utilized.

Cycle 4, the first transition cycle, was initiated by shuffling of the fuel isotopics from Oconee 2 cycle 3 at 308 EFPD. Forty-one twice-burned fuel assemblies and fifty-six once-burned assemblies from cycle 3 were utilized in cycle 4. The cycle 4 fuel loading pattern and LBP concentrations are shown in Figure E-1. Cycle 4 was depleted to 400 EFPD and shuffled to the next cycle.

Cycles 5, 6, and 7 were loaded using the same fresh fuel pattern as cycle 4. The fuel shuffles and LBP concentrations for cycles 5, 6, and 7 are presented in Figures E-2, E-3, and E-4, respectively. The desired cycle lifetime of 460 EFPD was attained in all three cycles.

2. Cycle Lifetimes and Uranium Utilization

The cycle lifetime attained were 396, 450, 462, and 460 EFPD for cycles 4 through 7. These cycles were run to the same EOL effective multiplication factor (k_{eff}) using a constant feed batch size. When all transition effects die out, the projected equilibrium cycle length is 462 EFPD compared to a target value of 460 EFPD. Thus, the initial equilibrium cycle estimate of 3.46 wt % ^{235}U for the 80-FA feed was reasonably accurate, although the detailed fuel management evaluation gave a cycle length that was slightly greater than estimated. An equilibrium feed enrichment of 3.445 wt % ^{235}U is projected for 460 EFPD cycles based on the results from this study. The equilibrium uranium utilization would be 11.24 MWy/2000 lb U_3O_8 , 4.2% lower than the three-batch annual cycle base case using the LBP shuffle scheme.

3. Core Power Distribution

The maximum allowable radial peak for these studies, 1.651, is based on the design radial peak for the Oconee-class plants. All of the 80-FA feed fuel cycles met this criterion for radial peaking as shown below. Power distributions at the beginning, middle, and end of cycle for each cycle are given in Figures E-5 through E-8.

<u>Cycle</u>	<u>Maximum calculated peak</u>	<u>Percent margin</u>
4	1.395	15.5
5	1.395	15.5
6	1.458	11.7
7	1.512	8.4

4. Burnup Distributions

The burnup accumulated by each batch of fuel during each cycle and the discharge batch average burnups are given in Table E-2 for the 80-FA feed case. The maximum assembly discharge burnup was 39,552 MWd/mtU at EOC 7.

5. Control Rod Worths

The hot zero power (HZP) control rod pattern worth was run with PDQ for BOL and EOL of all cycles. These worths are listed in Table E-3 along with the maximum stuck rod worth for cycles 4 and 7.

A two-dimensional FLAME model was used at the BOL and EOL of each cycle to identify the stuck rod of maximum worth. Then the PDQ pattern worths and power deficits, along with the FLAME maximum stuck rod worth, were used to calculate a shutdown margin for each cycle. The cycles with the lowest EOC shutdown margin were selected for full-core PDQ stuck rod worth calculations and the shutdown margins recalculated. The resultant shutdown margins are given in Table E-3.

Table E-1. Fuel Inventory Plan — 80-FA Feed

<u>Batch</u>	<u>Enrichment</u>	<u>Cycle</u>						
		<u>1</u>	<u>2</u>	<u>3</u>	<u>4</u>	<u>5</u>	<u>6</u>	<u>7</u>
1	2.06	56		5				
2	2.75	61	61					
3	3.05	60	60	60				
4	2.64		56	56	41			
5A	2.53			4	4			
5B	3.03			52	52	17		
6	3.22				80	80	17	
7A	3.306					36	36	
7B	3.622					44	44	17
8	3.53						80	80
9	3.376							80

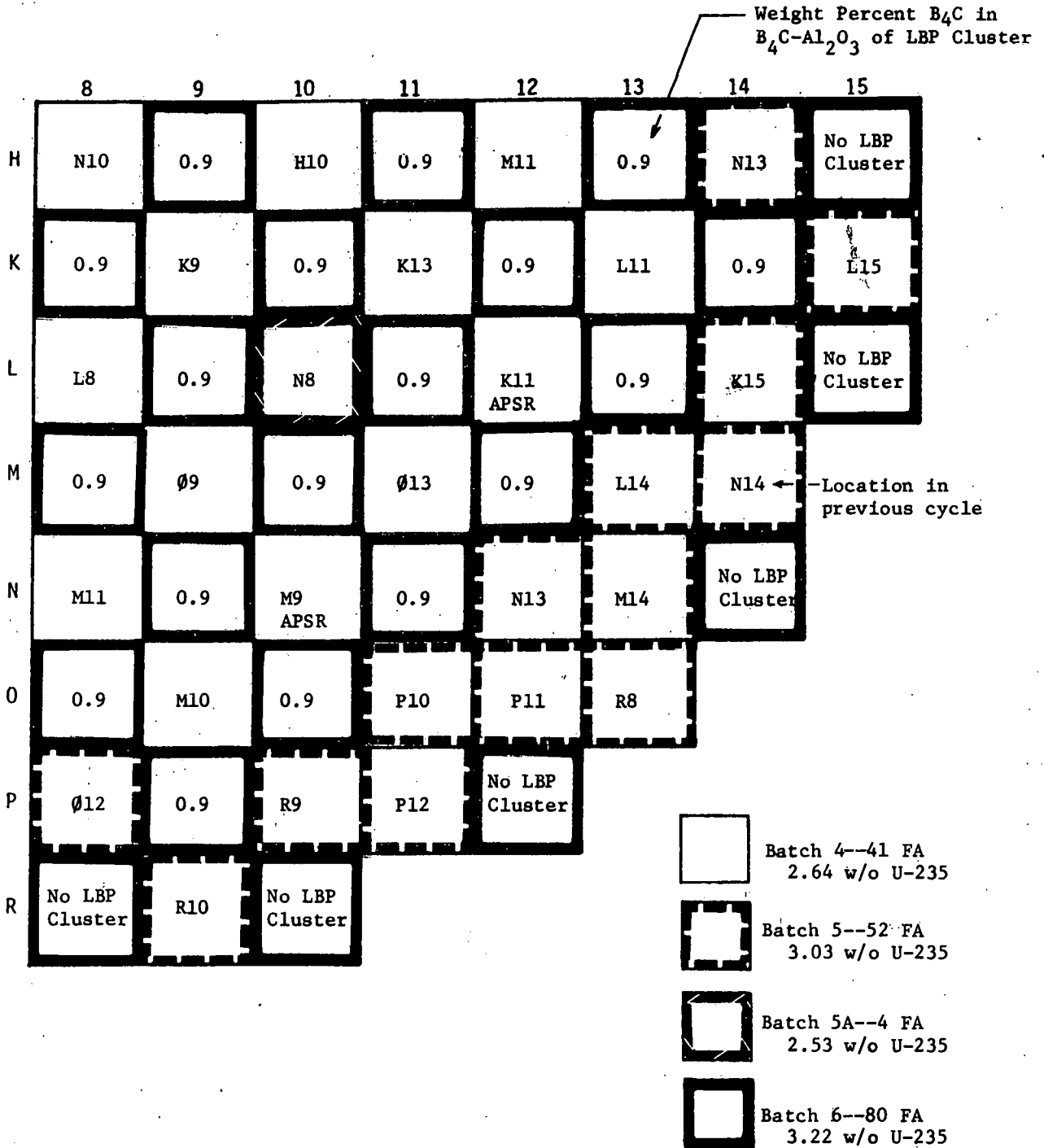
Table E-2. Fuel Burnup Distribution

Batch No.	Initial enrich't	No. of assemblies	Mwd/mtU by cycle									Batch average burnup
			Cycle 1	Cycle 2	Cycle 3	Cycle 4	Cycle 5	Cycle 6	Cycle 7	Cycle 8	Cycle 9	
1A	2.06	5	11338	--	10326	--	--	--	--	--	--	21664
1B	2.06	51	15352	--	--	--	--	--	--	--	--	15352
2	2.75	61	15901	8732	--	--	--	--	--	--	--	24633
3	3.05	60	10459	10103	8974	--	--	--	--	--	--	29536
4A	2.64	41	--	6808	10738	13388	--	--	--	--	--	30934
4B	2.64	15	--	9604	10335	--	--	--	--	--	--	19939
5A	2.53	4	--	--	12822	14813	--	--	--	--	--	27635
5B	3.03	35	--	--	9869	12886	--	--	--	--	--	22755
5C	3.03	17	--	--	7303	9322	16701	--	--	--	--	33326
6A	3.22	63	--	--	--	16213	15098	--	--	--	--	31311
6B	3.22	17	--	--	--	8970	9949	17419	--	--	--	36338
7A	3.31	36	--	--	--	--	19671	15950	--	--	--	35621
7B	3.62	27	--	--	--	--	17702	12858	--	--	--	30560
7C	3.62	17	--	--	--	--	9415	11102	18487	--	--	39004
8	3.53	80	--	--	--	--	--	16801	13926	--	--	(30727)
9	3.38	80	--	--	--	--	--	--	16526	--	--	(16526)
Core			13769	8825	9639	13513	15539	15539	15539			
(Not discharged)												

Table E-3. Control Rod Worths

	Cycle			
	4	5	6	7
HZP control rod worths, % $\Delta\rho$				
BOC	8.71	8.43	8.23	8.61
EOC	9.12	8.85	8.63	8.73
Max stuck rod worth, % $\Delta\rho$				
BOC	2.15	--	--	1.70
EOC	1.96	--	--	1.73
Shutdown margin, % $\Delta\rho$				
BOC	3.20	--	--	3.27
EOC	2.10	--	--	1.91

Figure E-1. Cycle 4 Core Loading Plan



APSR - Location of Axial Shaping Rod

Figure E-2. Cycle 5 Core Loading Plan

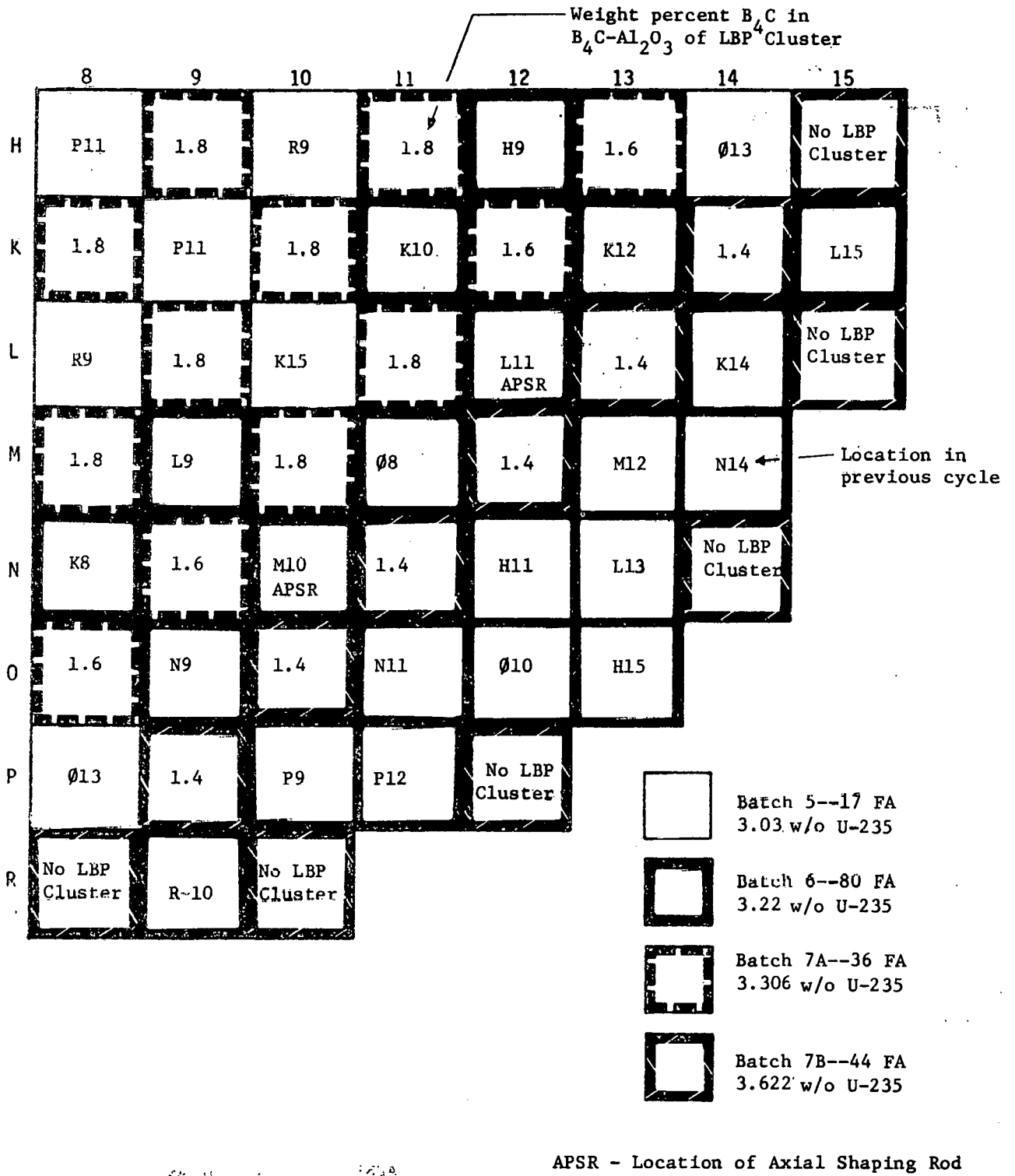
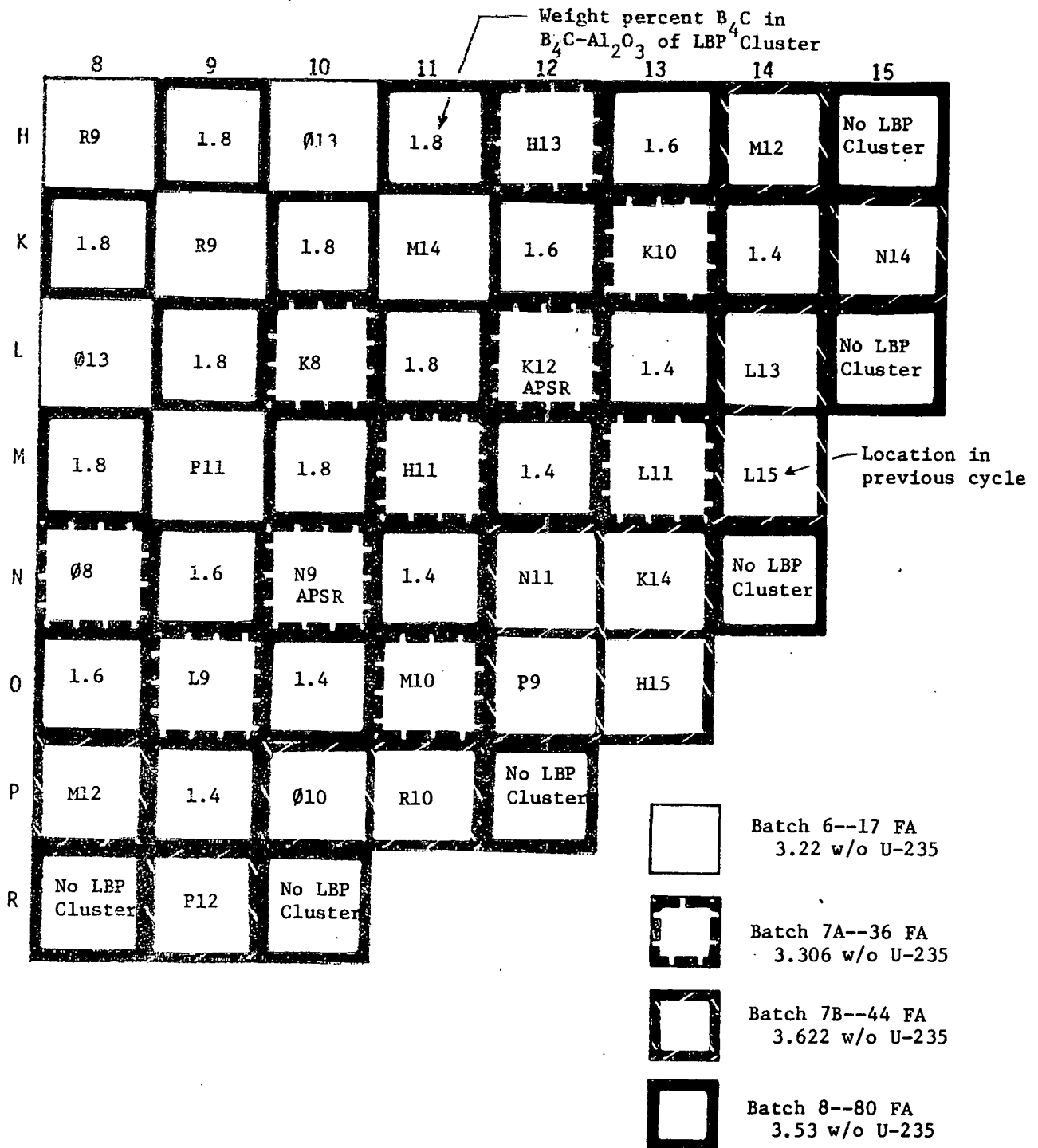
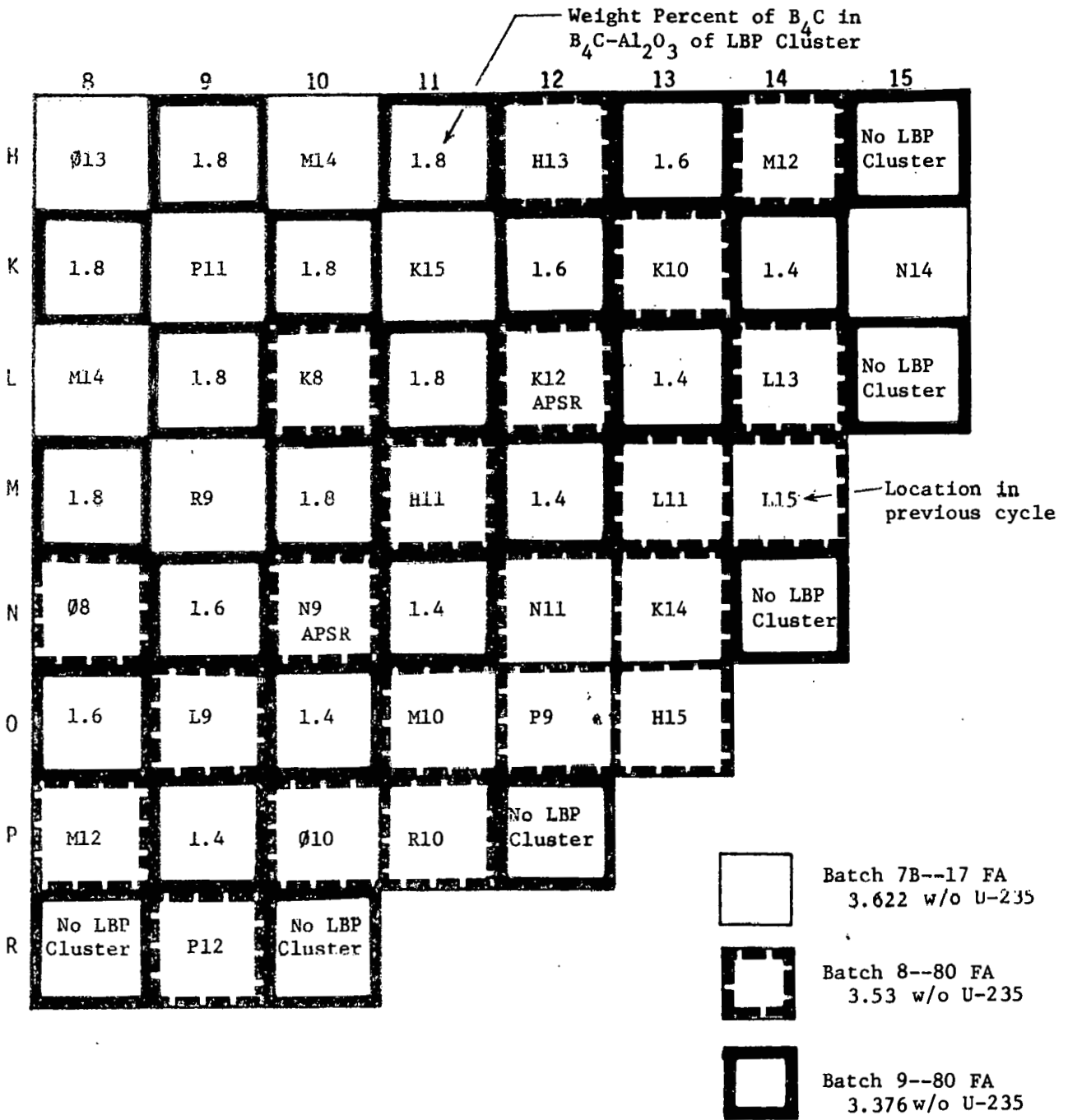


Figure E-3. Cycle 6 Core Loading Plan



APSR - Location of Axial Shaping Power

Figure E-4. Cycle 7 Core Loading Plan



APSR - Location of Axial Shaping Rod

Figure E-5. Cycle 4 Core Power Distribution - 80-FA Feed

	8	9	10	11	12	13	14	15
H	0.947	1.175	0.963	1.198	1.015	1.266	1.186	0.937
	1.040	1.318	1.041	1.301	1.041	1.276	1.088	0.853
	0.994	1.241	0.999	1.244	1.020	1.244	1.065	0.875
K		0.964	1.217	0.962	1.179	1.008	1.180	0.759
		1.049	1.332	1.016	1.242	0.992	1.143	0.710
		1.001	1.252	0.989	1.214	0.992	1.151	0.752
L			1.079	1.215	0.874	1.183	1.031	0.640
			1.120	1.283	0.886	1.175	0.956	0.614
			1.059	1.227	0.888	1.177	0.972	0.682
M				1.094	1.224	1.065	0.772	
				1.085	1.215	0.989	0.727	
				1.050	0.198	1.002	0.786	
N					1.115	0.875	0.571	
					1.029	0.813	0.552	
					1.031	0.866	0.642	
O						0.526	Beginning of Cycle	
						0.511	Middle of Cycle	
						0.598	End of Cycle	

Figure E-6. Cycle 5 Core Power Distribution — 80-FA Feed

	8	9	10	11	12	13	14	15
H	1.041	1.182	1.094	1.269	1.250	1.281	1.053	0.925
	1.113	1.313	1.122	1.320	1.169	1.265	0.978	0.851
	1.059	1.255	1.065	1.255	1.102	1.230	0.979	0.878
K		1.060	1.218	1.200	1.261	1.196	1.162	0.713
		1.113	1.312	1.163	1.274	1.107	1.134	0.689
		1.059	1.254	1.097	1.224	1.074	1.151	0.730
L			1.096	1.207	1.046	1.190	0.890	0.612
			1.107	1.260	1.005	1.184	0.855	0.621
			1.059	1.225	0.980	1.188	0.887	0.684
M				1.151	1.181	0.923	0.677	
				1.107	1.195	0.901	0.690	
				1.076	1.200	0.933	0.754	
N					0.906	0.679	0.498	
					0.897	0.702	0.544	
					0.933	0.771	0.632	
O						0.388	Beginning of Cycle	
						0.442	Middle of Cycle	
						0.526	End of Cycle	

Figure E-7. Cycle 6 Core Power Distribution - 80-FA Feed

	8	9	10	11	12	13	14	15
H	1.161	1.340	1.171	1.324	1.217	1.296	1.161	0.945
	1.162	1.368	1.165	1.337	1.178	1.281	1.093	0.891
	1.054	1.270	1.065	1.269	1.085	1.245	1.035	0.874
K		1.164	1.331	1.143	1.268	1.131	1.130	0.778
		1.161	1.352	1.131	1.274	1.095	1.114	0.751
		1.057	1.272	1.055	1.236	1.046	1.132	0.773
L			1.204	1.239	0.988	1.102	0.885	0.599
			1.183	1.258	0.979	1.117	0.872	0.603
			1.087	1.238	0.956	1.156	0.899	0.675
M				1.092	1.098	0.857	0.669	
				1.083	1.126	0.865	0.686	
				1.050	1.172	0.911	0.769	
N					0.918	0.688	0.472	
					0.926	0.711	0.503	
					0.968	0.799	0.623	
O						0.402	Beginning of Cycle	
						0.437	Middle of Cycle	
						0.551	End of Cycle	

Figure E-8. Cycle 7 Core Power Distribution - 80-FA Feed

	8	9	10	11	12	13	14	15
H	1.322	1.410	1.304	1.358	1.281	1.235	1.079	0.837
	1.193	1.356	1.187	1.334	1.182	1.254	1.031	0.821
	1.078	1.237	1.086	1.249	1.114	1.234	1.035	0.861
K		1.317	1.385	1.257	1.259	1.133	1.033	0.699
		1.191	1.346	1.166	1.268	1.090	1.081	0.714
		1.083	1.245	1.089	1.222	1.071	1.119	0.767
L			1.301	1.257	1.035	1.055	0.833	0.536
			1.187	1.268	1.008	1.120	0.854	0.588
			1.101	1.221	0.985	1.147	0.900	0.663
M				1.149	1.075	0.870	0.634	
				1.105	1.140	0.896	0.608	
				1.075	1.160	0.939	0.764	
N					0.904	0.666	0.441	
					0.926	0.719	0.515	
					0.968	0.795	0.610	
O						0.382	Beginning of Cycle	
						0.452	Middle of Cycle	
						0.542	End of Cycle	

DISTRIBUTION

Mr. Thomas Abernathy, Chief (150)
Document Management Branch
U.S. Department of Energy
Technical Information Center
P. O. Box 62
Oak Ridge, TN 37830

Babcock & Wilcox

Andrews, JB
Brunson, WT
Chipman, EE
Coleman, TA (25)
Coppola, EJ (26)
Croft, MW
Davis, HH
DeMars, RV
Gudorf, MR
Kane, ER
Library
Mayer, JT
Meyer, GA
Montgomery, MH
Papazoglou, TP
Pyecha, TD
Romano, JJ (6)
Sapyta, JJ
Shipman, GA
Smotrel, JR
Stein, KO
Travis, CC/TRG
Trost, RJ
Tulenko, JS
Wilson, HW

Others

Mr. S. Armijo
GENERAL ELECTRIC CO.
Nuclear Energy Division
175 Curtner Avenue
San Jose, CA 95125

Mr. Gordon Bond
GPU SERVICE CORP.
260 Cherry Hill Road
Parsippany, NJ 07054

Mr. F. W. Buckman
CONSUMERS POWER COMPANY
1945 Parnall Road
Jackson, MI 49201

Mr. J. P. Cagnetta
NORTHEAST UTILITIES SERVICE CO.
P. O. Box 270
Hartford, CT 06101

Mr. Dennis R. Coleman
NUCLEAR ASSOCIATES INTERNATIONAL
6003 Executive Boulevard
Rockville, MD 20852

Mr. C. E. Crouthamel
EXXON NUCLEAR COMPANY, INC.
Richland, WA 99352

Mr. Orville Cypret
ARKANSAS POWER & LIGHT
P. O. Box 551
Little Rock, AK 72203

Mr. G. F. Daebeler
PHILADELPHIA ELECTRIC CO.
2301 Market Street
P. O. Box 8699
Philadelphia, PA 19101

Others (Cont'd)

Mr. R. N. Duncan
COMBUSTION ENGINEERING, INC.
1000 Prospect Hill Road
Windsor, CT 06095

Mr. M. S. Freshley
BATTELLE-NORTHWEST LABORATORY
Richland, WA 99352

Mr. F. E. Gelhaus
ELECTRIC POWER RESEARCH INSTITUTE
P. O. Box 10412
Palo Alto, CA 94303

Mr. S. J. Groetch
GENERAL ELECTRIC COMPANY
Knolls Atomic Energy Laboratory
P. O. Box 1072
Schenectady, NY 12301

Mr. R. M. Grube
YANKEE ATOMIC ELECTRIC COMPANY
20 Turnpike Road
Westboro, MA 01581

Mr. John Hallam
NUCLEAR SERVICES CORP.
1700 Dell Avenue
Campbell, CA 95008

Mr. C. R. Hann
BATTELLE-NORTHWEST LABORATORY
Richland, WA 99352

Mr. W. R. Harris
RAND CORPORATION
1700 Main Street
Santa Monica, CA 90406

Mr. W. M. Kiefer
COMMONWEALTH EDISON COMPANY
P. O. Box 767
Chicago, IL 60690

Mr. J. Korthever
DUKE POWER COMPANY
P. O. Box 2178
Charlotte, NC 28342

Mr. D. L. Larkin
WASHINGTON PUBLIC POWER SUPPLY SYSTEM
P. O. Box 968
Richland, WA 99352

Mr. M. L. Lee
CONSOLIDATED EDISON COMPANY OF
NEW YORK
4 Irving Place
New York, NY 10003

Mr. W. Lipinski
ARGONNE NATIONAL LABORATORY
9700 South Cass Avenue
Argonne, IL 60439

Mr. Kashmiri Mahna
PUBLIC SERVICE ELECTRIC & GAS CO.
80 Park Place
Newark, NJ 07101

Mr. R. S. Miller
WESTINGHOUSE ELECTRIC CORP.
Nuclear Fuel Division
Box 355
Pittsburgh, PA 15230

Mr. R. J. Mullin
TENNESSEE VALLEY AUTHORITY
1410 Commerce Union Bank Bldg.
Chattanooga, TN 37402

Mr. D. O'Boyle
COMMONWEALTH EDISON CO.
P. O. Box 767
Chicago, IL 60690

Mr. R. R. O'Laughlin
PUBLIC SERVICE OF INDIANA
1000 East Main Street
Plainfield, IN 46168

Mr. R. Omberg
HANFORD ENGRG DEVELOPMENT LABORATORY
P. O. Box 1970
Richland, WA 99352

Mr. B. A. Pasternak
BOOZ-ALLEN APPLIED RESEARCH
4330 East-West Highway
Bethesda, MD 20014

Others (Cont'd)

Mr. J. T. A. Roberts
ELECTRIC POWER RESEARCH INSTITUTE
P. O. Box 10412
Palo Alto, CA 94303

Mr. T. Row
OAK RIDGE NATIONAL LABORATORY
P. O. Box X
Oak Ridge, TN 37830

Mr. H. W. Schadler, Manager
Metallurgy Laboratory
GENERAL ELECTRIC CO. R&D CENTER
P. O. Box 8
Schnectady, NY 12301

Mr. Howard Sobel
AMERICAN ELECTRIC POWER SERVICE
Nuclear Materials and Fuel
Management Section
2 Broadway
New York, NY 10004

Mr. G. Sofer
EXXON NUCLEAR COMPANY, INC.
Richland, WA 99352

Mr. I. Spiewak
OAK RIDGE NATIONAL LABORATORY
P. O. Box X
Oak Ridge, TN 37830

Mr. E. Straker
SCIENCE APPLICATIONS, INC.
8400 Westpark Drive
McLean, VA 22101

Mr. J. R. Tomonto
FLORIDA POWER & LIGHT CO.
P. O. Box 013100
Miami, FL 33101

Mr. W. J. Tunney
LONG ISLAND LIGHTING CO.
175 E. Old Country Road
Hicksville, NY 11801

U.S. Department of Energy
NASAP Control Office
Room F-409 (Mail Stop B-107)
Germantown, Maryland 20767

Mr. D. B. Wehmeyer
DETROIT EDISON CO.
2000 Second Avenue
Detroit, MI 48226

Mr. W. A. Weinreich
WESTINGHOUSE ELECTRIC CORP.
Bettis Atomic Power Laboratory
P. O. Box 79
West Mifflin, PA 15122

Mr. S. W. Wilczek, Jr.
NIAGARA MOHAWK POWER CORP.
300 Erie Boulevard West
Syracuse, NY 13202

Mr. K. Woods
EXXON NUCLEAR COMPANY, INC.
Richland, WA 99352